

**STRUCTURAL DYNAMIC MODIFICATION OF  
VIBRATING STRUCTURES USING  
TOPOLOGY OPTIMIZATION**

**SAJJAD ZARGHAM**

**FACULTY OF ENGINEERING  
UNIVERSITY OF MALAYA  
KUALA LUMPUR**

**2012**

**STRUCTURAL DYNAMIC MODIFICATION OF  
VIBRATING STRUCTURES USING  
TOPOLOGY OPTIMIZATION**

**SAJJAD ZARGHAM**

**DISSERTATION SUBMITTED IN FULFILMENT OF THE  
REQUIREMENTS FOR THE DEGREE OF  
MASTER OF ENGINEERING**

**FACULTY OF ENGINEERING  
UNIVERSITY OF MALAYA  
KUALA LUMPUR**

**2012**

## **Original Literary Work Declaration**

Name of the candidate: **Sajjad Zargham** (I.C/Passport No.)

Registration/Matric No: **KGH080030**

Name of the Degree: **Master of Engineering (M. Eng.)**

Title of Dissertation: **Structural Dynamic Modification of Vibrating Structures Using Topology Optimization**

Field of Study: **Mechanical Engineering**

I do solemnly and sincerely declare that:

(1) I am the sole author /writer of this work;

(2) This work is original;

(3) Any use of any work in which copyright exists was done by way of fair dealings and any expert or extract from, or reference to or reproduction of any copyright work has been disclosed expressly and sufficiently and the title of the Work and its authorship has been acknowledged in this Work;

(4) I do not have any actual knowledge nor do I ought reasonably to know that the making of this work constitutes an infringement of any copyright work;

(5) I, hereby assign all and every rights in the copyrights to this Work to the University of Malaya (UM), who henceforth shall be owner of the copyright in this Work and that any reproduction or use in any form or by any means whatsoever is prohibited without the written consent of UM having been first had and obtained actual knowledge;

(6) I am fully aware that if in the course of making this Work I have infringed any copyright whether internationally or otherwise, I may be subject to legal action or any other action as may be determined by UM.

Candidate's Signature

Date:

Subscribed and solemnly declared before,

Witness Signature:

Date:

Name:

Designation:

## **Abstract**

This thesis presents a structural dynamic modification of vibrating structures by using topology optimization method in order to find the most effective design of a structure supporting rotating machinery. Modal testing and operating deflection shape (ODS) measurement were applied to identify the dynamic characteristics of a pedestal structure. The dynamic characteristics of the structure were ascertained to validate the finite element model. Then, topology optimization method was used to determine the optimum design of the structure. Results from modal testing showed that the structure has two natural frequencies at 12.1 Hz (left to right bending), and 16.7 Hz (rear to front bending). The ODS measurement indicated the exact deflection shapes of the structure related to these two natural frequencies. Afterwards, a topological optimization was applied to ascertain optimized design of the structure. It was observed that, by applying the finite element modal analysis to the new design, both of the natural frequencies were shifted from 12.1 Hz and 16.7 Hz to 27.5 Hz and 25.7 Hz, respectively. Accordingly, there would not be any natural frequency within the motor operating frequency range. In addition, by applying some conditions on designable area and optimization constraint, proposed design has advantage of uncomplicated manufacturability. As a result, topology optimization method is capable of getting optimum design in less time and a more effective way in comparison with trial and error methods.

## **Abstrak**

Tesis ini membentangkan tentang pengubahsuaian struktur dinamik yang bergetar dengan menggunakan kaedah pengoptimuman topologi untuk mencari rekaan yang paling berkesan bagi struktur kekaki yang dipasang dengan sebuah motor elektrik. Ujian modus dan pengukuran bentuk pesongan operasi (ODS) telah digunakan untuk mengetahui ciri-ciri dinamik struktur kekaki. Ciri-ciri dinamik struktur telah ditentukan untuk mengesahkan model unsur terhingga struktur. Kemudian, kaedah pengoptimuman topologi telah digunakan untuk menentukan rekabentuk optimum struktur. Ujian modus berjaya menunjukkan struktur mempunyai dua frekuensi tabii pada 12.1 Hz (lentur kiri ke kanan), dan 16.7 Hz (lentur belakang ke depan) di bawah julat frekuensi operasi motor yang diambil. Ukuran ODS menunjukkan bentuk pesongan sebenar struktur yang berkaitan dengan frekuensi tabii ini. Seterusnya, pengoptimuman topologi telah digunakan untuk mendapatkan keadaan struktur dan bentuk baru. Adalah diperhatikan bahawa, dengan menjalankan mod analisis unsur terhingga ke atas rekabentuk baru, kedua-dua frekuensi tabii beralih dari 12.1 Hz dan 16.7 Hz ke 27.5 Hz dan 25.7 Hz. Jadi, tiada mana-mana frekuensi tabii berada di bawah julat frekuensi operasi motor. Di samping itu, dengan mengenakan beberapa syarat-syarat ke atas kawasan bolehubah dan kekangan pengoptimuman, reka bentuk yang dicadangkan mempunyai kelebihan kebolehubatan yang tidak kompleks. Hasilnya, kaedah pengoptimuman topologi mampu mendapatkan reka bentuk optimum dalam masa yang singkat dan merupakan cara yang lebih berkesan berbanding dengan kaedah cubajaya.

## **Acknowledgement**

First and foremost I offer my sincerest gratitude to my supervisor, Dr Rahizar Bin Ramli, who has supported me throughout my thesis with his patience and knowledge. I attribute the level of my Master's degree to his encouragement and effort and without him this thesis, too, would not have been completed or written. One simply could not wish for a better or friendlier supervisor.

Besides my supervisor, I would like to thank Mr Mohammad Sajad Naghavi, Mrs Sim Hio Yin, and Mr Behzad Rismanchi for their congenial help and guidance throughout my work.

Last but not least, I would like to thank my kindhearted parents; they have been always supporting and encouraging me with their best wishes.

# Table of Contents

Original Literary Work Declaration.....	i
Abstract.....	ii
Abstrak.....	iii
Acknowledgement.....	iv
List of Figures.....	ix
List of Tables.....	xiii
List of Symbols and Abbreviations.....	xiv
Chapter One.....	1
1 Introduction.....	1
1.1 Experimental Modal Analysis (EMA).....	2
1.2 Operating Deflection Shape (ODS) Measurement.....	2
1.3 Structural Optimization.....	3
1.4 Problem Statement.....	3
1.5 Objectives of the Study.....	4
1.6 Scope of the Study.....	4
1.7 Organization of the Study.....	4
Chapter Two.....	6
2 Literature Review.....	6
2.1 Structural Optimization, Types and Scopes.....	6
2.1.1 Method and the Mathematical Approach of an Optimization Problem.....	7

2.1.2	Classifications of Structural Optimization .....	8
2.1.2.1	Size Optimization .....	8
2.1.2.2	Shape Optimization .....	9
2.1.2.3	Topology Optimization .....	9
2.1.3	Solution Methods for Structural Optimization .....	10
2.2	Structural Topological Optimization .....	16
2.2.1	Topology optimization for Discrete Structures .....	17
2.2.2	Topology Optimization for Continuous Structures .....	18
2.3	Topology Optimization Related to Vibration Problem .....	21
Chapter Three .....		27
3	Methodology .....	27
3.1	Experimental Modal Analysis (EMA).....	27
3.1.1	FRF Measurements.....	29
3.1.2	Curve Fitting.....	31
3.1.3	EMA Instrumentation.....	34
3.2	ODS Measurement .....	48
3.2.1	Mode Shapes Versus ODS's .....	48
3.2.2	ODS Measurement .....	49
3.3	Finite Element Modal Analysis .....	50
3.4	Structural Optimization .....	52
Chapter four .....		55
4	Results .....	55



4.1	Experimental Modal Analysis .....	55
4.2	ODS Measurement .....	62
4.3	Finite Element Modal Analysis .....	68
4.3.1	Geometry Design and Performing Modal Analysis .....	68
4.3.2	Model Validation.....	71
4.4	Optimization .....	74
4.4.1	Maximizing the First Natural Frequency .....	76
4.4.2	Maximizing the Second Natural Frequency- First Approach.....	79
4.4.3	Maximizing the Second Natural Frequency- Second Approach .....	82
Chapter Five .....		86
5	Discussion .....	86
5.1	Experimental Modal Analysis .....	86
5.1.1	Modal Testing.....	87
5.2	ODS Measurement .....	88
5.3	Finite Element Modal Analysis .....	89
5.4	Structural Optimization .....	91
5.4.1	Maximizing the First Natural Frequency .....	92
5.4.2	Maximizing the Second Natural Frequency- First Approach.....	93
5.4.3	Maximizing the Second Natural Frequency- Second Approach .....	94
5.4.4	Benefits of Each Approach for Optimization of Second Mode .....	94
Chapter Six.....		95
6	Conclusion and Recommendations .....	95

6.1	Conclusions .....	95
6.2	Recommendations for Future Works.....	96
	Bibliography.....	97

## List of Figures

Figure 2.1 : Three different kinds of structural optimization of a truss structure a) Sizing optimization, b) shape optimization c) topology optimization (Bendsøe & Sigmund, 2003).....	10
Figure 3.1: Modal Testing major phases (Agilent, 2008) .....	28
Figure 3.2: Measurement FRFs on a structure(Schwarz & Richardson, 1999) .....	29
Figure 3.3 : Block diagram of an FRF (Schwarz & Richardson, 1999) .....	30
Figure 3.4 : Alternate formats of the FRF (Schwarz & Richardson, 1999).....	30
Figure 3.5 : FRF response as a summation of Modal responses (Schwarz & Richardson, 1999) .....	31
Figure 3.6 : A curve fitting example (Schwarz & Richardson, 1999) .....	32
Figure 3.7 : Impact testing (Schwarz & Richardson, 1999).....	33
Figure 3.8 : EMA flowchart .....	34
Figure 3.9 : Frequency response of transducer (Agilent, 2008).....	36
Figure 3.10 : Tri-axial accelerometer of model 3023A1T from Dytran .....	37
Figure 3.11 : Accelerometer calibrator of model VE-10 from RION.....	38
Figure 3.12 : Force pulse (Agilent, 2008).....	39
Figure 3.13 : Impact hammer of model 5800B2 from Dytran .....	40
Figure 3.14 : Four channel data acquisition module .....	41
Figure 3.15 : DAQ configuration in block diagram of FRF-analyzer VI (Chiat, 2008) .....	43
Figure 3.16 : Trigger configuration in block diagram of FRF-analyzer VI (Chiat, 2008) .....	43
Figure 3.17 : FRF configuration in block diagram of FRF-analyzer VI (Chiat, 2008) .....	44
Figure 3.18 : Front panel configurations of FRF-analyzer VI (Chiat, 2008).....	45

Figure 3.19 : Configurations and operations flow chart of FRF-analyzer VI (Chiat, 2008) .....	46
Figure 3.20 : A general view of MEScope software.....	47
Figure 3.21 : Graphical comparison of EMA and FEA frequencies (Agilent, 2008) ...	52
Figure 3.22 : Model validation strategy .....	52
Figure 4.1 : MEScope VES model of the structure .....	56
Figure 4.2 : Overlay FRFs between 0 and 70 Hz to indicate the rigid body modes .....	58
Figure 4.3 : Overlay FRFs between 10Hz and 70Hz .....	58
Figure 4.4 : Curve fitting the FRFs between 10Hz and 70Hz.....	59
Figure 4.5 : mode 1 at the frequency of 12.1Hz.....	60
Figure 4.6 : Mode 2 at the frequency of 16.7Hz .....	60
Figure 4.7 : mode 3 at the frequency of 31.4Hz.....	61
Figure 4.8 : mode 4 at the frequency of 53Hz.....	61
Figure 4.9 : Configurations and operations flow chart of ODS measurement VI (Chiat, 2008) .....	63
Figure 4.10 : Imaginary part of the ODS measurement FRFs of the pedestal structure at 12.1Hz .....	64
Figure 4.11 : Linear amplitude of the ODS measurement FRFs of the pedestal structure at 12.1Hz .....	64
Figure 4.12 : Operating Deflection shape of the pedestal structure at 12.1Hz .....	65
Figure 4.13 : Imaginary part of the ODS measurement FRFs of the pedestal structure at 16Hz .....	66
Figure 4.14 : Linear amplitude of the ODS measurement FRFs of the pedestal structure at 16Hz .....	66
Figure 4.15 : Operating Deflection shape of the pedestal structure at 16 Hz .....	67
Figure 4.16 : Designed model by SolidWorks – isometric view .....	68

Figure 4.17 : Designed model by SolidWorks .....	69
Figure 4.18 : Exported model to Hypermesh .....	70
Figure 4.19 : Meshed model by Hypermesh .....	71
Figure 4.20 : Analytical mode shape- mode1- 13.2 Hz .....	72
Figure 4.21 : Analytical mode shape- mode2- 17.9 Hz .....	73
Figure 4.22 : Analytical mode shape- mode3- 28.1 Hz .....	73
Figure 4.23 : Analytical mode shape- mode4- 58 Hz .....	74
Figure 4.24 : designable area of pedestal and platform .....	75
Figure 4.25 : Visual estimation results for optimizing the first mode after 30 iterations.....	77
Figure 4.26 : Visual estimation results for optimizing the first mode after 30 iterations.....	77
Figure 4.27 : Optimized design structure according to visual estimations for the first mode .....	78
Figure 4.28 : Optimized design structure according to visual estimations for the first mode .....	79
Figure 4.29 : Visual estimation results for optimizing the second mode after 26 iterations, first approach.....	80
Figure 4.30 : Visual estimation results for optimizing the second mode after 26 iterations, first approach.....	80
Figure 4.31 : Optimized design structure according to visual estimations for the first and second mode, first approach .....	81
Figure 4.32 : Optimized design structure according to visual estimations for the first and second mode, first approach .....	82
Figure 4.33 : Visual estimation results for optimizing the second mode after 26 iterations, second approach.....	83

Figure 4.34 : Visual estimation results for optimizing the second mode after 26 iterations, second approach .....	83
Figure 4.35 : Optimized design structure according to visual estimations for the first and second mode, second approach.....	84
Figure 4.36 : Optimized design structure according to visual estimations for the first and second mode, second approach.....	85
Figure 5.1 : graphical validation of FEA results .....	90

## List of Tables

Table 3.1 : Initial configurations in block diagram of FRF-analyzer VI (Chiat, 2008) .....	42
Table 3.2 : Front panel configurations of FRF-analyzer VI (Chiat, 2008) .....	44
Table 3.3 : Mode shapes versus ODS's .....	48
Table 4.1 : Modes obtained from Modal Testing .....	59
Table 4.2 : Modal parameter resulted from finite element modal analysis .....	72
Table 4.3 : Finite Element modal analysis results after optimization of the pedestal only .....	75
Table 4.4 : Modal properties of the optimized structure for the first mode .....	79
Table 4.5 : Modal properties of the optimized structure for the first and second mode, first approach .....	82
Table 4.6 : Modal properties of the optimized structure for the first and second mode, second approach .....	85
Table 5.1 : Comparison of obtained modal parameters with results from (Chiat, 2008) .....	87
Table 5.2 : comparison of FEA and EMA results by error method .....	91
Table 5.3 : Estimated changes of natural frequencies before and after the reinforcement for maximizing the first mode .....	92
Table 5.4 : Estimated changes of natural frequencies before and after the reinforcement for maximizing the second mode, first approach .....	93
Table 5.5 : Estimated changes of natural frequencies before and after the reinforcement for maximizing the second mode, second approach .....	94

## List of Symbols and Abbreviations

DOF	degree of freedom
MDOF	master degree of freedom
SDOF	single degree of freedom
EMA	experimental modal analysis
FEA	finite element analysis
FEM	finite element method
ODS	operating deflection shape
MP	mathematical programing
OC	optimality criteria
NLP	non-linear programing
GA	genetic algorithm
H/e	homogenization and evolutionary
CATO	constrained adaptive topology optimization
SDM	Structural Dynamics Modifications
SIMP	Solid Isotropic Material with Penalization
ESO	evolutionary structural optimization
BESO	Bi-directional Evolutionary Structural Optimization
OMD	Optimal Material Distribution



I-ECP	internal element connectivity parameterization
FRF	Frequency Response Function
FFT	Fast Fourier Transform
SIMO	single input multiple outputs
MIMO	multiple inputs multiple outputs
$\rho$	Density
RMS	root mean square
ADC	analog-digital converter
VI	virtual instrument
DAQ	data acquisition

# Chapter One

## 1 Introduction

Topology optimization is a novel method to minimize the vibration effects of the structure or machine, but yet there are not many works have been done in this area. In general, all vibration is a combination of both forced and resonant vibration. The sources of forced vibration are usually internally generated forces, ambient excitations, unbalances, and external loads. The role of resonant vibration is to amplify the vibration response of a machine or structure far beyond the design levels for static loading.

Modes (or resonances) are among the innate features of a structure and are defined by dynamic properties of the structure consisting of natural frequency, modal damping and mode shapes. Modes depend on material properties (mass, stiffness, and damping), geometrical properties, and boundary conditions; meaning, via changing the material properties, geometrical properties or the boundary conditions the modes will change.

Mode shape is the overall vibration shape of the structure at a natural frequency or resonance and it is divided into rigid and flexible modes. Rigid modes consist of three translational and three rotational modes. Fundamental flexible modes have names such as first bending, second bending, first torsion, etc. However, in the higher frequency, modes do not have names because of their complexity. Flexible modes are the cause of many vibration problems in case of acting excitation forces on the structure or system.

Modal Analysis is defined as a technique to extract the dynamic characteristics of a structure or a system (natural frequency, damping, and mode shapes). It should be noted that linear behaviour and time-invariant are the assumptions for modal analysis.

Real systems are Multiple Degree of Freedom (MDOF) and nonlinear. But for vibration analysis, the system is assumed as a superposition of single degree of freedom (SDOF) linear models.

Generally, there are two ways to obtain modal parameters, experimentally (EMA) and numerically (FEA). In this research, the numerical solutions were used in the form of finite element methods (FEM), and the experimental solution was done by modal testing method. Furthermore, an operating deflection shape (ODS) measurement was done to determine the vibration pattern of the structure under machine operating condition.

### **1.1 Experimental Modal Analysis (EMA)**

For the modal parameters of a structure or a machine to be recognized, Experimental Modal Analysis (EMA) can be seen as a very effective means. EMA has grown rapidly especially after the advent of digital FFT analysers in the early 1970's. Today, EMA is widely employed in identifying modal parameters due to its application speed and economical methods. Different methods of EMA are used nowadays; among them, the modal testing is one of the most popular ones. The modal testing is based on the excitation of the system, usually by an impact hammer, and it collects the structure or the machine responses.

### **1.2 Operating Deflection Shape (ODS) Measurement**

ODS measurement is a method used in structural vibration analysis to visualize the structure vibration pattern as influenced by its own operating forces. In the Operating Deflection Shape (ODS) measurement, data are collected from different points and directions of the structure or machine during its operation, and analysing

such collected data to identify the deflection shape which is mainly influenced by the structural dynamic properties. The vibration pattern can be shown as an animated geometry model of the structure or listed in a shape table.

### **1.3 Structural Optimization**

Structural optimization is about finding the best potential solution which can satisfy all the requirements imposed by functionality and manufacturing conditions. In other words, it is a rational establishment of a structure which is the best of all possible solutions within a prescribed objective and a set of constraints.

Structural optimization has a wide range of applications from automotive to aeronautics and naval. It is used in several fields of engineering such as civil, mechanical, nuclear, off-shore, etc. This wide range of applications makes it more and more interesting for so many scientists and engineers.

### **1.4 Problem Statement**

Previous works for dynamic modification are mainly done based on trial and error methods. Technically, these methods could not be proper ones as they are very time consuming, and also, in the most of cases they cannot lead to the optimized results. The topology optimization method is applied to reduce the time of achieving to the optimum design of a dynamically loaded structure.

Manufacturability is an industrial key for the optimized design. Usually, topology optimization results are complicated to be fabricated. Therefore, manufacturability of the new designed structure becomes very important within the optimization process. Later, by applying some conditions on designable area and optimization constraint, a simple design solution is obtained.

## **1.5 Objectives of the Study**

This thesis presents a structural dynamic modification of vibrating structures by using topology optimization method in order to find the optimum design of a structure supporting rotating machine. In the process to achieve this main objective, the following goals will be addressed:

- To ascertain the dynamic characteristics of a vibrating structure
- To determine the optimum design of the vibrating structure using topology optimization

## **1.6 Scope of the Study**

The scope of this research is based on the modal testing and operating deflection shape (ODS) measurement of a pedestal structure to determine its dynamic characteristics, namely natural frequencies, mode shapes and damping factor. Then, these data are employed to validate the Finite Element Model of the structure. Finally, the topology optimization is applied on account of this validated finite element model to predict the newly optimized structure based on the vibration and dynamic loading of the structure.

## **1.7 Organization of the Study**

In the context of this study, chapter 2 presents a comprehensive review on the structural optimization and topology optimization related to vibration. The proposed methodology in this research for the three main areas of this work, namely, experimental modal analysis (EMA), finite element modal analysis, and structural optimization which will be explained and discussed in chapter 3 in details. After that,

the results which were obtained in these three main areas are presented in chapter 4. Chapter 5 discusses the results from previous chapter. The concluding remarks of the study are summarized in the conclusion and recommendation chapter.

## **Chapter Two**

### **2 Literature Review**

#### **2.1 Structural Optimization, Types and Scopes**

Nowadays, due to the limitation in material resources, technological competition, environmental impact, etc. the need of efficient methodologies to design gaining more importance; which can consequently lead to high-performance, low cost and light weight structures. In the field of engineering, optimization plays a very significant role, because it seeks to find the best possible solution for engineering problems. In this perspective, structural optimization is defined as a tool to achieve maximum efficiency in a structure at the same time as removing different constraints, like the availability and the amount of the material(Huang & Xie, 2010).

The concept of an optimum design in an engineering problem is intriguing which has been under intensive investigation for decades. In the past, engineering design was based on the creativity and experience of the designer and the use of a trial and error process. The designer had to start with an early design rooted in his knowledge and experience. Then, according to the performance of the design, a new design was developed.

But today, engineering field aim at reducing the design time and cost while making products with high functionality and quality. Due to this reason and with the advent of high speed computers, the concept of engineering design has been changed. In recent decades, an evolution has been occurred due to the development of computer technology and it has changed the engineering design from using of a trial and error

process to scientific methods of rational design and optimization. This has already been accomplished through structural optimization.

### 2.1.1 Method and the Mathematical Approach of an Optimization Problem

The major influencing factors in a structural optimization design problem are to clearly define the objectives of the problem, the design variables and the constraints. A general structural optimization problem can be put forward as: “Minimize (or maximize) an objective function subject to behavioural and geometrical constraints.”

Among these constraints, behavioural constraints can be mentioned as the cost of material or manufacturing process; stress, strain or displacement structural responses at a local area or in the whole of the structure; the weight or the volume of a structure and the performance of the structure for stiffness, dynamic response, natural vibration frequency, etc.

Also, geometrical constraints can be mentioned as manufacturing limitations, availability of member sizes, fabrication and physical limitations.

Mathematically, searching for the minimum (or maximum) value of a function  $f(\mathbf{x})$  and the related variable vector,  $\mathbf{x} = (x_1, x_2 \dots x_n) \in \mathbf{R}^n$ ,  $\mathbf{R}^n$  is  $n$  dimensional space, which yields the optimal solution subject to some constraints is known as an optimization problem. Generally, the optimization problem could be expressed as (Haftka & Gürdal, 1992):

Minimize  $f(\mathbf{x})$

Such that  $h_j(\mathbf{x})=0$   $j=1, 2 \dots n_n$

$g_k(\mathbf{x})\leq 0$   $k=1, 2 \dots n_k$

In this case  $h_j$  and  $g_k$  are constraints; the number of equality and inequality of constraints will be  $j$  and  $k$ , respectively.



The sets of design variables which overcome all constraints constitute the feasible domain. The infeasible domain is the assortment of all design points that violates as a minimum one of the constraints. The optimization problem can be assumed to be linear when both equality constraints and inequality constraints and the objective function are linear functions of the design variables. The optimization problem is linear providing that both equality and inequality constraints and the objective function are linear functions of the design variables, and it is non-linear on the condition that either at least one of the constraints or the objective function is a non-linear function. From the engineering point of view, the objective function  $f(\mathbf{x})$  is usually chosen as the structural volume, weight, cost, performance, serviceability or their combination. Structural optimization problems are usually non-linear optimization problems (Chu, 1997).

### **2.1.2 Classifications of Structural Optimization**

For the design variables to be optimized, the structural optimization in engineering field is classified into three types: size, shape and topology.

#### **2.1.2.1 Size Optimization**

In this type of optimization, the domain of the structure is fixed. Additionally, design variables can be continuous or discrete. Size optimization can usually be considered as the implementation of optimization at detailed design stage. Discovering the optimal design by adjusting the size parameters can be considered as the objective of size optimization. For example, finding the optimal thickness distribution of a plate or the cross-sectional dimensions in truss structures or frames can be the objective of size optimization problem. The optimal thickness distribution minimizes (or maximizes) a physical quantity such as the mean compliance (external work), peak stress, deflection, etc. by maintaining equilibrium and other constraints on the state and design variables

are satisfied. The thickness of the plate is the design variable and the deflection of the plate will be the state variable. It also should be mentioned that size optimization is the earliest and easiest type of approach to optimization (Bendsøe & Sigmund, 2003; Huang & Xie, 2010).

#### **2.1.2.2 Shape Optimization**

This type of optimization problems requires the topology to be fixed while the domain is not. In most cases, shape optimization is employed to select the optimum shape of external boundary surfaces or curves. Finding the optimal values for parameters which define the middle surface of a shell structure and finding the boundaries of a structure or locations of joints of a skeletal structure are some examples of shape optimization. Generally, the implementation of this optimization technique is performed at the preliminary design stage. Additionally, it is also used in the aerospace and the automotive industry and in the design of electromechanical, electromagnetic and acoustic devices (Huang & Xie, 2010).

#### **2.1.2.3 Topology Optimization**

In some cases, size and shape optimization methods may be resulted to sub-optimal shapes. Hence, topology optimization can be performed to get over this shortage. In fact, topology optimization can be regarded as discovering of the layout of a structure which is optimum within a defined design domain. It seeks to determine characteristics of the model like the location, number and the connectivity of the domain and the shape of holes. Unlike the shape or size optimization method, the initial design domain in topology optimization is a grand or universal structure, such as a rectangular plate, in some two dimensional design problems. In a typical topology optimization

problem, the recognized parameters are the support conditions, applied loads, structure volume and numerous other additional design restrictions defined by the designer. Besides, the unknowns of the problem would be the physical shape, size and connectivity of the structure. Standard parametric functions do not represent the topology, size, and the shape of the structure. They, however, are represented by a set of distributed functions which are defined over the fixed design domain. These functions in turn represent a parameterization of the stiffness tensor of the continuum and a suitable choice of this parameterization, which would lead to the proper design formulation for topology optimization (Bendsøe & Sigmund, 2003). It also should be mentioned that among different versions of structural optimization, the most challenging one is topology optimization.

Figure 2.1 shows three different classifications of structural optimization.

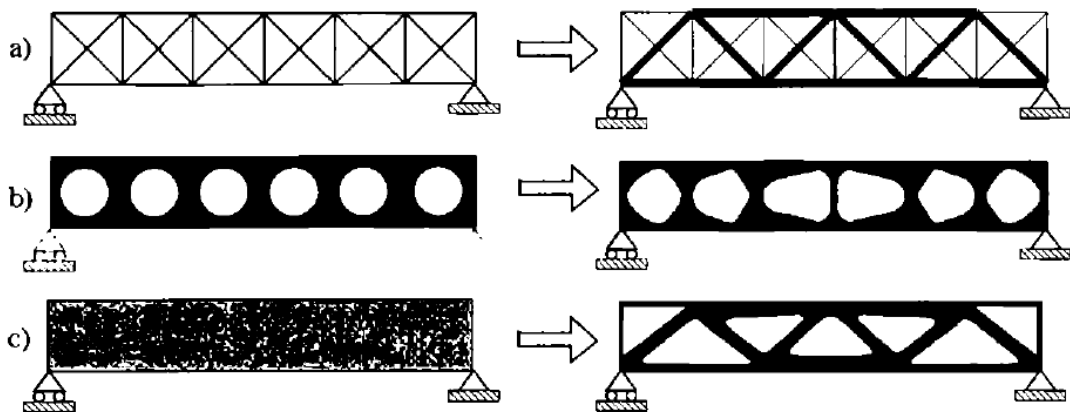


Figure 2.1 : Three different kinds of structural optimization of a truss structure a) Sizing optimization, b) shape optimization c) topology optimization (Bendsøe & Sigmund, 2003)

### 2.1.3 Solution Methods for Structural Optimization

Various approaches for resolving the issue of the structural optimization can be categorized into classical calculus methods and numerical methods.

### 2.1.3.1 Calculus Methods

In the 17th century, the differential calculus was initially introduced into optimization problem. Maxwell (Maxwell, 1895) was the first to use the calculus methods to structural design when he designed the least weight layout of frameworks. The later research on the optimal topology of trusses by Michell (Michell, 1904) led to the renowned Michell type structures. The typical calculus methods are differential calculus and calculus of variations.

#### Differential Calculus

The method of differential calculus holds that the conditions for the existence of extreme values are the first order partial derivatives of the objective function regarding the design variable to be zero.

The formula of differential calculus is as follows:

$$\nabla F(x_i) = 0 \quad , \quad i=1, 2 \dots n \quad 2.1$$

where the vector  $\mathbf{X} = \{x_1, x_2 \dots x_n\}$  is the extreme points.

The differential calculus generally can only be applied to very straightforward cases such as unconstrained optimization problems.

#### Calculus of Variations

Calculus of variations is a generalization of the differentiation theory. It deals with optimization problems having an objective function  $F$  expressed as a definite integral of a functional  $Q$ ,  $Q$  which is defined by an unknown function  $y$  and some of its derivatives (Haftka & Gürdal, 1992) :

$$F = \int_a^b Q(x, y, \frac{dy}{dx}, \dots, \frac{d^ny}{d^nx}) dx \quad 2.2$$

where  $y=y(x)$  is directly related to the design variable  $x$ . Optimization is to find the form of function  $y=y(x)$  instead of individual extreme values of design variables.

The necessary condition for an extremum is the first order of variation that equals to zero.

$$\delta F = \int_a^b \left( \frac{\partial Q}{\partial y} \delta y + \frac{\partial Q}{\partial \dot{y}} \delta \dot{y} + \dots \right) dx = 0 \quad 2.3$$

where  $\dot{y} = \frac{dy}{dx}$

Taking into account the boundary conditions at fixed  $y(a)$  and  $y(b)$  (Haftka & Gürdal, 1992), Equation (2.4) can be expressed as

$$\frac{\partial Q}{\partial y} - \frac{d}{dx} \left( \frac{\partial Q}{\partial \dot{y}} \right) = 0 \quad 2.4$$

This is the well-known Euler-Lagrange equation.

Even though the application of this method is fairly restricted, it has been a crucial stage in the development of optimization methods. This method has also the fundamental significance in exploring the mathematical nature of optimization and also in providing the lower bound optimum against which the results by alternative methods can be checked (Haftka & Gürdal, 1992).

### 2.1.3.2 Numerical Methods

Generally, structural optimization problems are highly non-linear and due to this fact, employing numerical methods can be considered fundamental for designing real structures.

The numerical methods of structural optimization can be classified into three categories:

- Direct minimization techniques (e.g. mathematical programming, MP)
- Indirect methods (e.g. optimality criteria, OC)
- Genetic Algorithms method

#### **Mathematical Programming (MP)**

One of the most well-liked optimum search techniques formulated in 1950s was Mathematical programming (MP) (Heyman, 1951). MP is a stage-by-stage search approach concerning iterative processes and every iteration has two main steps:

a) Differentiating the value the objective function is assigned to and its gradients considering all design variables,

b) Calculation of a change of the design variable that would result in a reduction of the objective function.

Steps a) and b) needs to be recurred until a local minimum of the objective function is reached.

In the early days, the mathematical programming method was solely restricted to linear problems where the constraints and objective functions happen to be linear functions of design variables. Since 1960, many algorithms of nonlinear programming techniques have been developed such as nonlinear programming (NLP) (Schmit, 1960), feasible direction (Zoutendijk, 1960), gradient projection (Rosen, 1961) and penalty function method (Fiacco & McCormick, 1968). Simultaneously, approximation techniques which employ the standard linear programming to address nonlinear problems (Arora, 1993) have been studied, such as sequential linear programming.

One of the main advantages of MP methods is that MP methods are able to be employed in most problems of structural optimization field. On the other hand, the main disadvantage of MP methods is that as the number of design variables and constraints increases, the cost of computing derivatives becomes expensive.

### **Optimality Criteria**

Optimality criteria are the necessary conditions for minimality of the objective function and these can be derived by either using variational methods or extremum principles of mechanics. Optimality criteria (OC) method was analytically formulated by Prager and his co-workers in 1960s (Prager & Taylor, 1968; Prager & Shield, 1968).

It was later developed numerically and became a widely accepted structural optimization method (Venkayya, Khot, & Reddy, 1968).

OC methods can be divided into two types. One type is rigorous mathematical statements such as the Kuhn-Tucker conditions. The other is algorithms used to resize the structure for satisfying the optimality criterion. Different optimization problems require different forms of the optimality criterion.

In Kuhn-Tucker conditions (Haftka & Gürdal, 1992), by adding slack variables, the inequality constraints can be changed into equality constraints. In this case, the inequality constraints in Equation (2.1) can be written as

$$g_k(\mathbf{x}) + t_k^2 = 0, \quad k = 1, 2, 3, \dots, n_g \quad 2.5$$

$t_k^2$  is slack variables

The definition of the Lagrangian function of the optimization can be put forward as:

$$L(\mathbf{x}, t, \lambda, \xi) = f(\mathbf{x}) + \sum_{j=1}^{n_h} \xi_j h_j(\mathbf{x}) + \sum_{k=1}^{n_g} \lambda_k (g_k(\mathbf{x}) + t_k^2) \quad 2.6$$

where  $\xi_j$  and  $\lambda_k$  are Lagrangian multipliers.

Differentiating the Lagrangian function (2.7) with respect to  $\mathbf{x}$ ,  $t$ ,  $\lambda$ , and  $\xi_i$  we obtain

$$\frac{\partial L}{\partial x_i} = \frac{\partial f}{\partial x_i} + \sum_{j=1}^{n_h} \xi_j \frac{\partial h_j(\mathbf{x})}{\partial x_i} + \sum_{k=1}^{n_g} \lambda_k \frac{\partial g_k(\mathbf{x})}{\partial x_i} = 0, \quad i = 1, 2, \dots, n \quad 2.7$$

$$\frac{\partial L}{\partial \xi_j} = h_j = 0 \quad j = 1, 2, \dots, n_h$$

$$\frac{\partial L}{\partial \lambda_k} = g_k + t_k^2 = 0 \quad k = 1, 2, \dots, n_g$$

$$\frac{\partial L}{\partial t_k} = 2\lambda_k t_k = 0 \quad k = 1, 2, \dots, n_g$$

From (2.10) and (2.11) we can get

$$g_k(\mathbf{x}) \leq 0, \quad k = 1, 2, \dots, n_g$$

$$\lambda_k g_k = 0, \quad k = 1, 2, \dots, n_g$$

This implies that when an inequality constraint is not active, the Lagrangian multiplier associated with the constraint is zero.

By using Kuhn-Tucker conditions, the optimality conditions for the problem of optimization can be expressed as:

$$\frac{\partial L}{\partial x_i} = \frac{\partial f}{\partial x_i} + \sum_{j=1}^{n_h} \xi_j \frac{\partial h_j(x)}{\partial x_i} + \sum_{k=1}^{n_g} \lambda_k \frac{\partial g_k(x)}{\partial x_i} = 0, \quad i = 1, 2, \dots, n \quad 2.8$$

$$\frac{\partial L}{\partial \xi_j} = h_j = 0 \quad j = 1, 2, \dots, n_h$$

$$g_k(x) \leq 0, \quad k = 1, 2, \dots, n_g$$

$$\lambda_k g_k = 0, \quad k = 1, 2, \dots, n_g$$

$$\lambda_k \geq 0, \quad k = 1, 2, \dots, n_g$$

The optimal criteria method is one of the best-established and widely accepted optimization techniques.

As dual methods search the optimum direction in the space of Lagrangian multipliers, instead of the initial design variables, it can save considerable computing efforts when the constraints value is smaller than that of the design variables (Fleury, 1979).

### **Genetic Algorithms**

Genetic Algorithms (GA) were first developed in the 1970s (Holland, 1975). The GA method employs genetic processes of reproduction, crossover and mutation. The procedures of GA can be described as follows:

- a) Creating an initial population of designs randomly
- b) Evaluating the fitness of each individual according to a fitness function.
- c) Reproducing the fittest members and allowing the fittest members to cross among themselves



d) Developing a new generation with member having higher degree of desirable characteristics than the parent generation

e) Repeating the procedure until reaching a near optimum solution

Although the GA method may not yet be as popular as MP or OC method, this method has merits of being reliable and robust (Haftka & Gürdal, 1992; Nagendra, Haftka, & Giirdal, 1993).

## **2.2 Structural Topological Optimization**

Considering the numerical methods in structural optimization design, the research begins with element stiffness design through shape and geometric, and then moves to topology optimization design. Similarly, at the conceptual stage, a main impact on the structural efficiency is carried out by the topology and the structure shape. This normally is the case in the sense of stress/volume or stiffness/volume ratio. If there exists an error in the topology or the structural shape, any amount of cross-sections and fine-tuning will not compensate for this (Olhoff, Bendsoe, & Rasmussen, 1991).

With the development of high-speed computers, the topology optimization method using numerical approach has been growing quickly (Haftka & Grandhi, 1986; Kirsch, 1989; Rozvany, 1995). In the first attempt in performing numerical approaches, a domain of material was used and boundary conditions and external loads were applied to this domain. Afterwards, the optimization algorithm proceeds with removing the ineffectual material to get the best structural optimization. In most cases, the objective function for topology optimization problems is often the compliance (Taylor, 1977).

Generally, structural topology optimization could be considered as a material distribution problem. Topology optimization can be divided into two classes; for discrete and continuous structures. Early solutions for topology optimization of discrete structures were put forward by Don et al. (Dorn, Gomory, & Greenberg, 1964); Dobbs

and Felton (Dobbs & Felton, 1969). Afterwards, instances of applying the concept to large-scale structures have been given by Zhou and Rozvany (Zhou & Rozvany, 1991). The continuum is normally separated into suitable finite elements. Each element carries intrinsic structural features. They are reviewed in the following sections.

### **2.2.1 Topology optimization for Discrete Structures**

Topology optimization for discrete structures has mainly been employed for structures like trusses and frames. Its core concept is figuring out the optimal number, mutual connectivity and position of the structural members. In other word, it can be seen as exploring the optimal connectivity and spatial order of the bars.

Based on the survey by Topping (Bendsøe & Mota Soares, 1993), topology optimization method for discrete structures can be categorized into three classes:

- a) Geometric approach
- b) Hybrid approach
- c) Ground structure approach

#### **2.2.1.1 Geometric Approach**

In the geometric approach, the design variables are the properties of cross-section and the coordinates of joints. While the optimization process is in progress, the number of connecting members and joints are fixed as some joints are allowed to coalesce.

#### **2.2.1.2 Hybrid Approach**

In the hybrid approach, the design variables are divided into size design variables and geometrical design variables and are separated in the design space. While the optimization process is in progress, firstly, the element size is changed while the

topology is kept unchanged; after that, the searching begins for the optimum position of the element nodes.

### **2.2.1.3 Ground Structure Approach**

In this method, a ground structure is considered as a dense group of nodes and a number of potential connections between the nodes. While the optimization process is in progress, the size and the number of connecting elements are altered, however, the position and the number of nodes are kept intact. If the section area of elements is decreased to zero during the optimization process, the elements are deemed as non-existent and the topology is changed accordingly.

A notable advantage of the ground structure approach method is that the design domain is fixed thus the problem of mesh regeneration can be evaded.

## **2.2.2 Topology Optimization for Continuous Structures**

Continuum topology optimization seeks to determine the inner holes and also the internal and external boundaries (Bendsøe & Sigmund, 2003; Huang & Xie, 2010; Krog & Olhoff, 1999), or as it came in reference (Huang & Xie, 2010), topology optimization of continuum structures will determine the optimal designs through indicating the best geometries and cavity locations in the design domain.

It also should be mentioned that whilst the shape and size structural optimization still have applications in various industries, but technically and economically aspects have made the topology optimization of continuum structures the most common approach. It is due to the freedom of creating entirely efficient and new conceptual designs that topology optimization of continuous structures makes in comparison to the shape and size structural optimization. It also should be added that this technique has a

wide range of applications, from large-scale structures such as buildings and bridges to micro and nano-levels (Huang & Xie, 2010).

As it was mentioned earlier, numerical methods have a vast usage in topology optimization especially for topology optimization of continuum structures. The first work published in this area was by Bendsoe and Kikuchi in 1989 (Bendsøe & Kikuchi, 1989). Numerical methods mostly have its grounds in Finite Element Analysis (FEA) that discrete the design domain into a fine mesh element. In such situation, finding the topology of the structure by identifying each single point in the design domain and whether there should be material (solid element) or not (void element) could be seen as the optimization procedure.

According to the survey by Topping (Bendsøe & Mota Soares, 1993), topology optimization method for continuum structures could be categorized into four classes as mentioned as follow.

#### **2.2.2.1 Heuristic Methods**

Heuristic methods are those addressing structural optimization problems in a less mathematical but more intuitive way. Instead of complex mathematical formulation, the heuristic methods are based on simple concepts or natural laws.

#### **2.2.2.2 Evolutionary Structural Optimization Method (ESO)**

The evolutionary structural method was initially put forward by Xie and Steven (Xie & Steven, 1993; Xie & Steven, 1994). This method has its grounds in the notion of removing the inefficient material from the structure slowly and/or moving the material from the strongest to the weakest part of the structure gradually until the desired optimum is achieved. The ESO approach offers a simple way to obtain optimum

designs using standard finite element analysis codes. Compared to other structural optimization methods, the ESO approach is overwhelmingly interesting because of its effectiveness and ease of use. During the last ten years, the capability of ESO to solve numerous problems of shape, size and topology optimum designs for static and dynamic problems has been proven in many instances (Rong, Xie, Yang, & Liang, 2001).

### **2.2.2.3 Homogenization Method**

Compared to the Heuristic and ESO methods, the homogenization method is more complex. This method is based on the mathematical theory of homogenization. This theory was developed in the 1970's (Babuska, 1976; Cioranescu & Paulin, 1979). The homogenization method can be employed to discover the helpful features of the equivalent homogenized material and are applicable to numerous areas of engineering and physics. Since being firstly proposed for topology optimization in 1988 by Bendsøe and Kikuchi (Bendsøe & Kikuchi, 1988), homogenization method has attracted many researchers and design engineers. It has been used by industrial companies around the world for product development, particularly in the automobile industry.

The homogenization approach has successfully been followed both in static and dynamic problems with weighted constraints (Ma, Kikuchi, & Cheng, 1995; Tenek & Hagiwara, 1993). With regard to the algorithm aspect, the homogenization method uses traditional mathematical programming or optimality criteria as search techniques. The advantages of homogenization method are precise theoretical basis and good convergence behaviour. On the other hand, the disadvantage of homogenization method is that difficulties associated with those traditional methods are magnified in the homogenization method.

#### **2.2.2.4 H/e-method**

The h/e-method is a hybrid method. It is an abbreviation of the combination of homogenization and evolutionary methods in various degrees. Bulman, Sienz and Hinton (Bulman, Sienz, & Hinton, 2001) developed the constrained adaptive topology optimization (CATO) algorithm, combined of two methods: the homogenization method which is mathematically more rigorous and also the evolutionary method which is more intuitive. Through a set of benchmarks, they systematically investigated the performance of the algorithm for topology optimization. The results of the study show that in general cases, the h/e CATO algorithms was very well comparable with the homogenization method.

### **2.3 Topology Optimization Related to Vibration Problem**

This section will explain the topology optimization related to vibration problems as an application and category of structural optimization.

Improving the dynamic behaviour of a structure is very essential. For example, minimizing the noise and vibration when the loading condition is known is a very important consideration in a car body design. In this case and similar cases like this, it is to treat the dynamic behaviour of the system as an object of the optimization process, not as a constraint (Ma, Cheng, & Kikuchi, 1994).

On the other hand, one of the most challenging and difficult parts of applying the topology optimization method is to develop sensible combinations of objective functions and constraints. In the design of dynamic systems, For example, structural vibration control is particularly a central consideration. On the other hand, the main idea of the structural optimization is to obtain an optimal material layout of a load bearing structure. But traditionally, these two have been considered independently, the structural designers develops their designs according to stiffness and strength necessities and the

control designers constructs the control algorithm in order to decrease the dynamic response of a structure (Kang, Wang, & Wang, 2009; Ou & Kikuchi, 1996). Here, the means of “topology optimization related to vibration problem” is a simultaneously consideration of structural vibration control and structural optimization.

Generally, topology optimization related vibration problems follows some aims in concept. The first aim is that, it intends the specified structural eigenvalues to reach a maximum. The second one is that, it aims at maximizing the distances of the specified structural eigenfrequencies from a given frequency. The third aim is to optimize a structure for the purpose of obtaining prescribed desired eigenfrequencies (Ma et al., 1994). On the other hand, topology optimization for vibration problems can be categorized in two main categories; with respect to free vibration and with respect to forced vibration.

Eigenvalue optimization for free vibrations can be considered as one of the initial applications of topology optimization method. This problem is important for the design of structures and machines which are dependent on dynamic load. For example, one may wish to maintain the eigenfrequencies of a structure away from the driving frequency of an attached engine or one may wish to keep the fundamental eigenfrequencies well above possible disturbance frequencies. Also, structures with high fundamental eigenfrequency are inclined to be reasonably stiff for all conceivable loads and therefore maximization of the fundamental frequency results in designs that are also good for static loads (Bendsøe & Sigmund, 2003).

There are some important considerations involving Structural Dynamics Modifications (SDM) and topology optimization related to vibration problem. Structural dynamics modification (SDM) is extensively employed to alter mode shapes and/or natural frequencies through the addition or the elimination of auxiliary members in order to improve the dynamic response of a target structure. The differences of SDM

and topology for vibration problems can be summarized in two general factors. The first one is that the application of SDM is modifying the existing structures for the next generation design cycle. The second one is that SDM is used as a tool to remove the non-smoothness of eigenvalues (Jung, Park, & Park, 2005).

As it has been mentioned in the previous parts, the main objective of the topology optimization problem is to discover a material distribution which minimizes a given objective functional, subjected to a set of constraints, achieved by a consistent parameterization of the material properties in each part of the design domain. A natural question is whether there exists or not material in a given point, which leads to a discrete problem. It is well-known that this integer parameterization leads to numerical difficulties, associated with the integer problem convergence (Bendsøe & Kikuchi, 1988; Bendsøe & Sigmund, 1999; Cardoso & Fonseca, 2003). Minimizing the vibration effects of the dynamic response is an important goal for the structural vibration control, and the effectiveness of the control depends on the weighting matrices (Molter, Fonseca, Bottega, & Silveira, 2010).

There are two main numerical methods of topology optimization that are being used in practical applications nowadays, including the Solid Isotropic Material with Penalization (SIMP) method and Evolutionary Structural Optimization (ESO) method. Bendsøe (1989) put forward the original idea of SIMP. ESO is the abbreviation for “Evolutionary Structural Optimization”. ESO is a design method which has its roots in the notion of eliminating inefficient material gradually from a structure. Bi-directional Evolutionary Structural Optimization (BESO) is a new algorithm which has its grounds in the improvement of ESO method (Huang & Xie, 2010).

Taking another perspective, structural optimization could be considered in two main categories: one that is considering materials in level of macroscopic design and the other in micromechanics subject. In macroscopic design, a macroscopic definition of



geometry is given by, for example, thicknesses or boundaries considered. On the other hand, micromechanics are about studying the relation between microstructure and the macroscopic behaviour of a composite material.

Since the focus of this project is related to the macroscopic structures, in the following part, some of the works and researches in the area of structural optimization with respect to vibration for macroscopic structures will be reviewed from the earliest papers published in.

The first work in this scope has been done by Dias and Kikuchi in 1992 (Dias & Kikuchi, 1992). They considered topology optimization with reference to eigenfrequencies of structural vibration. The concept of their work was maximizing a natural frequency of a structure and presenting a strategy to discover its topology and shape. The method they used is homogenization method that was applied for a two dimensional, plane elasticity problem for a disk in which through a prescribed of material, an offered structure is reinforced.

Ma et al. (Ma et al., 1994) defined a mean eigenvalue equivalent to the multiple eigenvalues of a structure, and then according to the notion of Optimal Material Distribution (OMD), three types of optimization problems was considered for arriving at the desired eigenvalues. They obtained desired eigenvalues for maximization of the particular structural eigenvalues, the amplification of the distances of the specified structural eigenvalues from a given frequency, and the optimization of the structure to achieve prescribed eigenvalues.

Zhao et al. (Zhao, Steven, & Xie, 1998) propose a method to resolve the natural frequency optimization of membrane vibration by using of evolutionary method according to the finite element method and evolutionary standard. Founded on the general finite element formulation along with the energy conservation principle of structural eigenvalue problem, they defined a contribution factor of an element for a

discretized system. From a physical point of view, the contribution factor of an element entails that an element has contributed directly to the natural frequency of the structure. As an instance, they applied their method on a square membrane with four sides fixed.

Generally vibration optimization amounts to the optimization of eigenvalues in free vibration problems. But there are some works that are done for optimization of structures which are subject to periodic loading. Jog (Jog, 2002) has done a work for the minimization of vibrations of structures which were subjected to periodic loading with respect to two kinds of measures, one global and the other local. Means of Global measures was to reduce the vibration in an overall sense. It can be termed as “dynamic compliance”, and thus, it has important implications for the noise reduction of a structure. Means of Local measures is the reduction of the vibration at a local point. The aim here is to minimize the frequency response amplitude at a given point in the structure, although it might increase the amplitudes at other points in the structure. Both measures are based on reducing the vibration level by moving the natural frequencies and the driving frequencies away from one another. By presenting some numerical examples, it turned out that the structure of dynamic compliance optimization problem is very similar to the structure of the static compliance optimization problem.

Jensen et al. (Jensen & Pedersen, 2006) worked on structures with two material components . They used finite element analysis and material distribution method of topology optimization to maximize dividing of two nearby eigenvalues in structures. They used two different formulations to maximize the separation of the eigenvalues. In the formulation that was out forward firstly, the objective of the optimization was considered as the maximum difference in the frequencies. The second formulation is maximizing the ratios of two adjacent eigenvalues. The methods are considered for optimal design of 1D and 2D structures.

An integrated design procedure was introduced by Molter et al. (Molter, Fonseca, Bottega, Otávio, & Silveira, 2010) for topology optimization and structural control system. In his work, a structural topology optimization methodology derived from the notion of optimizing the material density distribution is presented for a cantilever beam, which includes an optimal control design for vibrations reduction. The concept of this work is to design the structure and controls simultaneously, meanings that the cost function includes not only the strain energy, but also the control energy. A continuum finite element modelling is applied to simulate the dynamic characteristics of the structure and the modal basis is used to derive an optimal control.

Whilst the nature of dynamic problems is non-linear, for simplicity, dynamic problems are usually solved using of linear methods. Yoon (Yoon, 2010) used topology optimization rooted in the internal element connectivity parameterization (I-ECP) for non-linear dynamic problems. The I-ECP method has more advantages to solve non-linear problems because it uses topology optimization method to solve non-linear dynamic problems. Such methods are based on standard density and they are influenced by element instability, numerical difficulties, and localized vibration modes. However, the I-ECP method avoids element instability and a new patch mass model in the I-ECP formulation is offered for controlling the problem of localized vibration modes.

All the works have been reviewed here were based on using topology optimization for solving the vibration problems. However, since all these works were done for the design stage, the manufacturability was not a condition of their work. In the present work, one of the most important conditions of the work was the manufacturability of the new structure to be appropriate for the industry.

## **Chapter Three**

### **3 Methodology**

The following chapter describes the methods used in this research. Here, three separate studies are conducted and the results of each part are used for the rest of the research. At first, an experimental modal analysis and an ODS measurement are conducted on the structure, and the results are used to validate the finite-element model. Optimization is then done based on this finite-element model to optimize the assumed structure.

The methods employed in these parts are described in the next section.

#### **3.1 Experimental Modal Analysis (EMA)**

The Experimental Modal Analysis (EMA) aims at identifying the dynamic properties of a structure. These properties are derived usually from acquired time domain signals. They can also be derived by using the frequency functions that are computed based on time domain signals. A multi-channel FFT (Fast Fourier Transform) analyser is often utilized to collect these signals and to measure the vibration response of a structure in multiple points and directions (DOFs). The vibration signals are amplified, digitized and stored in the analyser's for further post-processing. After that, the modal parameters can be calculated from these signals. Experimental modal data are also called modal testing.

Modal data of a structure consists of natural frequencies, damping factor and mode shapes. These data can be measured experimentally from Frequency Response Function (FRF) data between one or more reference positions, called Degree of Freedom (DOF). Each DOF has a direction and a point. To perform an accurate EMA, sufficient numbers of DOFs are needed.

Modal Testing is a four-step process to extract the modal parameters. It consists of vibration sensors, time domain data acquisition, measuring FRFs by performing FFT analysis on the collected time domain signals, and curve fitting the data and extracting the modal parameters. These steps are shown in Figure 3.1. It should be stressed that, while real structures possess an infinite number of DOFs (and therefore an infinite number of modes), however, it would be sufficient to accurately assess the modes of the structure by collecting a small subset of FRFs.

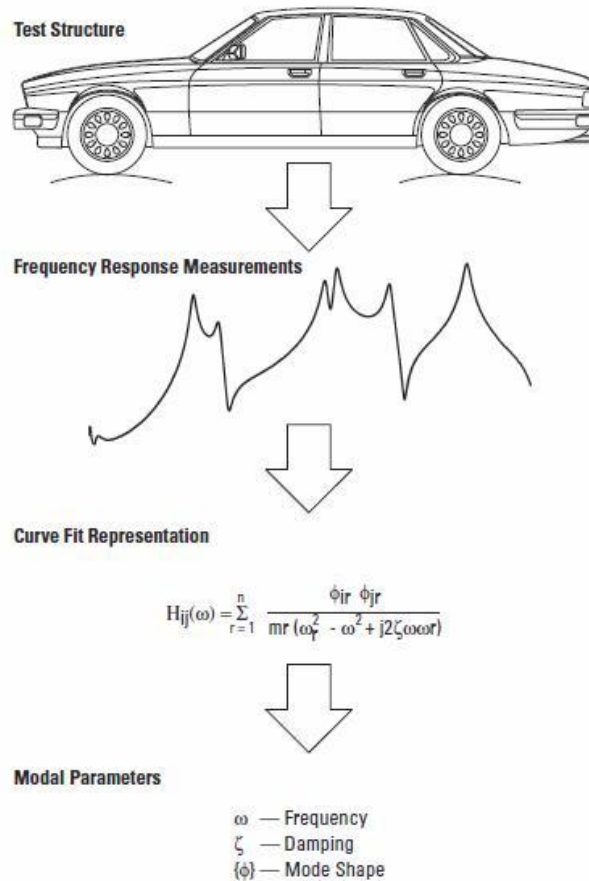


Figure 3.1: Modal Testing major phases (Agilent, 2008)

As shown in Figure 3.2, in order to perform a modal test, we must identify the elements of the FRF matrix;

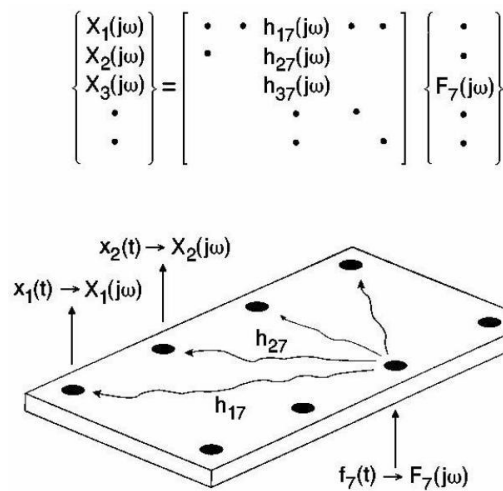


Figure 3.2: Measurement FRFs on a structure(Schwarz & Richardson, 1999)

Modal testing is normally done within a controlled condition. Between input and outputs, a multi-channel FFT analyzer is used to do the FRF measurement and the structure is also artificially excited. There are several ways to excite the structure but the most common are impact testing and shaker testing. In impact testing, output is fixed and FRFs are measured from multiple inputs. Elements are measured from a single row of the FRF matrix. In shaker testing, the input is fixed and the FRFs are measured by using multiple outputs. Elements are thus measured using a single column of the FRF matrix. Alternatively, modal testing can be done as single reference (SIMO) testing, or multiple references (MIMO) testing (Schwarz & Richardson, 1999). The mostly utilized method of modal testing is SIMO which is done by using either a single fixed input or a single fixed output. Meanwhile, two or more fixed inputs (or outputs) are used in MIMO testing and as a result, the FRFs are calculated between each input (or output) and also multiple outputs (or inputs).

### 3.1.1 FRF Measurements

FRF measurements describe the input-output relationship, as a function of frequency, between two points on a structure, a single input DOF and a single output DOF. As shown in Figure 3.3, FRF can be described to be the ratio of the Fourier

transform of an output response ( $X(\omega)$ ) divided by the Fourier transform of the input force ( $F(\omega)$ ) that caused the output (Schwarz & Richardson, 1999).

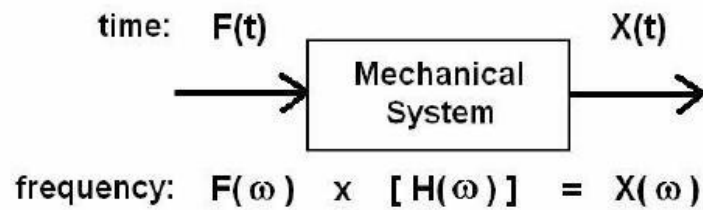


Figure 3.3 : Block diagram of an FRF (Schwarz & Richardson, 1999)

Since FRF is a complex valued function of frequency, there are several formats available to display the results. These include Nyquist, Bode, and Nichols. The most common format is Co-quad which shows the real and imaginary parts of the FRF. These formats are shown in Figure 3.4.

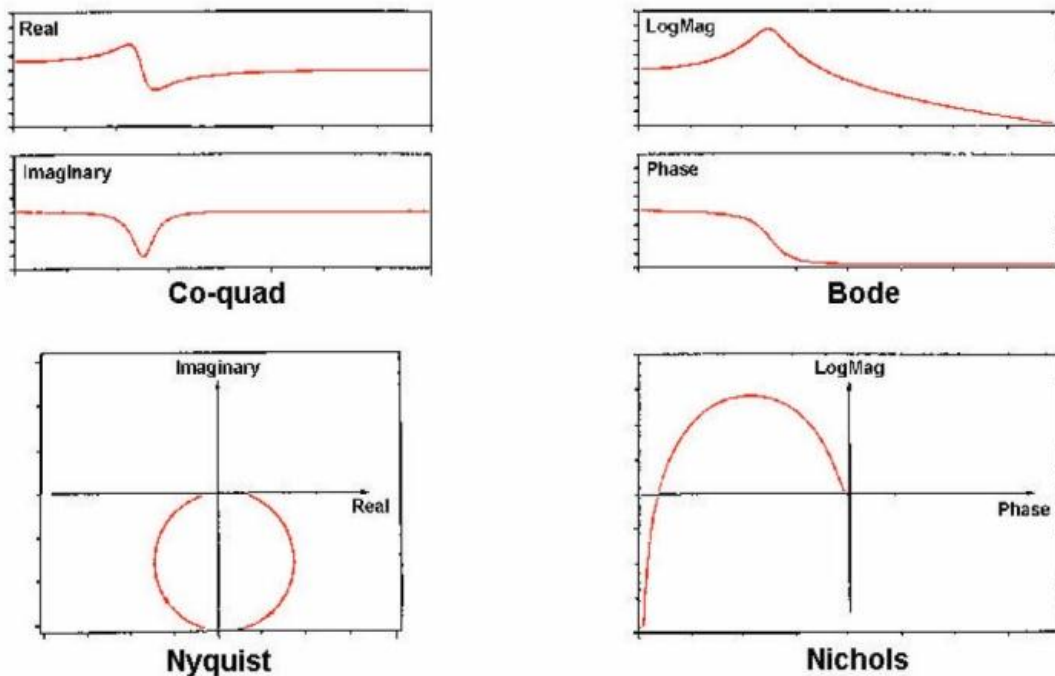


Figure 3.4 : Alternate formats of the FRF (Schwarz & Richardson, 1999)

FRF function, as shown in Figure 3.5, is the rundown of results due to each of its modes. In other words, FRF function at any frequency can show the modes (resonances) of the structure.

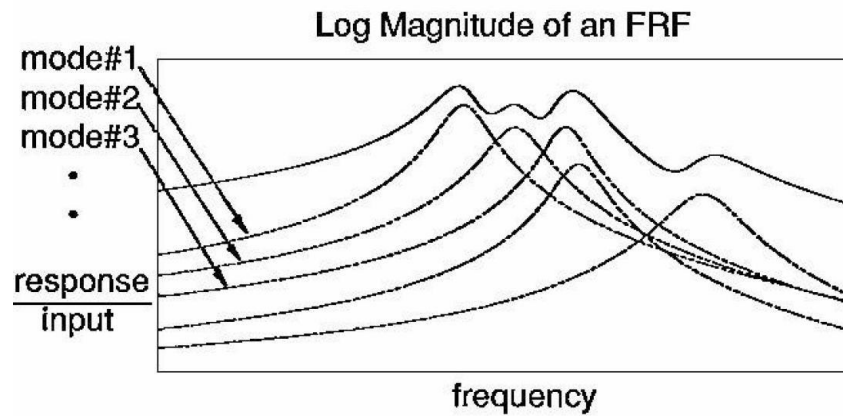


Figure 3.5 : FRF response as a summation of Modal responses (Schwarz & Richardson, 1999)

### 3.1.2 Curve Fitting

After collecting FRF data, by curve fitting a set of FRFs, one can identify the modal parameters. Curve fitting is generally a process in which a mathematical expression is matched to a set of empirical data points. This can be achieved through lessening the squared error (or squared difference) between the measured data and the analytical function. According to the complexity of the methods, curve fitting methods can be categorized as Local SDOF, Local MDOF, Global, and Multi-reference. A curve fitting example is depicted in Figure 3.6 (Schwarz & Richardson, 1999).



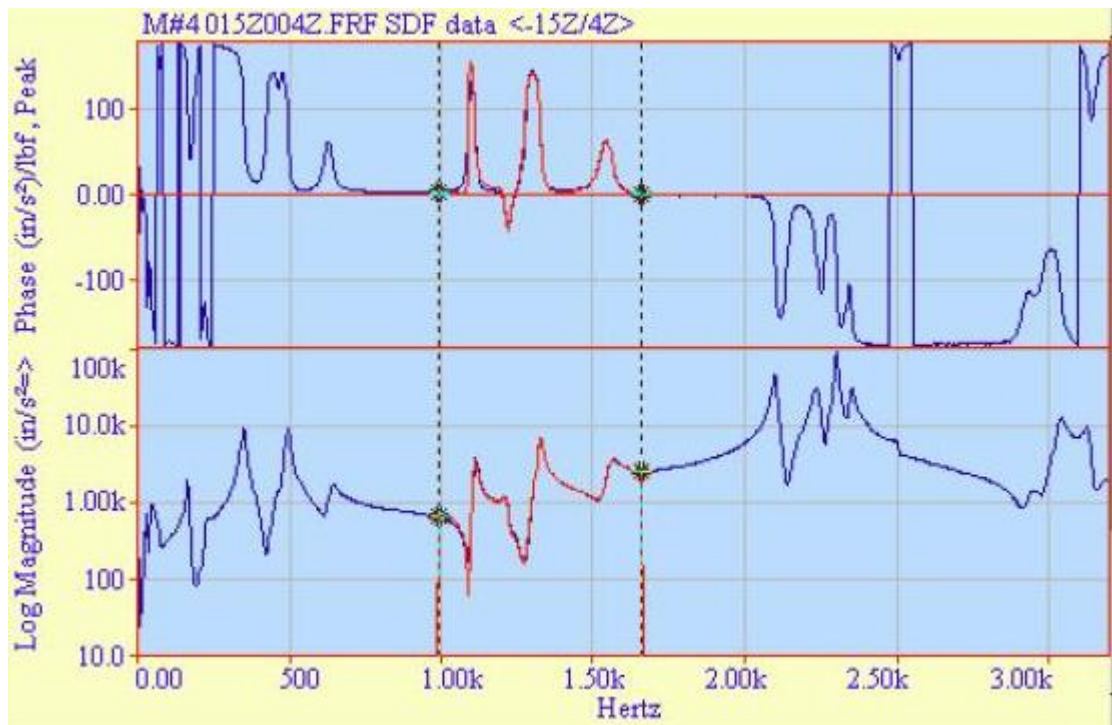


Figure 3.6 : A curve fitting example (Schwarz & Richardson, 1999)

In this research, along with various other types of modal testing, impact hammer testing was used. For this testing method, an impact hammer, an accelerometer, a 2 or 4 channel FFT analyser and post-processing modal software are needed. This test can be done in 2 ways, roving the hammer or roving tri-axial accelerometer. Here, a roving tri-axial accelerometer test was used because by applying this test, 3D motion of all DOFs can be obtained. For this test, we have impacted the structure at a fixed DOF. Also, a 4-channel analyser is used because the tri-axial accelerometer must be simultaneously sampled together with the force data. In Figure 3.7, a normal impact test is shown;

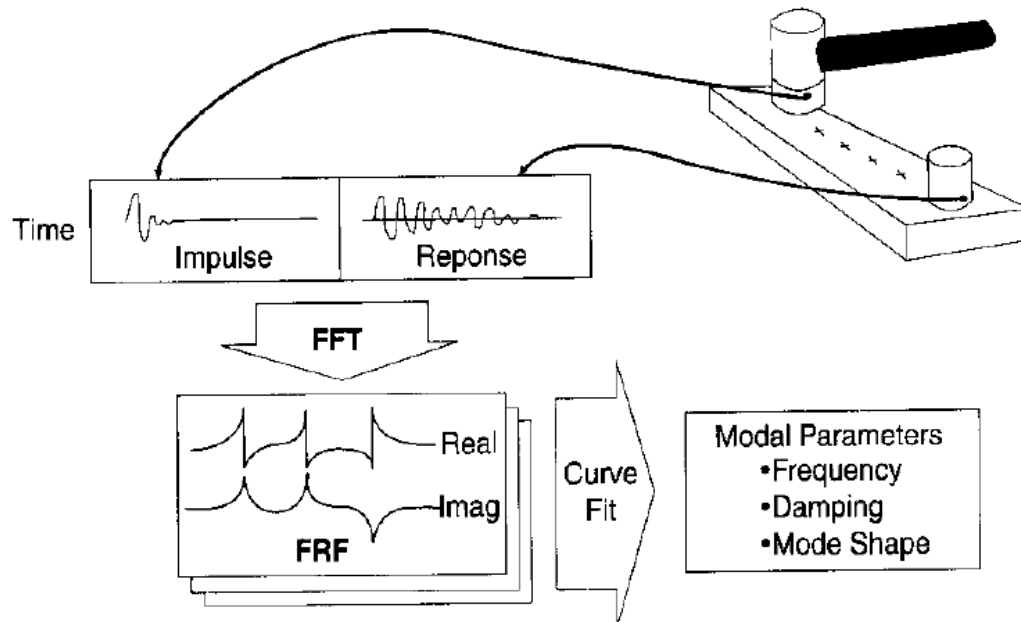


Figure 3.7 : Impact testing (Schwarz & Richardson, 1999)

As shown in Figure 3.7, impact testing consists of four major steps; vibration sensors, time domain data acquisition, measuring Frequency Response Functions (FRFs) by performing Fast Fourier Transform (FFT) analysis on the collected time domain signals, and curve fitting the data to extract the modal parameters. For this work, a SIMO (Single Input Multiple Output) method was performed where the input was the impact hammer, and the output was the 3-axis accelerometer. Impulse and response time domain signals were collected by fixing one point as the impact point and moving the accelerometer. Then these data are transformed to frequency-domain signals (FRFs) by using of an FFT analyser. Finally, the modal parameters are extracted from the results of curve fitting of the FRF data. The loop of an experimental modal analysis is depicted in Figure 3.8.

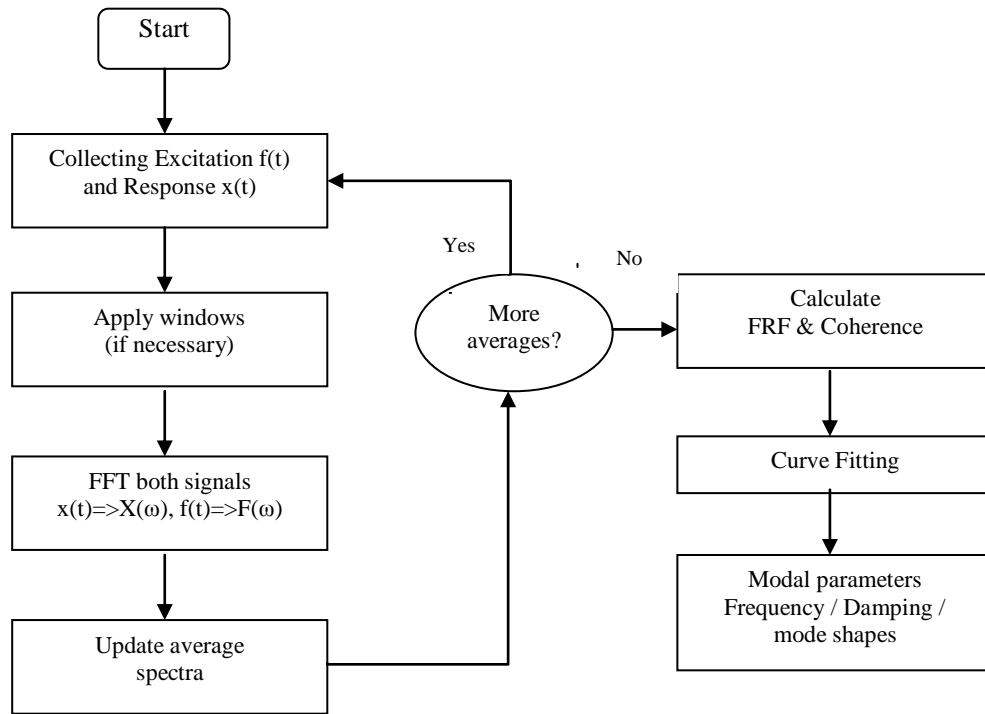


Figure 3.8 : EMA flowchart

Impact testing has two signal processing problems; noise, which can be detected in both the force or response signals, and leakage. To solve these problems, two kinds of windowing techniques are used; Force and Exponential windows. After the signals are sampled, these windows are applied to them, but it happens before the FFT is applied to them in the analyser.

Since precise impact testing results depend on skills of the person conducting the impacting, the FRF measurement process is better to involve spectrum averaging. Use of 3 to 5 impacts per measurement is required to measure the FRF (Schwarz & Richardson, 1999).

### 3.1.3 EMA Instrumentation

The hardware and software needed for EMA and ODS measurement are introduced in this section. The hardware parts included accelerometer, impact hammer, accelerometer calibrator and a four-channel data acquisition system. The software parts include a LabVIEW VI (Virtual Instrument) and the MEScope VES software.

### **3.1.3.1 Accelerometer**

An accelerometer is a piezoelectric transducer. Transducers are instruments that are used for sensing force and motion. The piezoelectric transducers are the most widely used for modal testing among different existing types because of their wide frequency and dynamic range, good linearity and durability. When subjected to vibration, a piezoelectric transducer generates an electrical output. A crystal element that creates an electrical charge when mechanically strained is in fact the main cause of this. When the accelerometer vibrates, the internal mass in the assembly applies a force to the crystal element which is proportional to the acceleration. This relationship is simply Newton's law: force equals mass times acceleration (Agilent, 2008).

There are also some operating specifications that should be considered when using an accelerometer. These are sensitivity, resonant frequency, temperature range and shock rating. A quality accelerometer enjoys high sensitivity, a wide frequency range and small mass. The unit for sensitivity is mV/G. The resonant frequency of the transducer is a function of the mass and stiffness of the transducer, and the stiffness of the mounting method used. Therefore, the frequency range of the test should be within the linear range below the resonance of the transducer. Generally, the usable frequency range is around one-third of the resonance frequency which is required to achieve a linear frequency response. It is shown in Figure 3.9 (Agilent, 2008; Ramli, 1998).

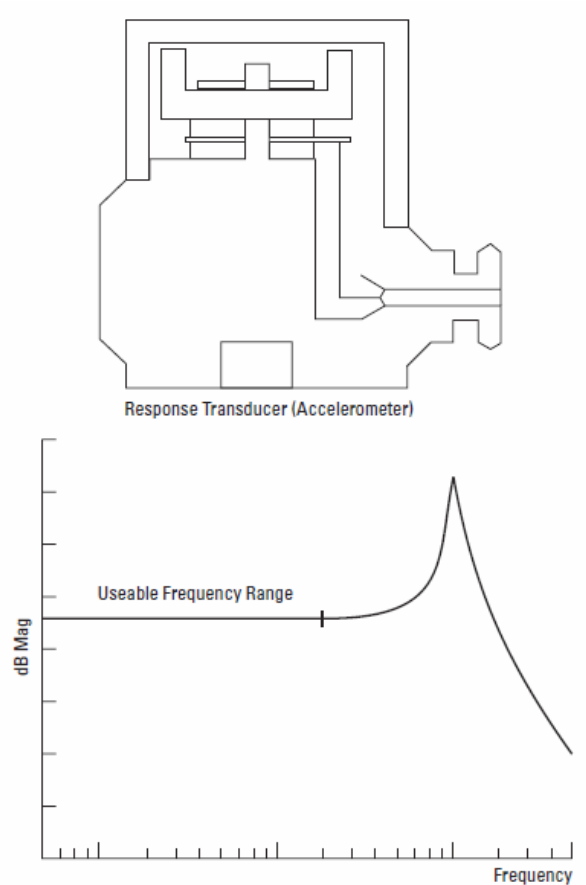


Figure 3.9 : Frequency response of transducer (Agilent, 2008)

The mounting method is another important factor that can affect the frequency response of an accelerometer. There are various mounting methods such as stud, Cement, Wax and Magnet. Stud is the best method, but it requires drilling to fix the accelerometer to a surface. The cement method uses Cyanoacrylate cement or epoxy for mounting, and is capable of producing a flat frequency response up to 80% of the usable range (Chiat, 2008). Wax can be used for fast and roving mounting, but it has a temperature limitation that should not exceed  $40^{\circ}\text{C}$ . The magnetic method has the advantage of fast mounting but gives a flat frequency response of only 20-30% of the specified range. For this work, the magnet mounting method was selected due to fast mounting. The other reason is that the maximum frequency range of an unbalanced motor is 50 Hz. The desired frequency range was 100 Hz. Magnet mounting satisfies this frequency requirement (Ramli, 1998).

The other factor that should be considered during the modal test is the additional mass that is added to the system due to mounting the accelerometer. Generally, the mass of the accelerometer should be less than 5% of the system mass. This condition is satisfactory for this work too.

For the EMA test in this work, a three axial accelerometer was used. The accelerometer model is the 3023A1T from Dytran with the usable frequency range of 1-10 Hz and is depicted in Figure 3.10.



Figure 3.10 : Tri-axial accelerometer of model 3023A1T from Dytran

### 3.1.3.2 Accelerometer Calibrator

Sensitivity is a conversion constant that is used to convert the output voltage to acceleration because the accelerometer output is in terms of voltage not acceleration. Therefore, a correct value of sensitivity can result in a correct amount of acceleration. The sensitivity unit is mV/g and defines as:

$$\frac{\text{Voltage}}{\text{Sensitivity}} = \text{Acceleration} \quad (3.1)$$

Calibration of the accelerometer is performed to obtain the correct value of sensitivity. A VE-10 model form RION calibrator was used for this research. It vibrates with an acceleration magnitude of root mean square (RMS) value  $10 \text{ m/s}^2$  at a frequency of 159.2 Hz.



Figure 3.11 : Accelerometer calibrator of model VE-10 from RION

### 3.1.3.3 Impact Hammer

Impacts hammer work based on a linear momentum principle. Therefore, the amplitude level of the energy is a function of the mass and velocity of the hammer. The velocity of the hammer is controlled by varying the mass since it is naturally hard to control. Therefore, by changing the stiffness of the hammer tip, we will be able to

control the frequency content of the test. The harder the hammer tip is, the shorter the pulse duration and higher-frequency content will be. A force signal is depicted in Figure 3.12.

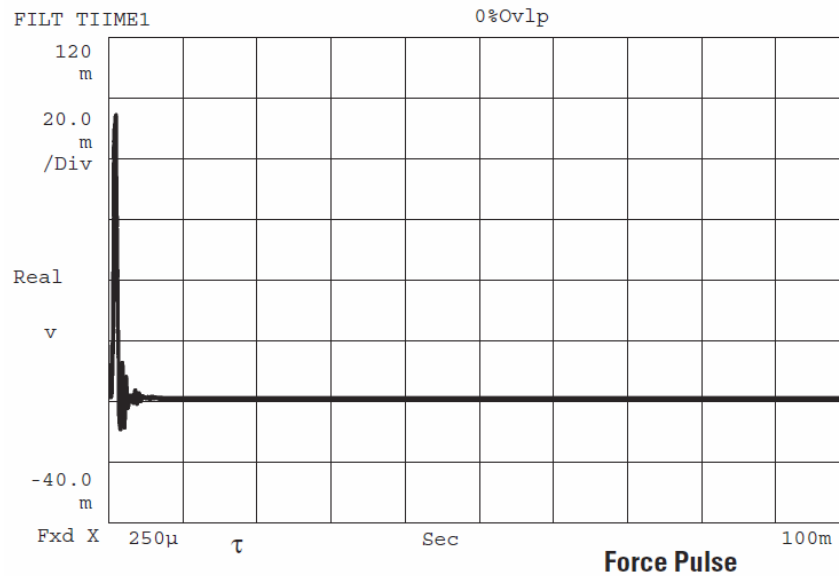


Figure 3.12 : Force pulse (Agilent, 2008)

The impact hammer that is used for this research is a 5800B2 model from Dytran. Three kinds of tip can be installed; a hard type that is made from stainless steel, a medium type that is made from plastic, and a soft type that is made from rubber. As mentioned earlier, the harder the tip, the higher the frequency content, thus this hammer covers a frequency range between 500 Hz (for the soft tip) and 700 Hz (for the hard tip). The hammer is shown in Figure 3.13 (Ramli, 1998).





Figure 3.13 : Impact hammer of model 5800B2 from Dytran

When performing a modal test, some errors may occur. One of them is the double impact that can decrease the accuracy of the FRF measurements. The other one is exhibiting non-linearity characteristics from the structure due to excessive impulsive force. Additionally, a variation in the position of the impact point can cause a phase shift in the FRF measurements and will affect the mode shapes. Averaging the results is a very effective way to reduce experimental errors during the test.

#### **3.1.3.4 Four-Channel Data Acquisition System**

A data acquisition system is an analog-digital converter (ADC) which converts the analog voltage data coming from the accelerometer to digital data readable by a computer. The data acquisition system connects to the computer through a USB cable.



Figure 3.14 : Four channel data acquisition module

The data acquisition system used for this research consists of NI-9233 four-channel analog input modules, assembled with an NI USB-9162 high speed USB carrier and shown in Figure 3.14.

### 3.1.3.5 Virtual Instruments (VI)

To obtain the modal parameters of a structure, the time data collected from the transducer must be transformed to frequency-domain data in an FFT analyzer. Conventional FFT analyzers are bulky, difficult to be customized by the user. It is also usually difficult to transfer FRF measurements to other hardware or programs. However, data acquisition software has recently made it possible to overcome the above problems.

For this research, a Virtual Instrument (VI) created by using the data acquisition software Lab VIEW was used. The VI had already been made by another student (Chiat,

2008) and was used for this research. This FRF-analyzer VI includes a front panel and a block diagram. The front panel contains controls and indicators and is the user interface. The block diagram contains graphical programming codes that control the front panel. The block diagram can be found in the reference (Chiat, 2008).

To be able to use the FRF analyzer VI, some initial configuration in the block diagram needs to be set as seen in Table 3.1 and Figure 3.15 to Figure 3.17.

**Table 3.1 : Initial configurations in block diagram of FRF-analyzer VI (Chiat, 2008)**

<b>LabVIEW module</b>	<b>Parameter</b>	<b>Features</b>
DAQ	Sampling rate	No. of digitized readings sampled in one second from analog data.
	No. of samples	No. of samples to be read.
	Sensitivity	Calibrated sensitivity of accelerometer and impact hammer.
Trigger	Threshold value	Data will be taken for FRF calculation starting from when impact force exceeded this value.
	No. of samples	No. of output samples for FRF calculation, counted from the moment the impact force exceeded threshold value.
FRF	No. of averages	No. of averages needed for FRF calculation.

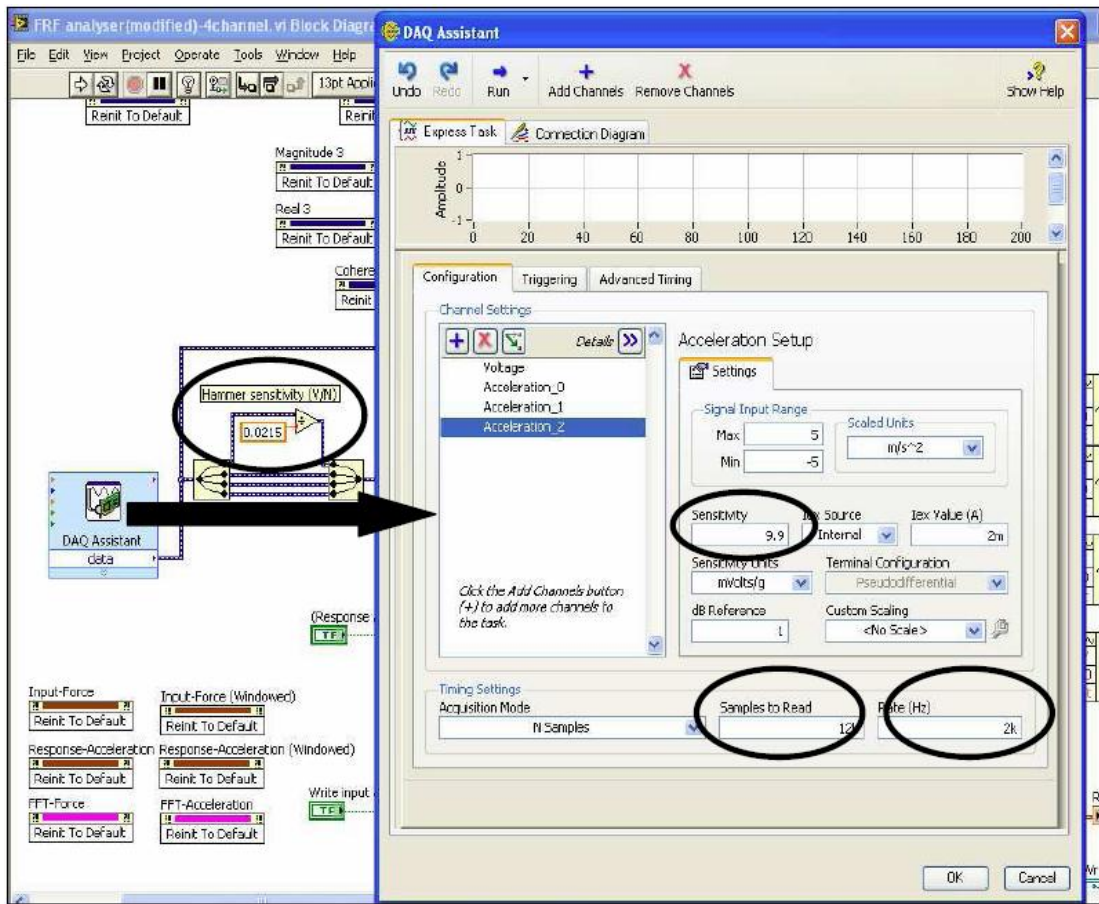


Figure 3.15 : DAQ configuration in block diagram of FRF-analyser VI (Chiat, 2008)

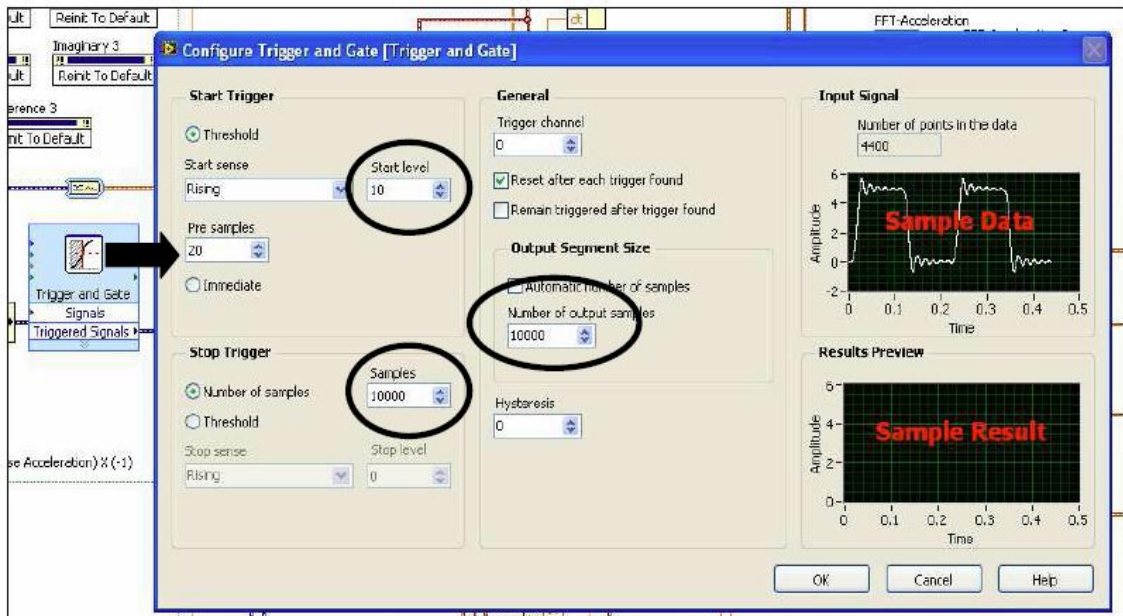


Figure 3.16 : Trigger configuration in block diagram of FRF-analyser VI (Chiat, 2008)



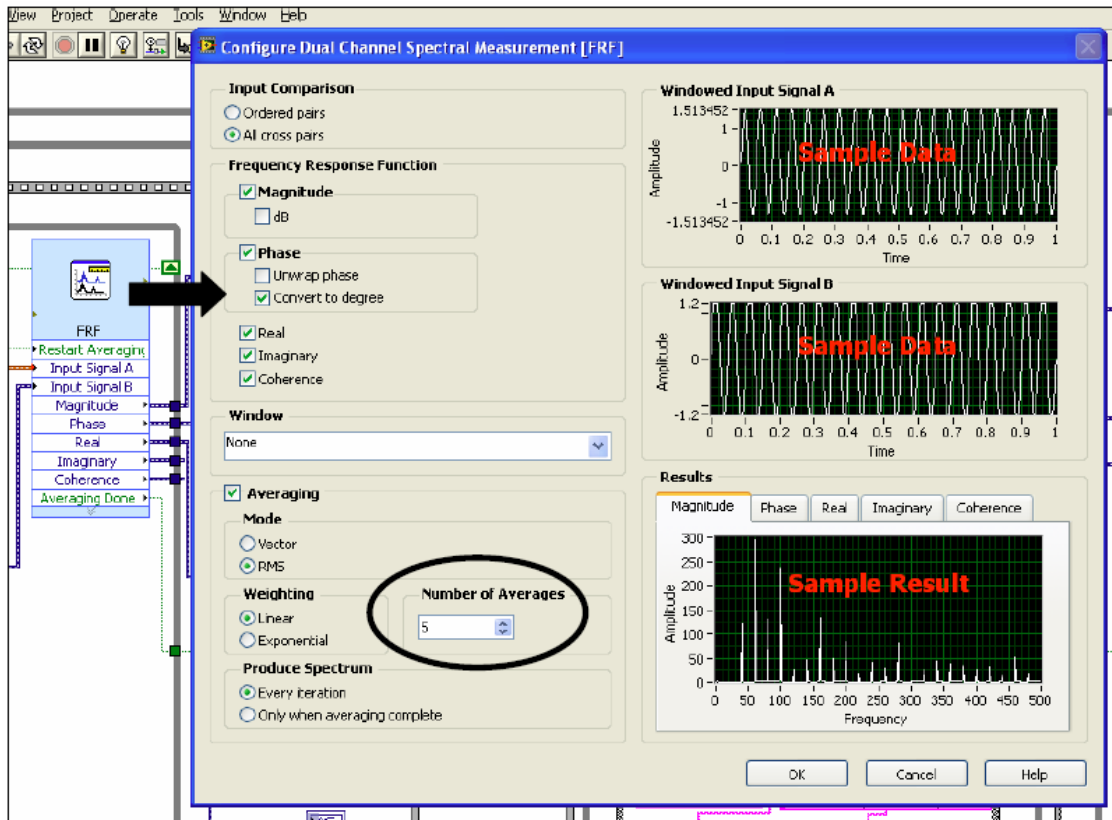


Figure 3.17 : FRF configuration in block diagram of FRF-analyzer VI (Chiat, 2008)

After configuring the block diagram, the front panel has to be configured as shown in Table 3.2 and Figure 3.18.

Table 3.2 : Front panel configurations of FRF-analyzer VI (Chiat, 2008)

Control	Features
Save input & response?	Select yes to save triggered time domain input and response signal at specified location.
File path	Defines the name and location where the (input, response, and) FRF will be saved.
Windowing	Applies windowing function to either input, response, or both.
DOF	Defined measurement point numbering and direction
Response x (-1)	Invert the sign of response signal acquired.

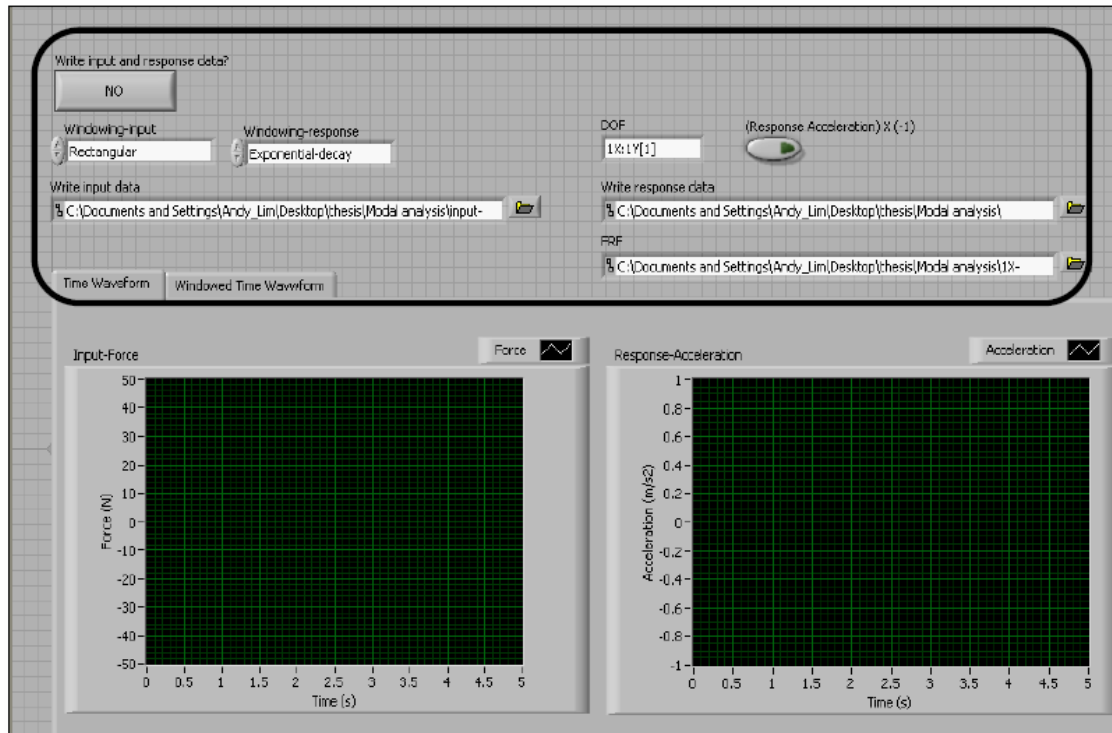


Figure 3.18 : Front panel configurations of FRF-analyzer VI (Chiat, 2008)

The configuration of the front panel makes the user able to save the data and locate the saved data files. Furthermore, the user can choose several types of windowing for input and response data, i.e. rectangular, hanning and flat-top for input, and rectangular and exponential decay for the response. The next step is to configure the DOF that will be followed by MScope VES. Writing the DOF configuration should be in a defined form. For example, 2X:1Y [1] means an impact at point 1 in the Y direction and reading the response from point 2 in the X direction. The button “response x (-1)” is used to inverse the sign of the response signal.

The front panel consists of 5 graph indicators. Input and response graphs show the triggered time domain signals of input and response. FFT input and response shows the frequency domain signals of input and response. The 3 other graphs are magnitude, phase and coherence of the averaged FRF. The flow chart of FRF-analyser VI is depicted in Figure 3.19.

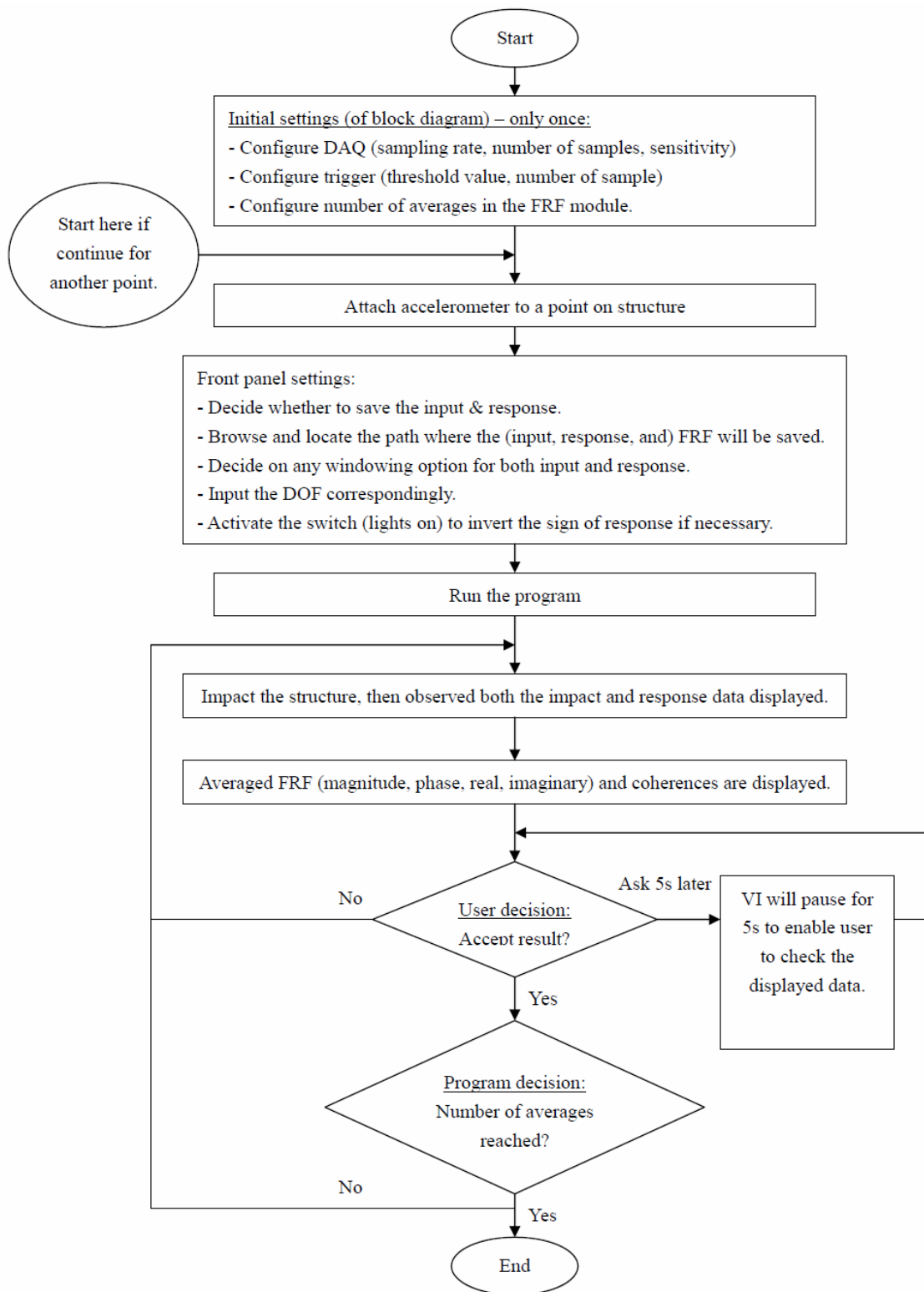


Figure 3.19 : Configurations and operations flow chart of FRF-analyzer VI (Chiat, 2008)

### 3.1.3.6 MEscape VES Software

MEscope VES is software to observe and analyse noise and vibration problems in machinery and structures, using either experimental or analytical data. MEscape VES can acquire and post-process multi-channel time or frequency data from machinery and structures. The software is equipped with an interactive 3D animation that makes it easy to observe operating deflection shapes from running machinery. It also displays resonances and mode shapes in structures and machinery, acoustic shapes and engineering shapes directly from acquired data.

In this work, acquired FRF data were transformed using this software to perform the curve fitting and extract the natural frequencies. It could also animate the mode shapes corresponding to each extracted natural frequency. A general view of the MEscape VES software is shown in Figure 3.20.

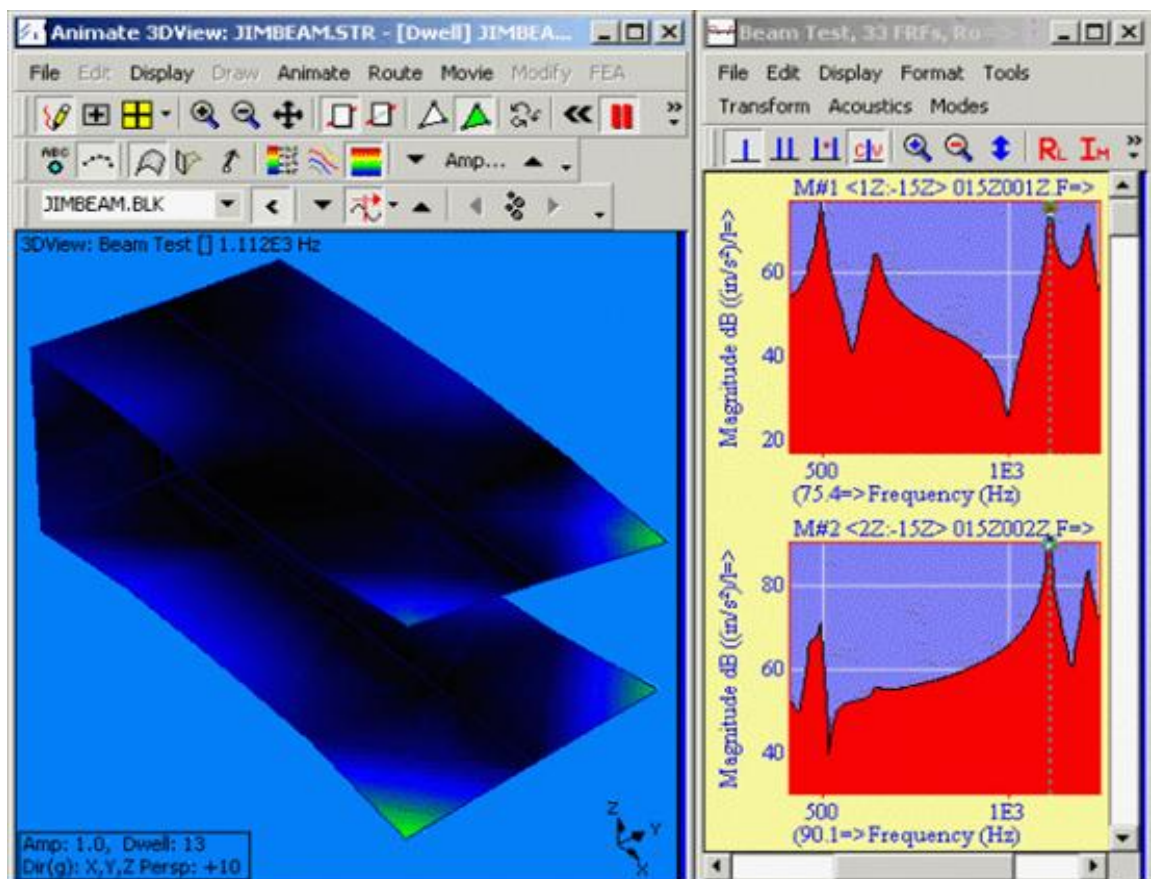


Figure 3.20 : A general view of MEscape software



## 3.2 ODS Measurement

*The deflection of a structure at a particular frequency* is the traditional definition that has been given to *ODS*. But in general, it can be defined as *any forced motion of two or more points* on a structure. In other words, the ODS contains both resonant and forced vibration whilst modes characterize only resonant vibrations (Richardson, 1997; Schwarz & Richardson, 1999).

### 3.2.1 Mode Shapes Versus ODS's

Whilst the mode shape and ODS are related (and for obtaining the mode shapes the ODS's should be measured) they are however completely different from one another. The differences can be summarized in some ways. These differences are tabulated in Table 3.3 (Schwarz & Richardson, 1999).

Table 3.3 : Mode shapes versus ODS's

<b>MODE SHAPES</b>	<b>ODS's</b>
each specific natural frequency is defined by a mode	can be defined at any frequency
for stationary and linear structures	for non-linear and non-stationary structures
characterize resonant vibration	characterize both resonant and non-resonant vibration
independent from the forces or loads	depends on forces and loads
only related to material properties and boundary conditions	related to not only material property and boundary conditions, but also to load changes
do not have units	have unique values and units
specify relative motion of one DOF versus another	show the actual motion of one DOF versus another

### 3.2.2 ODS Measurement

In both domains of time and frequency, the ODS can be obtained from any forced motion. As was described for modal data collection, ODS data collection can be made from a finite number of DOFs. Generally, it can be stated that “all experimental modal parameters are obtained from measured ODS’s”. To put it in other words, post-processing (curve fitting) a set of ODS data can result in obtaining the modal parameters. In other words, within a frequency range, a set of FRFs and a set of ODS’s could be similar. At or near a resonance peak, the ODS is dominated by a mode. As a result, the ODS can be thought of as being just about equivalent to the mode shape (Schwarz & Richardson, 1999).

Any ODS at each point is defined by magnitude and phase. To define a proper ODS vector, at all response points, at least the relative magnitude and phase are required. It denotes the fact that all the responses must be measured concurrently. This situation will make the measurement difficult and expensive. A way to solve this difficulty is via repeatable operation. This means that if the time waveform exactly repeats in the sampling window, one set of data can be acquired every time. This situation is also valid for steady state (stationary) operation situations that make using ODS possible for many situations in industry (Schwarz & Richardson, 1999).

FRF data is derived from dividing the response by the excitation, and both the magnitude and phase can be seen at each frequency. So, ODSs can be obtained from FRF measurements. However, it becomes difficult when we learn that while measuring the response, the excitation forces causing the response must be measured with it at the same time. If not impossible, this would be tremendously tough. For this reason, ODS data are obtained from Transmissibility measurements. When it is hard to measure the excitation forces, transmissibility measurements are made. The measurement method is similar to the way the FRF is measured, but instead of an excitation force, the response

is divided by a reference response signal. The units of the ODSs are response units per unit of response at the reference DOF (Schwarz & Richardson, 1999).

Another way to obtain ODS measurements is ODS FRF, which is used when excitation forces are immeasurable. In comparison to Transmissibility, the advantage of ODS FRF is that the ODS FRF has peaks at resonances that make it easy to locate these resonances. Like the Transmissibility, ODS FRF needs a reference response too (Schwarz & Richardson, 1999).

### **3.3 Finite Element Modal Analysis**

Finite Element Analysis (FEA) is a computational approach to solving engineering problems by applying numerical methods. FEA has a vast number of applications in the field of engineering such as stress analysis, heat transfer, fluid mechanics, etc. The most important benefit of FEA is its ability to predict the real-world behaviour of a structure or design concept. This leads to a considerable saving in both time and investment. FEA in vibration analysis is known to be an analytical method to determine the modal parameters of structures.

The main parameter in FEA is validation of the finite-element model because finite-element models are rarely correct or accurate due to the many parameters that create uncertainty in that model. Therefore, the results obtained from the FEA are needed to be validated with measured test data, for example experimental modal analysis data. So the test data themselves should have a high level of accuracy.

To validate a finite element modal analysis, corresponding natural frequency and mode shapes are both needed. It should be mentioned that to compare parameters, having corresponding amounts of natural frequencies is not enough. The mode shapes should be compared too. This ensures a one-to-one correspondence between the

frequency and the mode shape. It should be noticed that a distinct mode shape is associated with a distinct frequency (Schedlinski et al., 2004).

The finite-element model validation is accomplished through minimizing the deviation between the identified and analytical eigenvalues and mode shapes. For this purpose, it is assumed that the identified values are perfect and the whole error is from the finite-element model. In the finite-element model, there are some parameters that can be changed to decrease the deviation. These include geometry, element properties (i.e. density, modules of elasticity, Poisson's ratio, and the mesh size), and boundary conditions.

Two methods were used in this research to compare the natural frequencies. The first one is minimizing the error between the values obtained from FEA and EMA, which should be less than 10%. The second one, as is shown in Figure 3.21 is to compare the frequencies graphically through comparing the predicted and measured results against each other. This method shows both the relative differences between the frequencies as well as the global trends and advises possible reasons for these variances. With a direct correlation between the values, the points will lie on a straight line with a slope of 1.0 and if there is a random scatter, then an accurate representation of the structure cannot be obtained using the finite-element model. This could be a consequence of an inappropriate element type or a poor element mesh in the finite-element model. It is also possible that there have been incorrect boundary conditions in either the test or the analysis. If the points lie on a straight line, but with a slope other than 1, then the problem may be a mass loading problem in the modal test or an incorrect material property, such as elastic modulus or material density, in the finite-element model (Agilent, 2008).

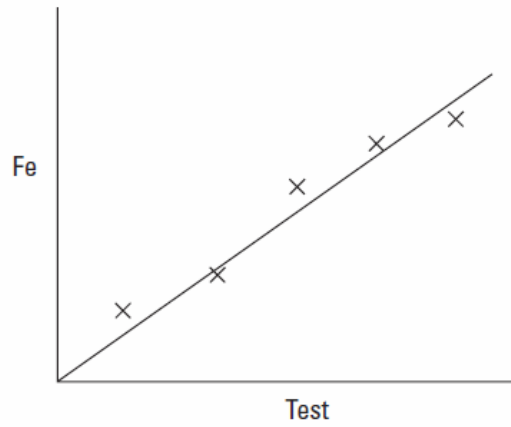


Figure 3.21 : Graphical comparison of EMA and FEA frequencies (Agilent, 2008)

According to what came in above, a block diagram can be defined as Figure 3.22 to validate modal parameters. As mentioned in the introduction, the assumption was that the EMA data are accurate enough, and the whole error comes from FEA data. Therefore, the modal validation is accomplished through FEA model updating to minimize the deviation between FEA and EMA results (Schedlinski et al., 2004).

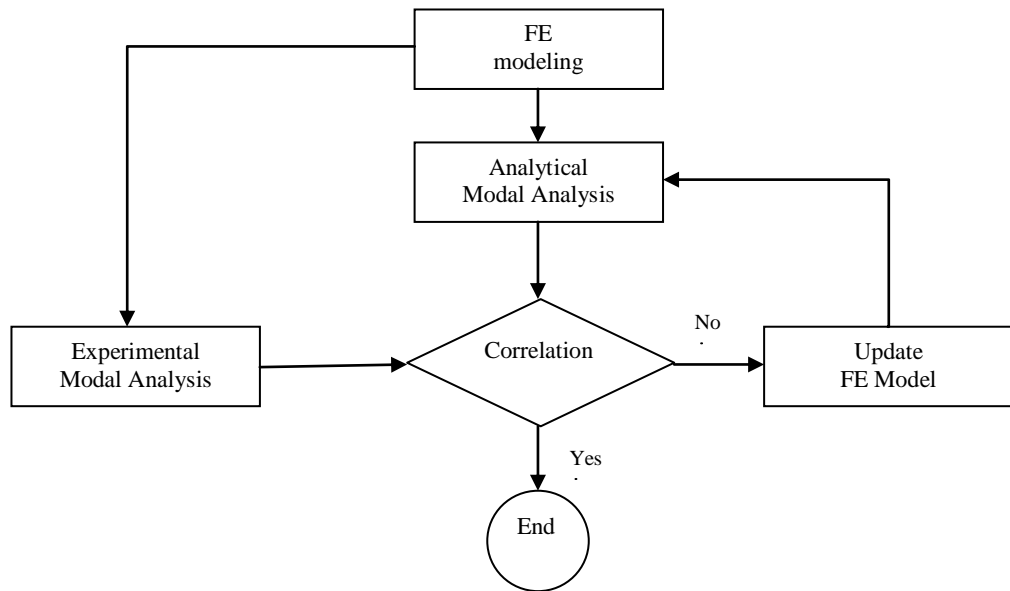


Figure 3.22 : Model validation strategy

### 3.4 Structural Optimization

For this research, the density method of topology optimization for continuum structures was used. This maximizes the structure's first and second natural frequencies

out of excitation frequency range with respect to the manufacturability of the new structure.

Continuum topology optimization seeks to determine the inner holes and also the internal and external boundaries. One of the methodologies used in continuum topology optimization is the density method. Each element should be solid or void meaning its density should take an amount of 1 or 0 or a value in between. The density of an element can be presented as:

$$\rho = 1 - (1 - a)(1 - b) \quad (3.2)$$

Where the (1-a) (1-b) represents the total volume of void in an element. As can be seen here, a=b=0 presents total void and a=b=1 presents solid element and the void size variables varying between 0 and 1 (Rosen, 1961).

The optimization in this research has been done using Altair-Hyper Works software. It is a finite-element based structural analysis and optimization software. This software is a response-based optimization tool. Responses are defined as quantities in the analysis which can be constrained or optimized. The aim of this research is to maximize the natural frequencies of the structure according to manufacturability of the new structure. Therefore, the objective function is assumed as frequency that should be optimized (maximized) and the constraint assumed as volume-fraction.

Altair-Hyper Works solves the optimization problems by either Homogenization or density method. The density method is the default method however. The main parameters in optimization problems that need to be solved are Objective, Constraints, and Design Variables. Objective function and constraint function are structural responses obtained from a finite-element analysis. Design variables depend on the type of optimization (Rosen, 1961).

The software uses an iterative solution. In the first step, the physical problem will be analysed, and then a convergence test is carried out. After that the design

sensitivity analysis is performed, and an approximate optimization solution is presented based on the sensitivity information. Finally, based on the postulation that only minor variations occur in the design with each optimization step, the steps will be repeated again. Furthermore, in this software, three types of elements are available; solid elements, shell elements, and 1-D elements. In the density method, each element has a variable that presents the material density. For this research, a solid element has been used to perform the optimization and modal analysis (Rosen, 1961).

As it turned out, the constraint in this research is manufacturability of the new structure. In this work, the assumption is that the structure should be reinforced by adding simple new parts to the structure rather than remanufacturing the structure. However, the problem is that software can only give a visual estimation of density variety for designable area and not an exact solution. Thus, the model should be defined in such a way that the best post processing can be realized. It is also assumed that the simplest form of optimization is needed because usually, the results from the software have complicated forms.

## **Chapter four**

### **4 Results**

In this chapter, the results obtained or calculated from different sections of this research are presented in the form of the text, tables and figures. In the first section, the results obtained from the Modal Testing and ODS analysis are presented. In the next section, the validated finite-element model and the validation methods are shown. Finally, the two different optimized models obtained from the Altair-Hyper Works software are presented.

#### **4.1 Experimental Modal Analysis**

In this section the results extracted from MEScope VES software for the Modal Testing is presented. Modal Testing consists of three main steps, i.e. modelling the geometry of the structure, setting up the system, acquire FRF data using FRF-analyser VI, and post processing the results (Chiat, 2008). Each step is described below, and the setting for each step and sub-step is detailed.

##### **Step 1: Modelling the Geometry of the Structure**

In this step, the measurement response points and the impact point were chosen. Numbered stickers were used to locate the point numbers. In total 72 measurement points were located on the structure. The structure was then modelled in MEScope VES according to its real dimensions and the measurement points and global coordinates defined in the MEScope VES software. The model is shown in Figure 4.1.



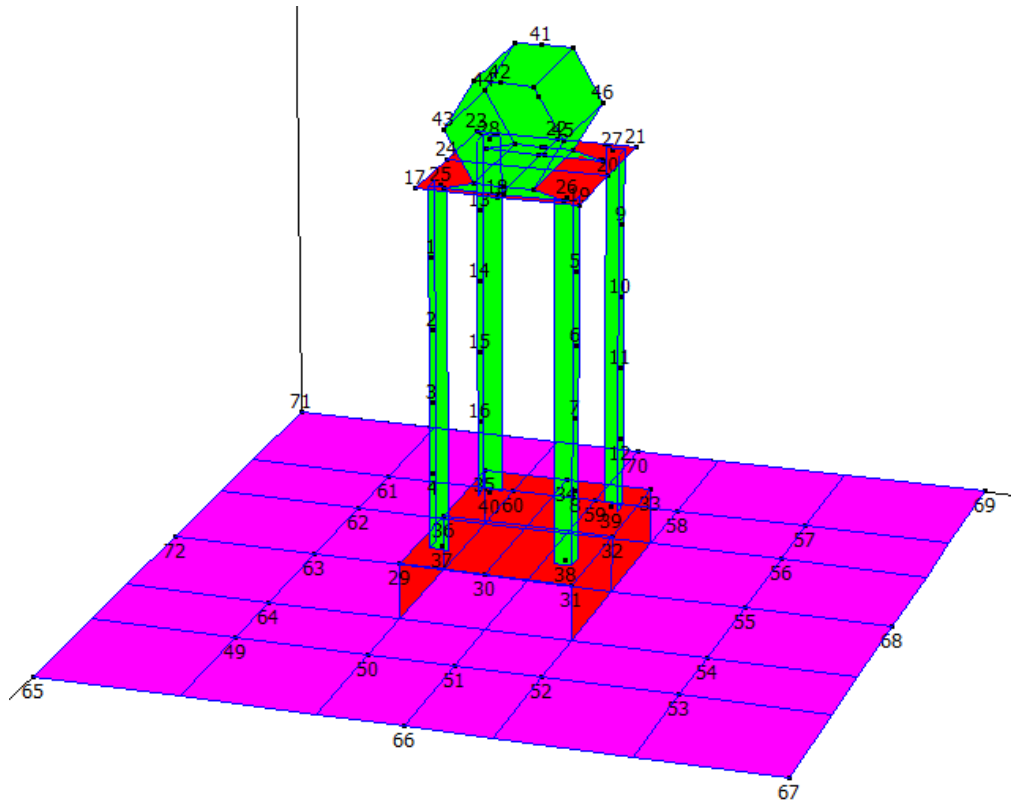


Figure 4.1 : MEscope VES model of the structure

**Step 2: Setting up the system and acquiring FRF data with FRF-analyser VI (LabVIEW software Virtual Instrument)**

In this step, the FRF data should be obtained and be saved using measured impact force and responses via the FRF analyser VI.

Before starting to obtain the data, the accelerometer needs to be calibrated. For this purpose, the accelerometer is connected to a calibrator which vibrates with an acceleration magnitude of RMS value  $10\text{m/S}^2$  at a frequency of 159.2 Hz. Furthermore, the accelerometer 3rd axis cable is connected to one of the channels of the 4-channel data acquisition hardware. This is connected to the laptop containing the LabVIEW software. The sensitivity calculated for this axis was 9.8 mV/g which is close the value printed on the case of the accelerometer; 9.9mV/g. Therefore, the other sensitivities for other axis are assumed to be correct. The accelerometer calibration needs to be done only once during the EMA.

Furthermore, the initial settings of the block diagram were configured as: sampling frequency=2000 Hz, number of samples of DAQ=14000, threshold value=1.0, number of samples of trigger=10000, number of averages=5. The windowing options were set to “Rectangular” for input and “Exponential” for the output response. These options also only need be configured once during the EMA.

The next step follows what introduced in the operation’s flow chart for the FRF-analyzer VI as depicted in Figure 3.8. The accelerometer is attached to a measurement point. The front pannel of the FRF-analyzer VI is set and the program is executed. The structure is excited at a fixed impact point by the impact hammer andthe time domain impulsive force is checkedto prevent double knocking.The results are then saved and the process is iterated acording to the flowchart. The measurment were done for 72 points in three x, y and z directions. This resulted in 216 FRF measurements.

### **Step 3: Post processing the results**

This step consists of importing the FRFs to MEscope VES software to determine the natural frequencies of the structure and animate the mode shapes corresponding to specific natural frequencies. The FRFs are imported to the software and assigned to the measurement points of the structure. The natural frequencies and mode shapes according to these natural frequencies are then obtained by performing curve fitting on the imaginary part of the FRFs. The frequency range for this analysis was set between 10 Hz and 70 Hz. It was set from 10 Hz to prevent the effects of rigid body modes on the flexible modes in the curve fitting results. The overlay FRFs for the frequency range between 0 Hz and 70 Hz is shown in Figure 4.2 to indicate the influence of the rigid body mode FRFs. After neglecting the rigid body modes, the resulted FRF between 10 Hz and 70 Hz is shown in Figure 4.3. Also, the curve fitting results are depicted in Figure 4.4.

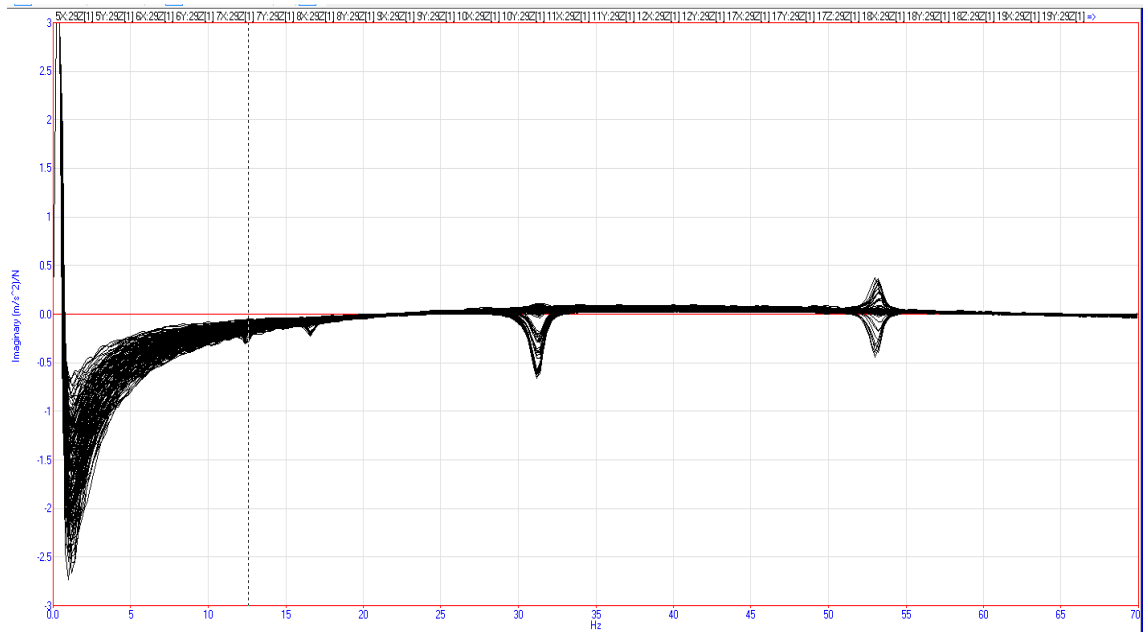


Figure 4.2 : Overlay FRFs between 0 and 70 Hz to indicate the rigid body modes

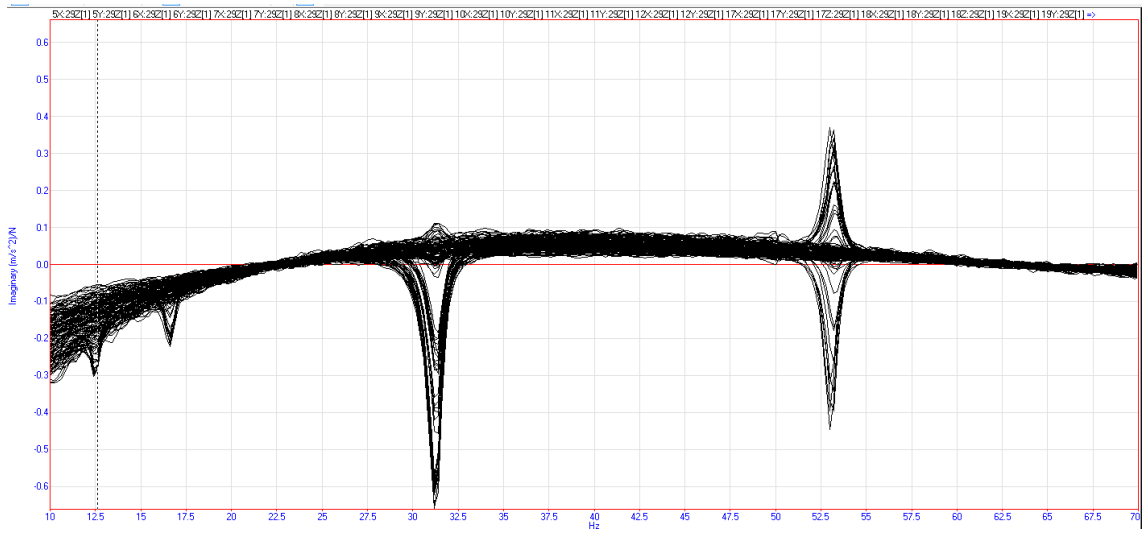
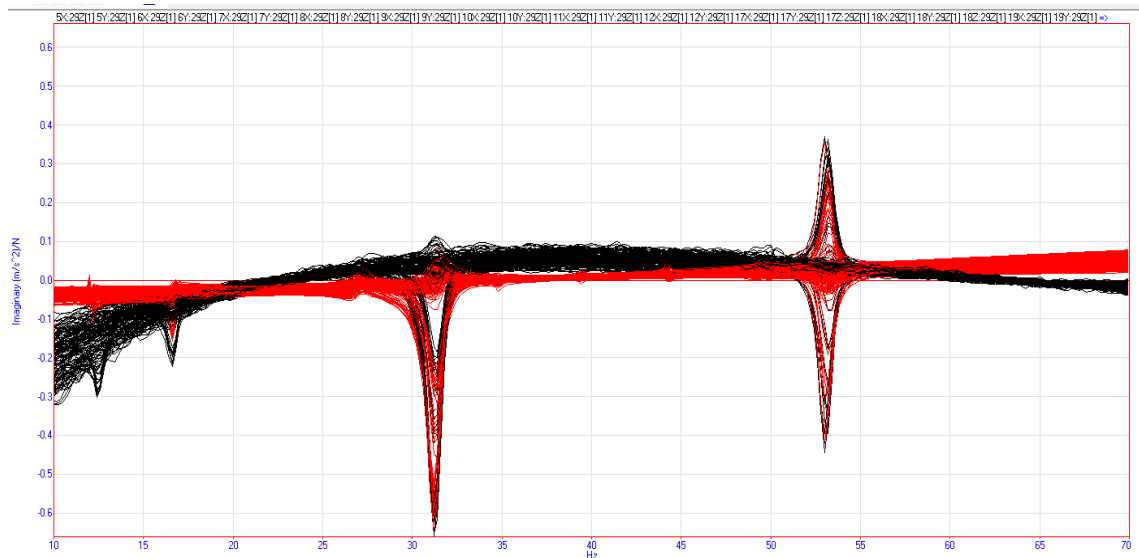


Figure 4.3 : Overlay FRFs between 10Hz and 70Hz



**Figure 4.4 : Curve fitting the FRFs between 10Hz and 70Hz**

As it can be seen from the curve fitting, the structure has four main peaks below 70 Hz. The mode shapes associated with each one of them can be seen in animation. The modes are tabulated in Table 4.1.

**Table 4.1 : Modes obtained from Modal Testing**

Mode Number	Frequency (Hz)	Mode Shape
1	12.1	Bending, left to right
2	16.7	Bending, front to rear
3	31.4	Bouncing
4	53	Torsional

The mode shapes associated with each natural frequency are depicted in Figure 4.5 to Figure 4.8. It should be mentioned that a scaling factor of 50 is used to exaggerate the mode shapes.

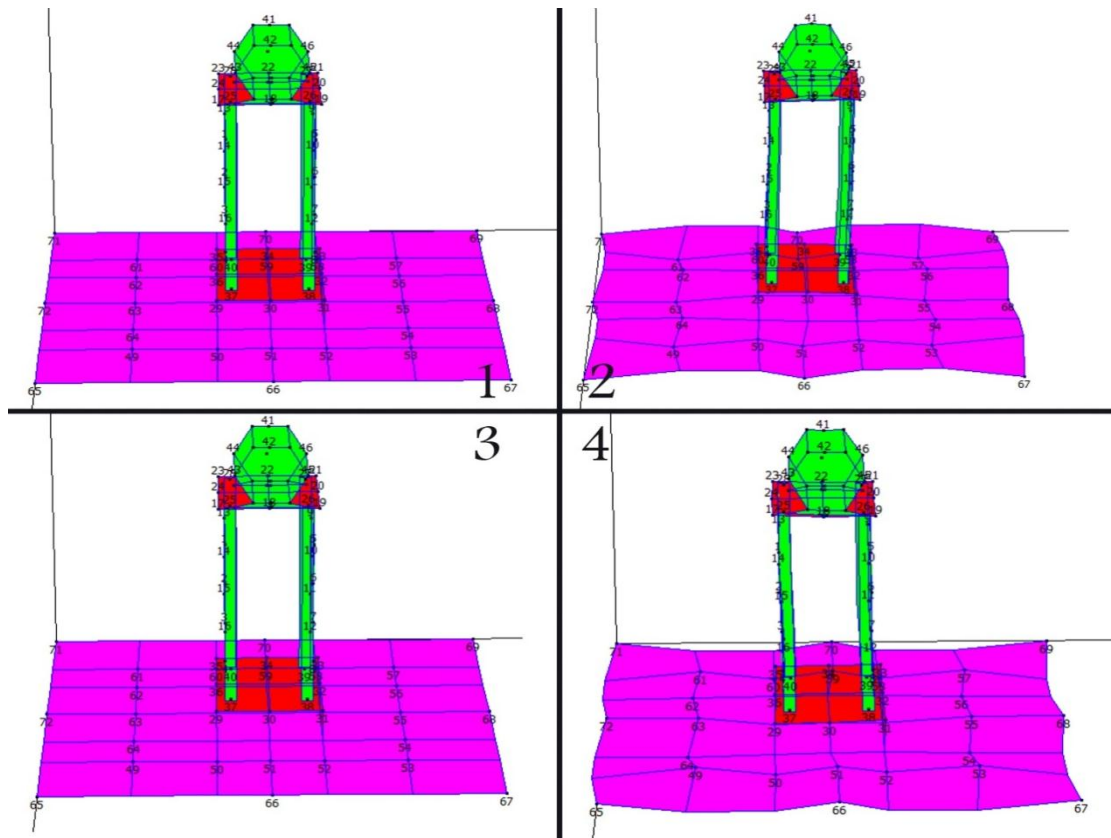


Figure 4.5 : mode 1 at the frequency of 12.1Hz

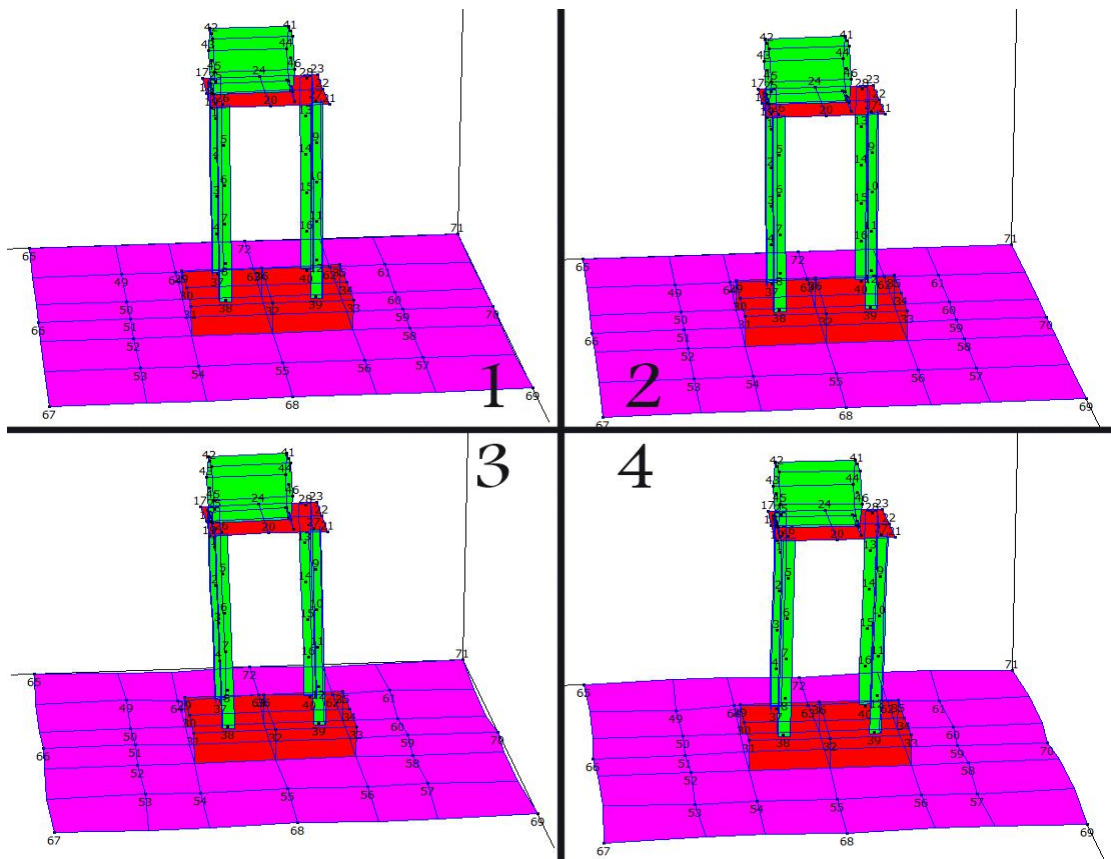


Figure 4.6 : Mode 2 at the frequency of 16.7Hz

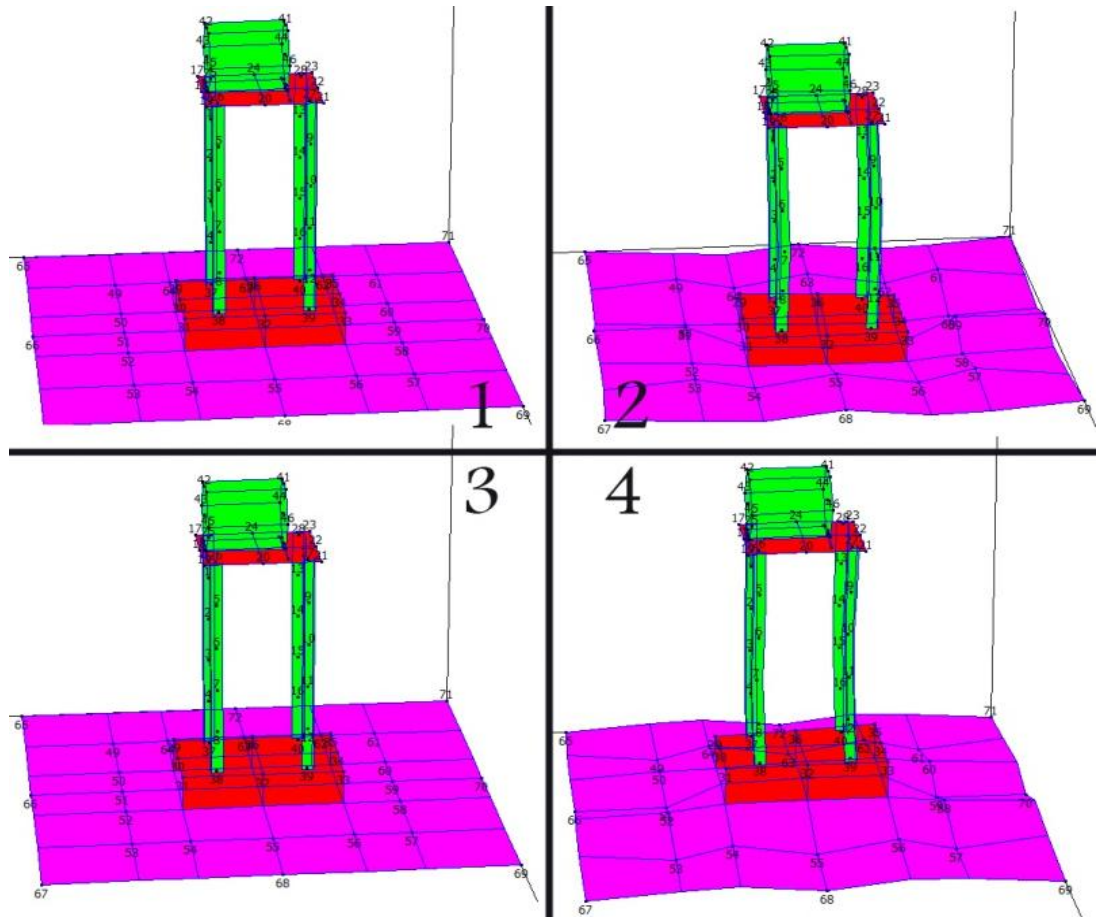


Figure 4.7 : mode 3 at the frequency of 31.4Hz

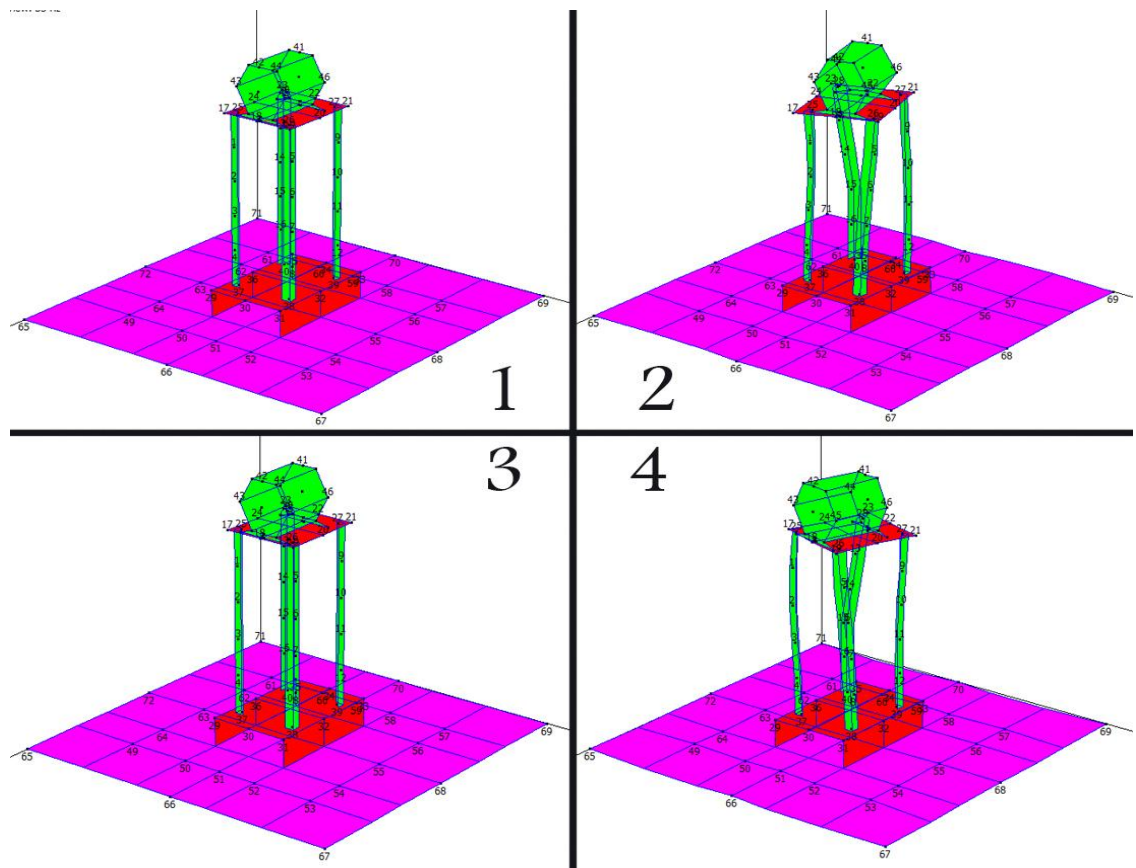


Figure 4.8 : mode 4 at the frequency of 53Hz

## 4.2 ODS Measurement

The set up for the ODS measurement is almost the same as the Modal Testing. However, instead of using an impact hammer to excite the structure, the time domain data are collected during the operation of the motor in specific frequencies. For this research, the ODS measurement has been done for two frequencies, namely, 12.1 Hz and 16 Hz. The main reason that these two frequencies were chosen was the fact that based on the Modal Testing results, there are two modes below 20 Hz at 12.1 Hz and 16 Hz. The three main steps of EMA are described below and the results are presented for the two frequencies separately.

### **Step 1: Modelling the geometry of the structure**

This step is completely the same as what was described in section 4.1.1.

### **Step 2: Setting up the system and acquire FRF data via FRF-analyser VI**

In this step, the FRF data should be obtained and be saved using measured impact force and responses via the FRF analyser VI.

The VI used for ODS measurement is similar to the one used for Modal Testing (Chiat, 2008). The initial settings of the block diagram were configured as follows: sampling frequency=2000 Hz, number of samples of DAQ=14000, threshold value=0, number of samples of trigger=10000, number of averages=5. The windowing options were set to “Hanning” for both input and output signals.

Performing ODS measurement is similar to Modal Testing but instead of the impact hammer, a uniaxial accelerometer is used as the reference point. The tri-axial accelerometer is roving and by following the flowchart as depicted in Figure 4.9, the FRF data was collected and saved for 72 points in three x, y and z directions. This resulted in 216 FRF measurements.

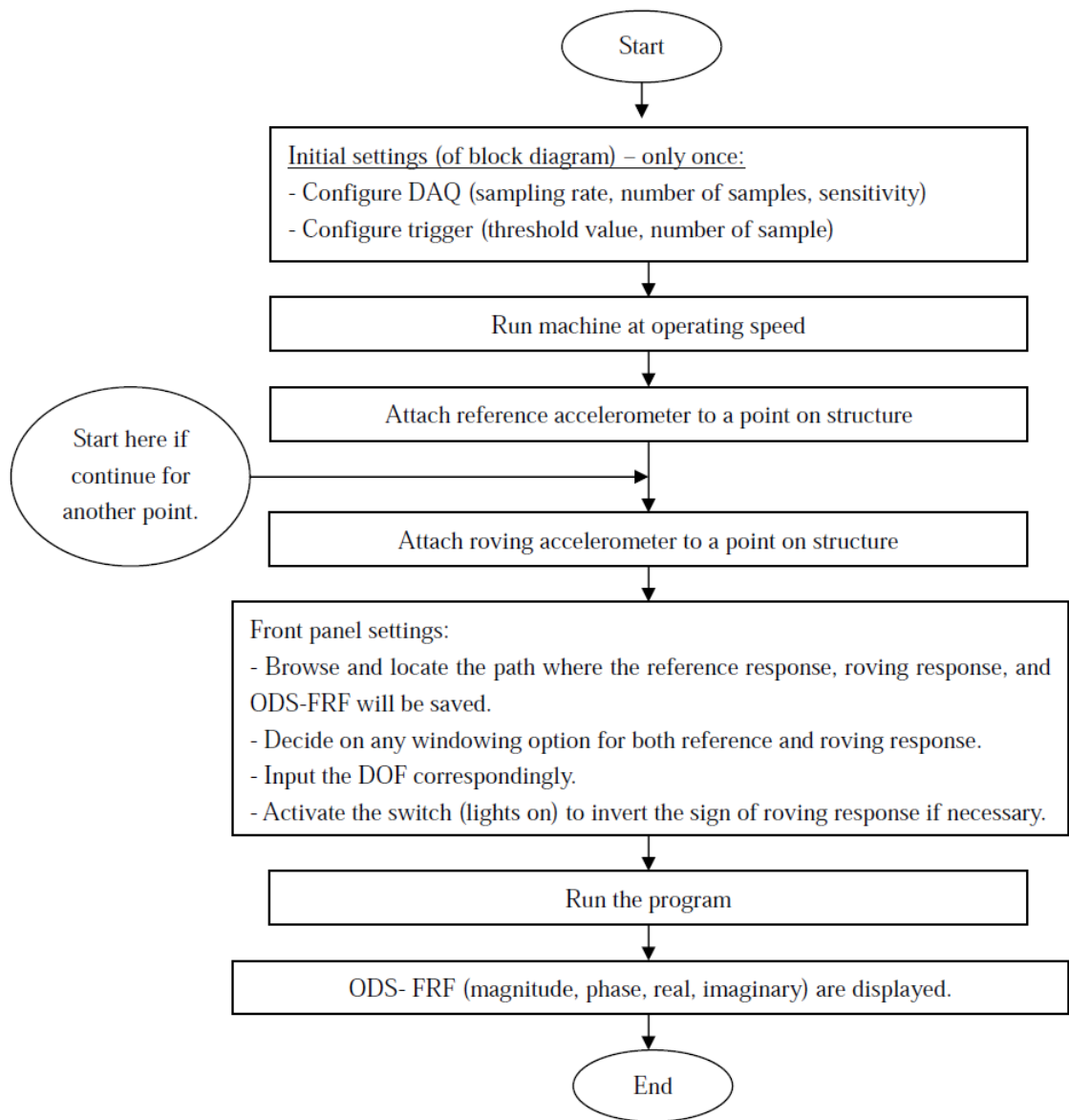


Figure 4.9 : Configurations and operations flow chart of ODS measurement VI (Chiat, 2008)

### Step 3: Post processing the results

This step consists of importing the FRFs to MEscope VES software to check out the results and animate the mode shapes corresponding to specific natural frequencies. Since the 12.1 Hz and 16.7 Hz are natural frequencies, the FRFs should show high peaks in these frequencies. Furthermore, the importance of ODS measurements is to depict an exact form of deflection shape of the structure in a specific frequency. These results are presented in Figure 4.10 to Figure 4.15.



## Results of ODS measurement at 12.1Hz

As we know from the EMA, 12.1 Hz is known to be the first natural frequency of the system. The FRFs at this frequency for the frequency range between 5 Hz and 60 Hz are depicted below. Figure 4.10 indicates the imaginary part of the FRFs and Figure 4.11 indicates the linear amplitude of the FRFs.

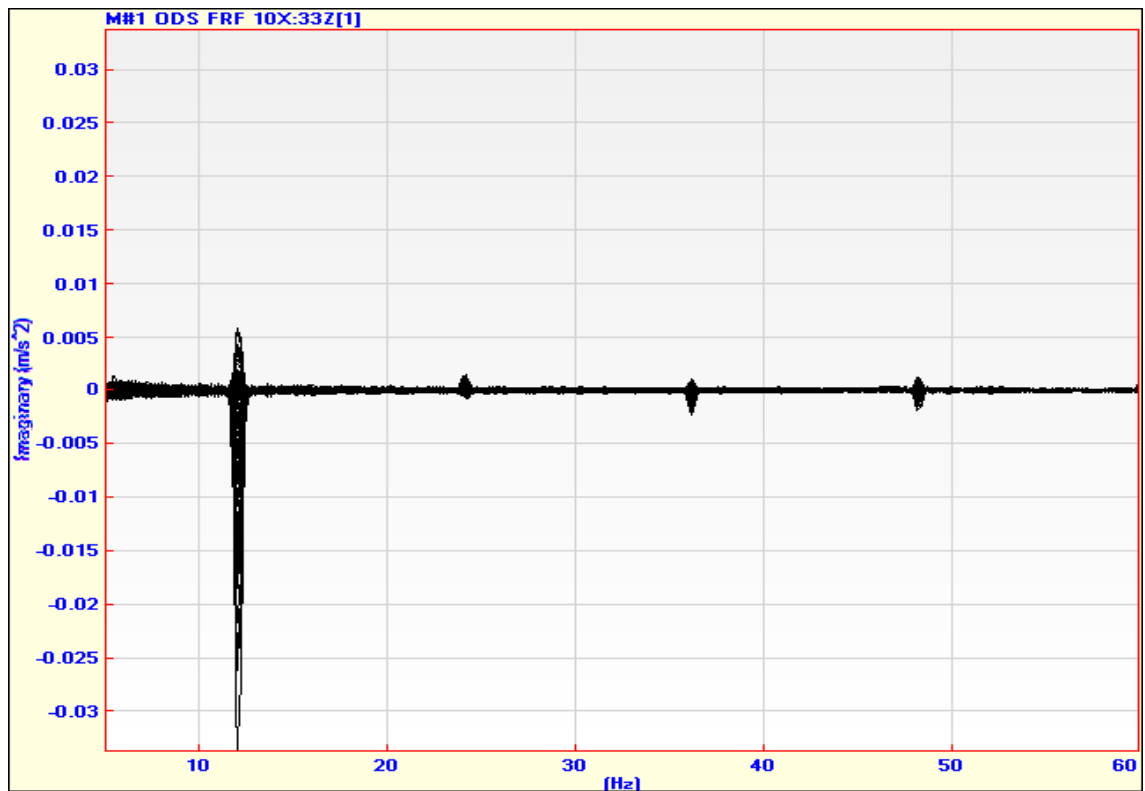


Figure 4.10 : Imaginary part of the ODS measurement FRFs of the pedestal structure at 12.1Hz

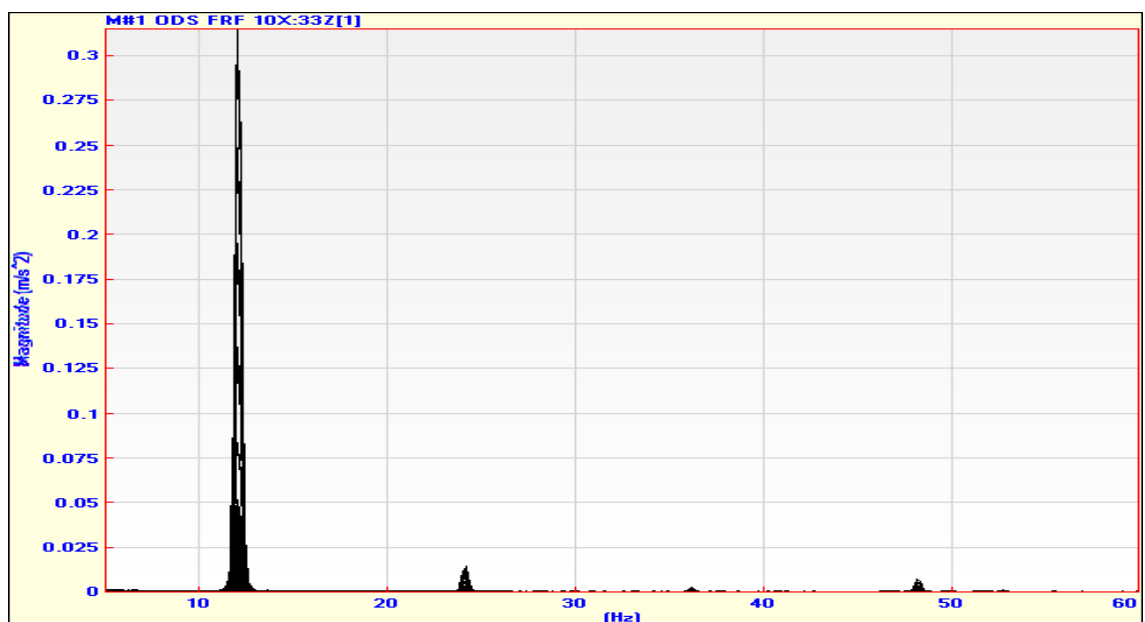


Figure 4.11 : Linear amplitude of the ODS measurement FRFs of the pedestal structure at 12.1Hz

Also, the Operating Deflection Shape at this frequency is depicted in Figure

4.12.

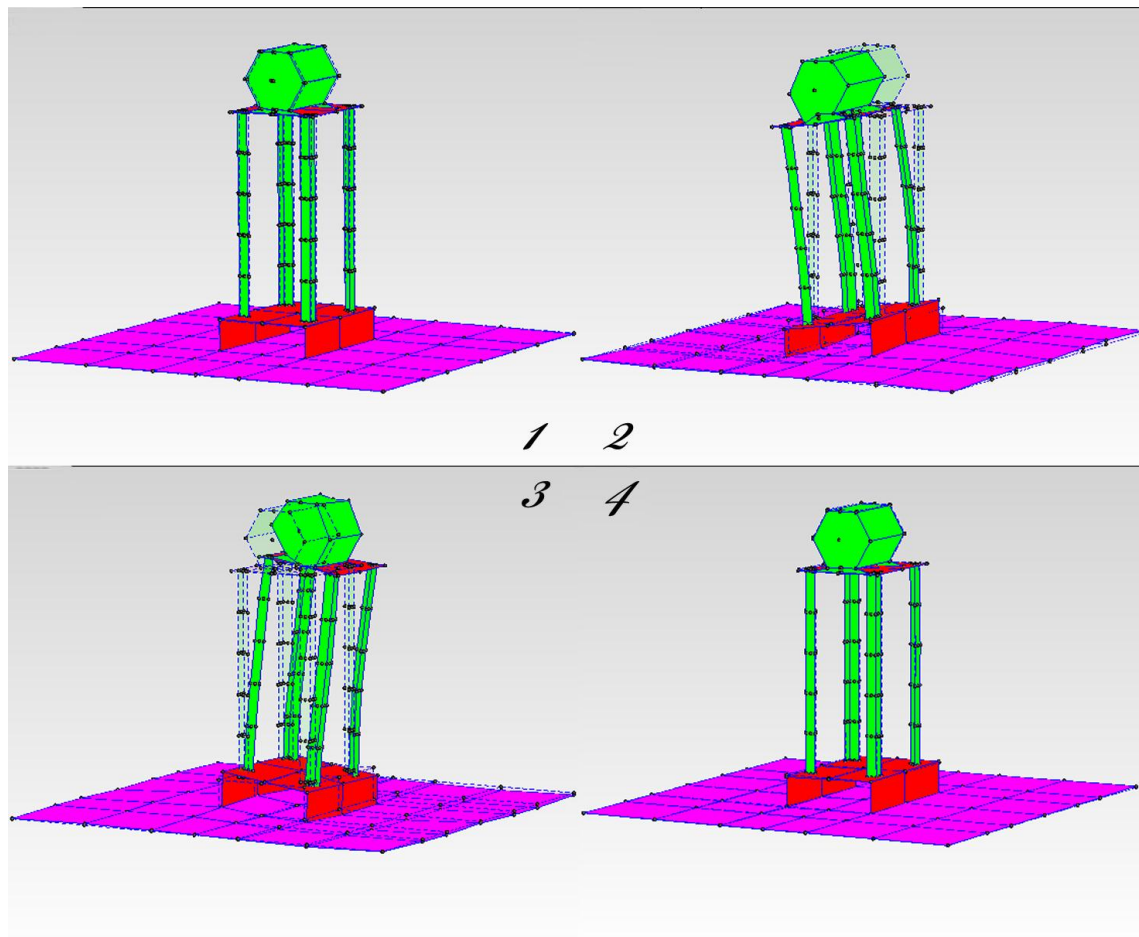


Figure 4.12 : Operating Deflection shape of the pedestal structure at 12.1Hz

### Results of ODS measurement at 16Hz

As we know from the EMA, the second natural frequency of the system is 16 Hz. The FRFs at this frequency for the frequency range between 5 Hz and 60 Hz are depicted below. Figure 4.13 illustrates the imaginary part of the FRFs and Figure 4.14 illustrates the linear amplitude of the FRFs.

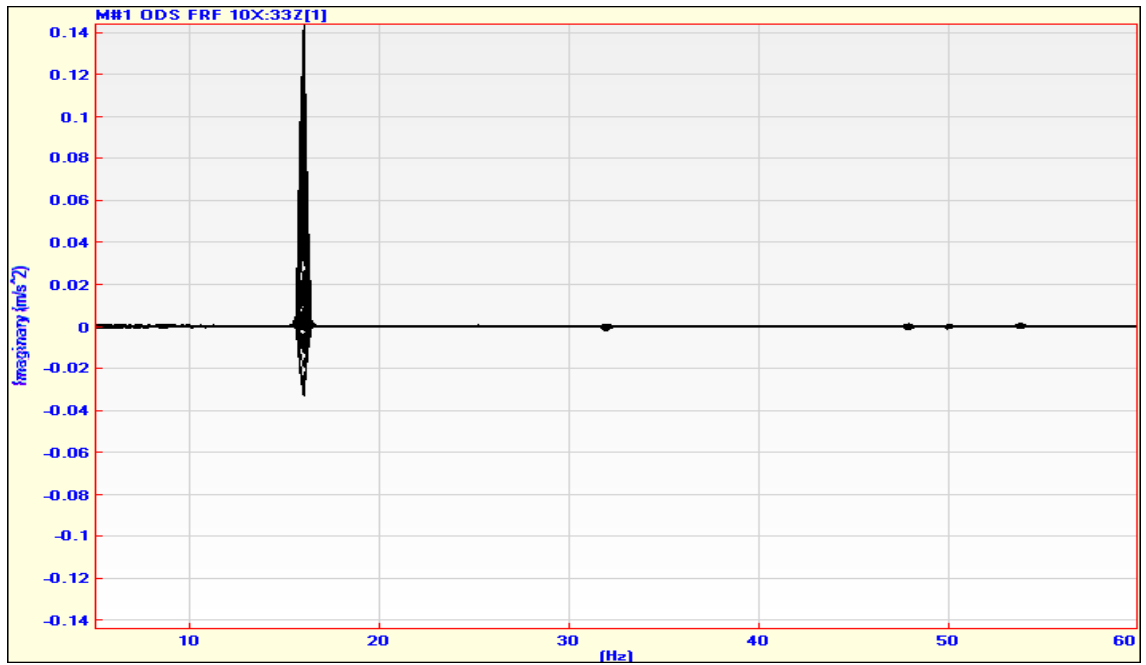


Figure 4.13 : Imaginary part of the ODS measurement FRFs of the pedestal structure at 16Hz

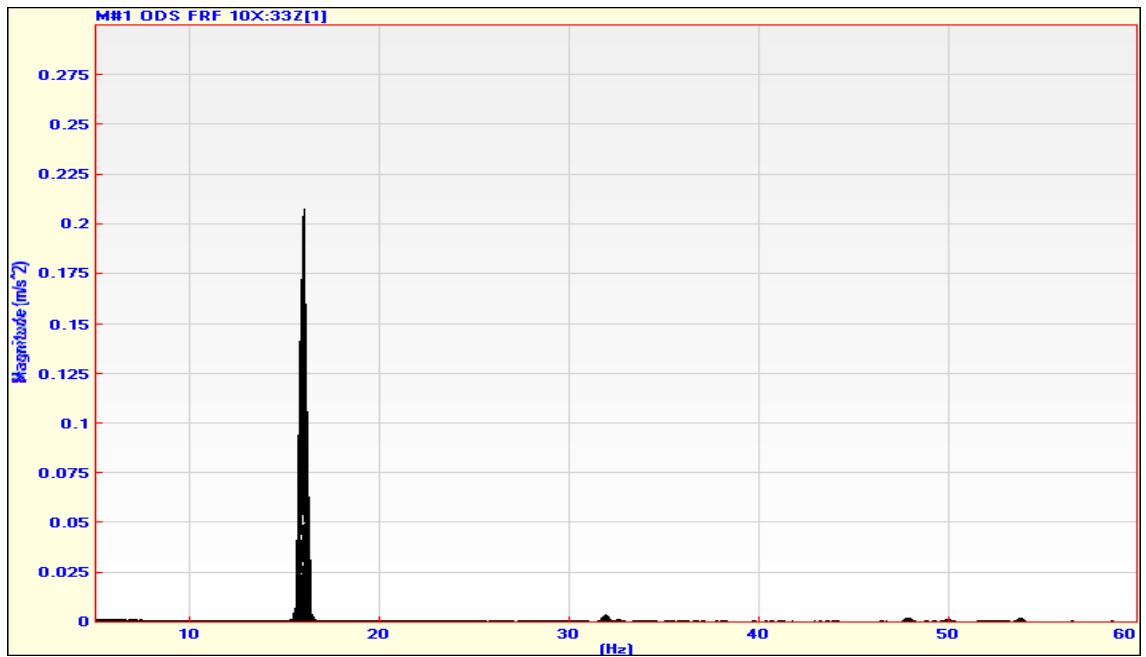


Figure 4.14 : Linear amplitude of the ODS measurement FRFs of the pedestal structure at 16Hz

Also, the Operating Deflection Shape at this frequency is depicted in Figure 4.15.

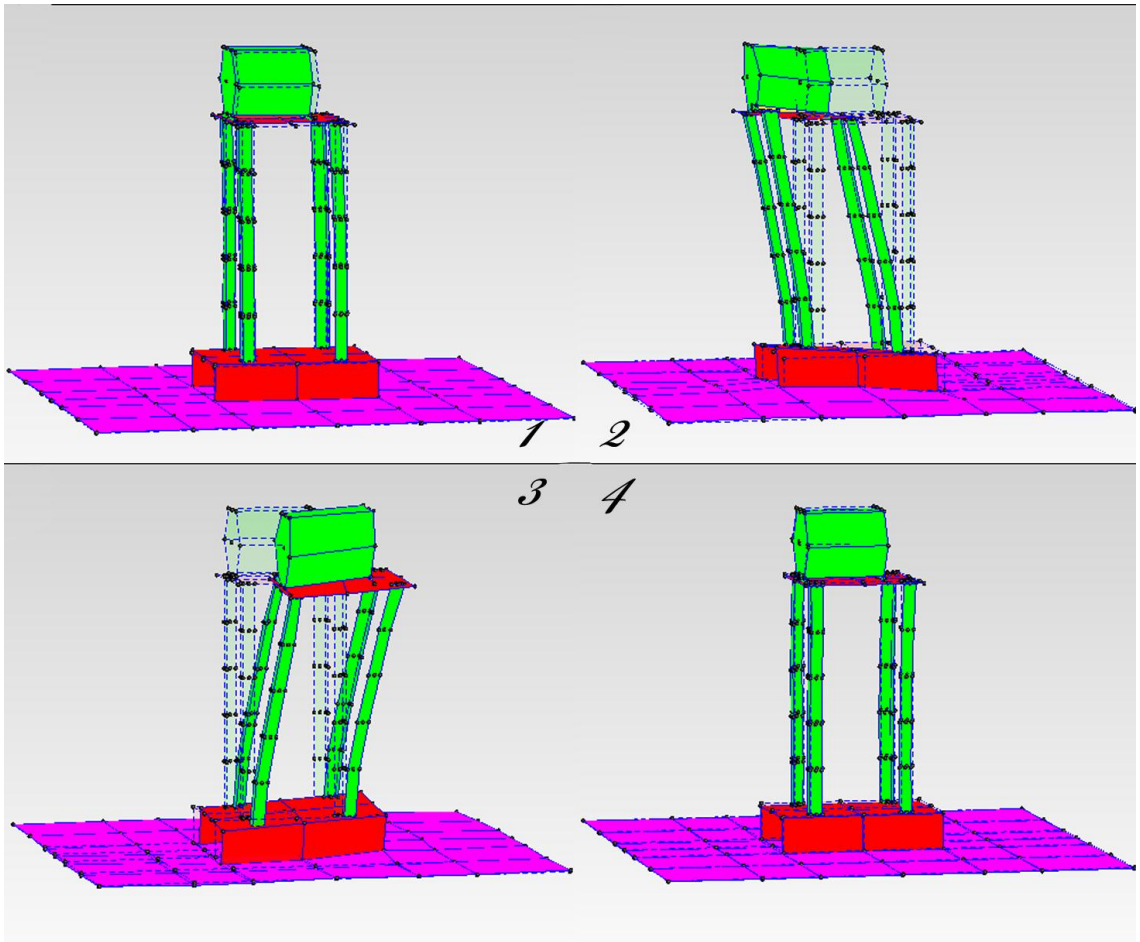


Figure 4.15 : Operating Deflection shape of the pedestal structure at 16 Hz

### 4.3 Finite Element Modal Analysis

As mentioned in the methodology, the main parameter in FEA is the validation of the model. For this research, the geometry of the structure was first modelled using SolidWorks software. This model was exported to Altair Hyper Works and the Modal analysis was performed on it. Then, according to methods introduced in the methodology, the FEA model was validated in comparison to EMA results. These two phases are described below.

#### 4.3.1 Geometry Design and Performing Modal Analysis

For this section of work, the geometry was modelled in SolidWorks according to the exact dimensions of the real structure. To simplify the model, some details such as washers, nuts, bolts and welding are neglected without significant loss in accuracy. Furthermore, for simplicity, the motor was designed in a way that its density is equal to the other parts of the structure. The designed geometry is shown in Figure 4.16 and Figure 4.17.

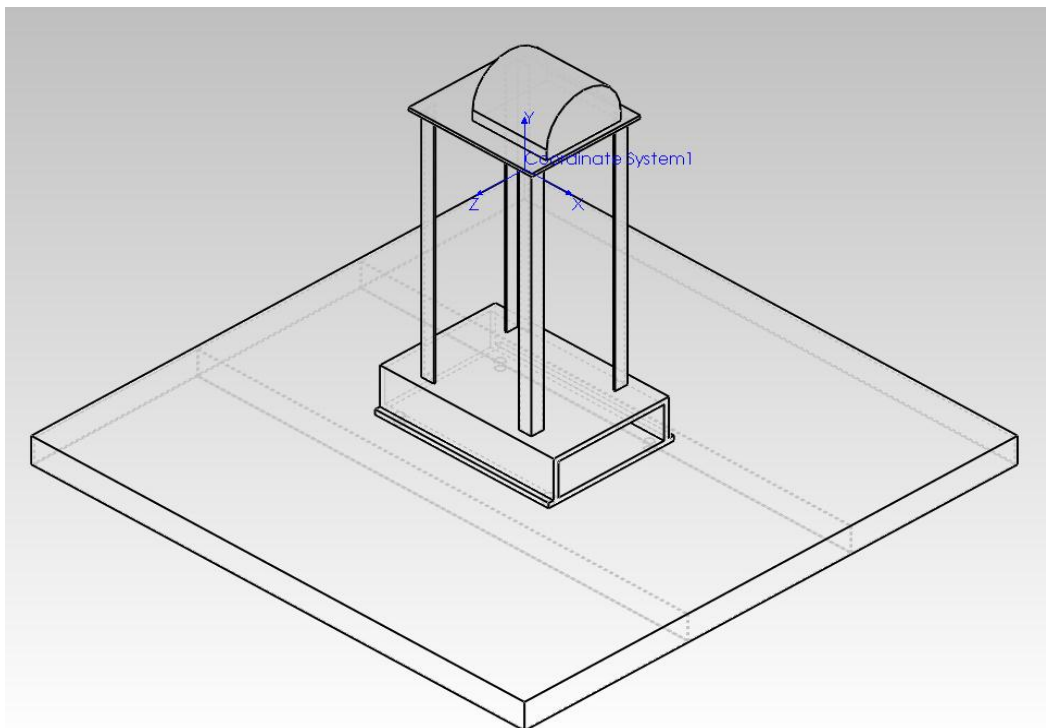
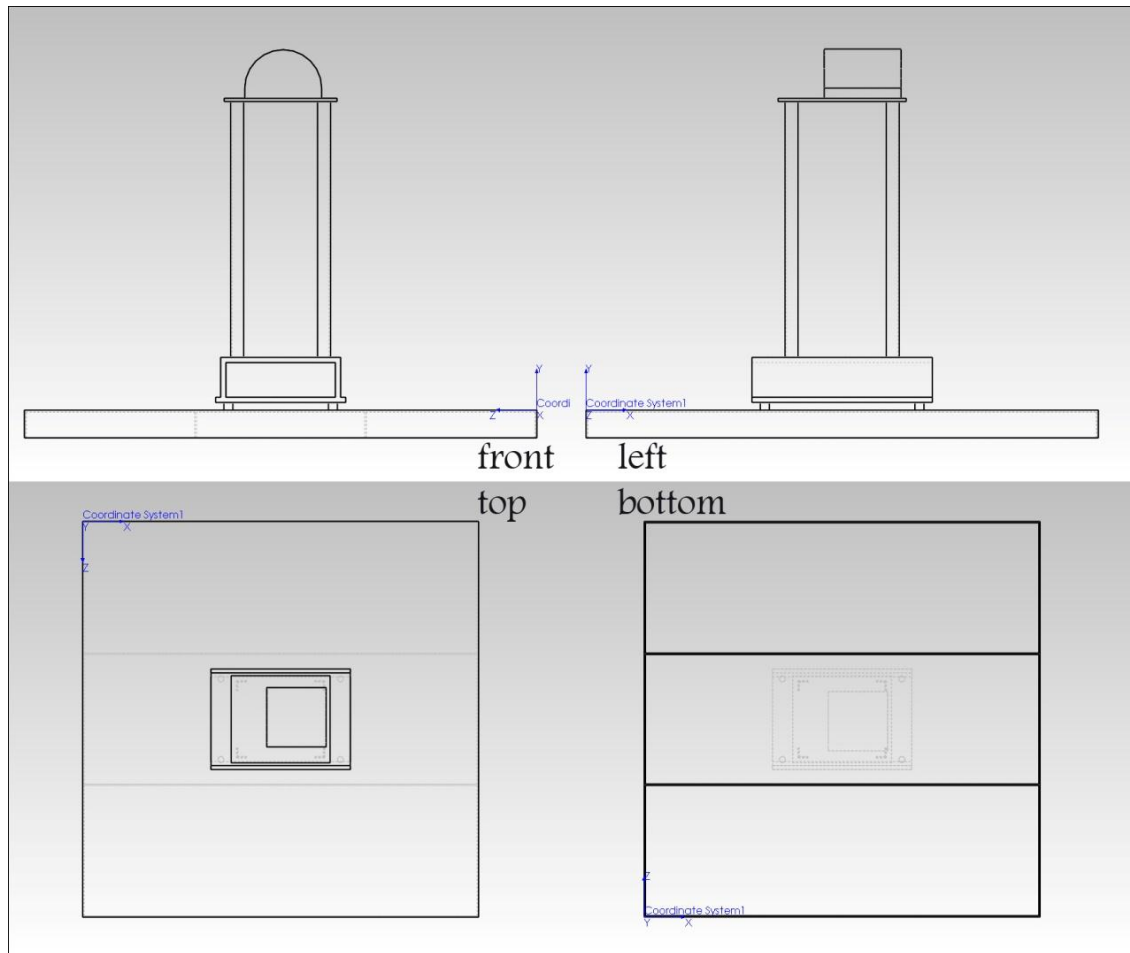
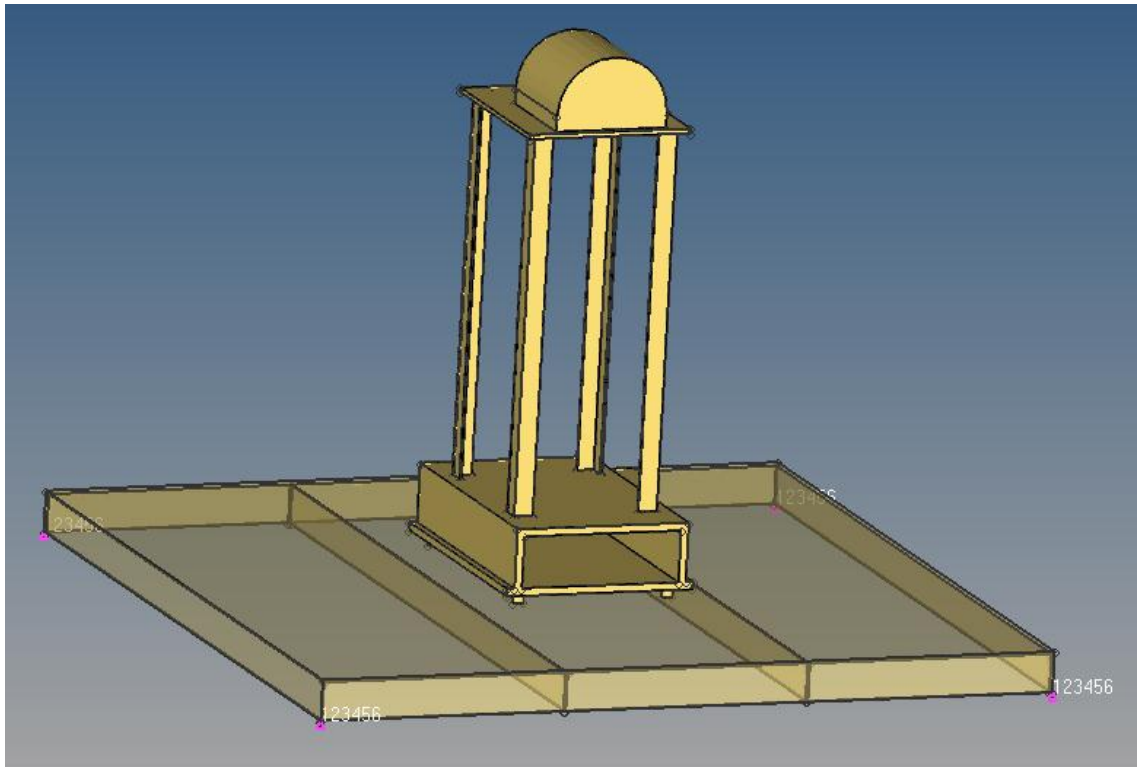


Figure 4.16 : Designed model by SolidWorks – isometric view



**Figure 4.17 : Designed model by SolidWorks**

In the next step, this geometry was exported to the Altair Hyper Works software as an \*.igs file. The model was then meshed with a fixed element size of 15 mm and a minimum of 3 mm for “Proximity”. The element type is the 3D tetra-mesh for solid volumes. This model is depicted in Figure 4.18.



**Figure 4.18 : Exported model to Hypermesh**

The properties assigned to the elements are Gray Cast Iron. These properties, also calculated by Chiat (Chiat, 2008), had the same values. There are three properties needed for modal analysis; Modulus of elasticity, density and Poisson ratio. For Gray Cast Iron, the modulus of elasticity=110 GPa, density=6719 Kg/m<sup>3</sup>, and the Poisson ratio is assumed to be 0.3. Furthermore, the boundary conditions are assumed as 6 DOF constraints at the 4 corners of the plat-form as depicted in Figure 4.19.

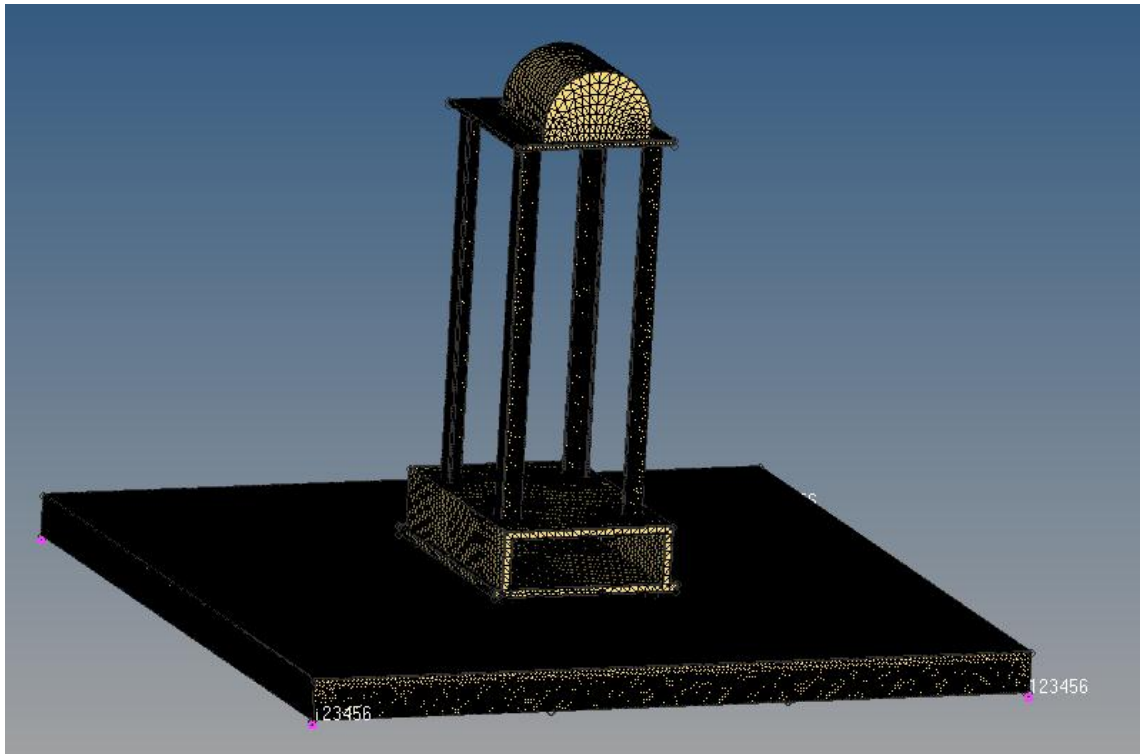


Figure 4.19 : Meshed model by Hypermesh

Next, the modal analysis was performed for the frequency range between 5 Hz and 70 Hz, since the maximum frequency range of the motor is 50 Hz.

#### 4.3.2 Model Validation

For this research, the flow chart in Figure 3.22 in the methodology was used to validate the model. Overall, the factors that are effective in the analysis are the geometry, boundary conditions, properties (modulus of elasticity, density, and Poisson ratio), and meshing. Among these properties, only boundary conditions and meshing were changed to get a reliable result since the other factors were distinctive. After each change in these parameters, the modal analysis was iterated and the results were checked with the EMA results. It also should be stressed that for model validation, the mode shapes and the natural frequencies were compared with the ones obtained from EMA. After many iterations and studying numerous models, the natural frequencies from Finite element modal analysis resulted in the data in Table 4.2.



Table 4.2 : Modal parameter resulted from finite element modal analysis

Mode number	Natural frequency (Hz)	Mode shape
1	13.2	Bending- left to right
2	17.9	Bending- front to rear
3	28.1	Bouncing
4	58	Torsional

The analytical mode shapes are depicted in Figure 4.20 to Figure 4.23.

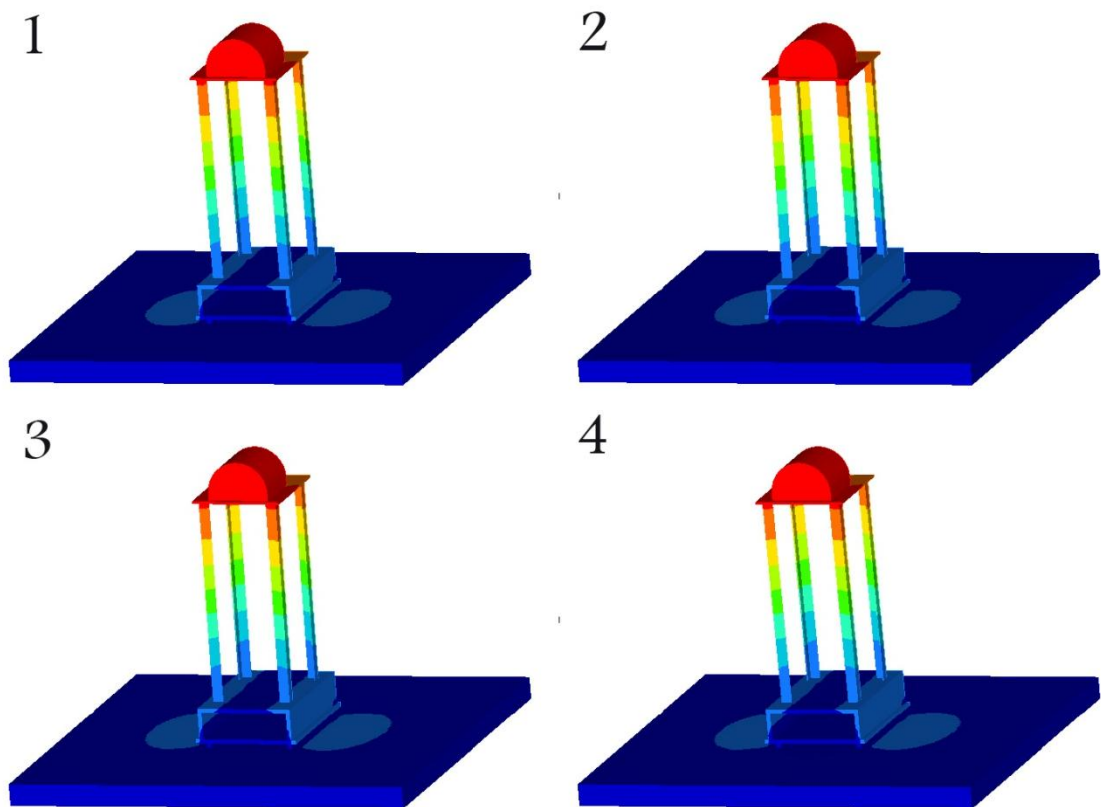


Figure 4.20 : Analytical mode shape- mode1- 13.2 Hz

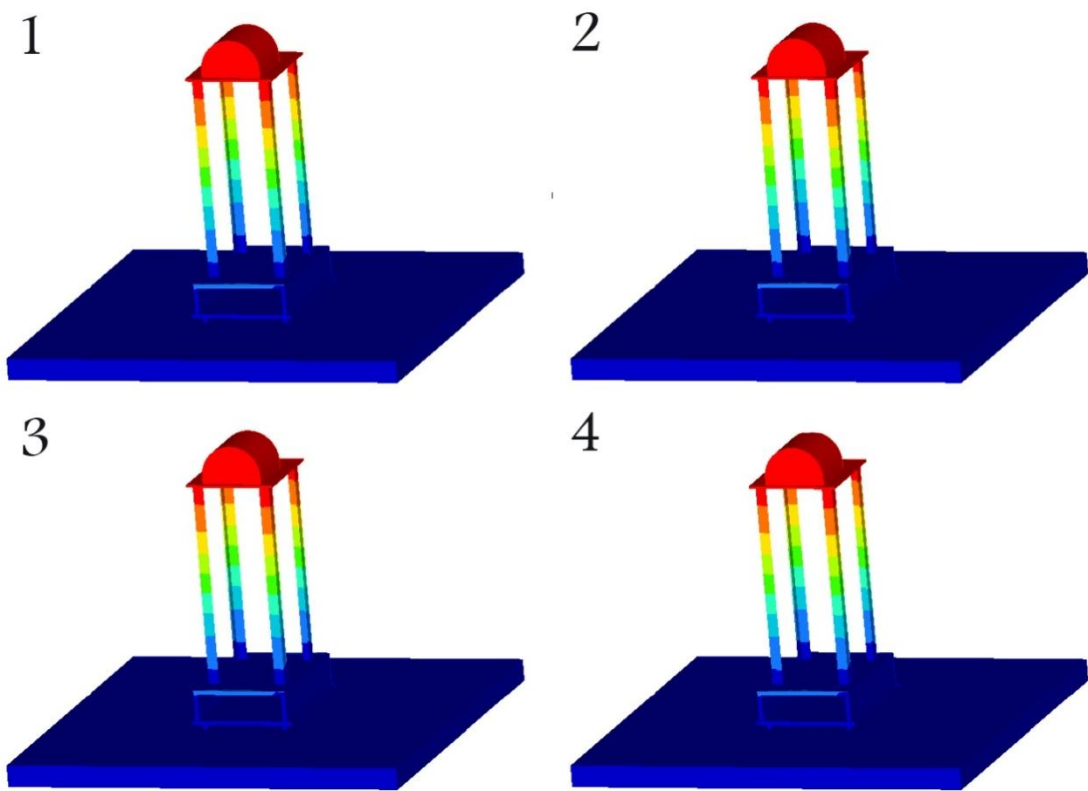


Figure 4.21 : Analytical mode shape- mode2- 17.9 Hz

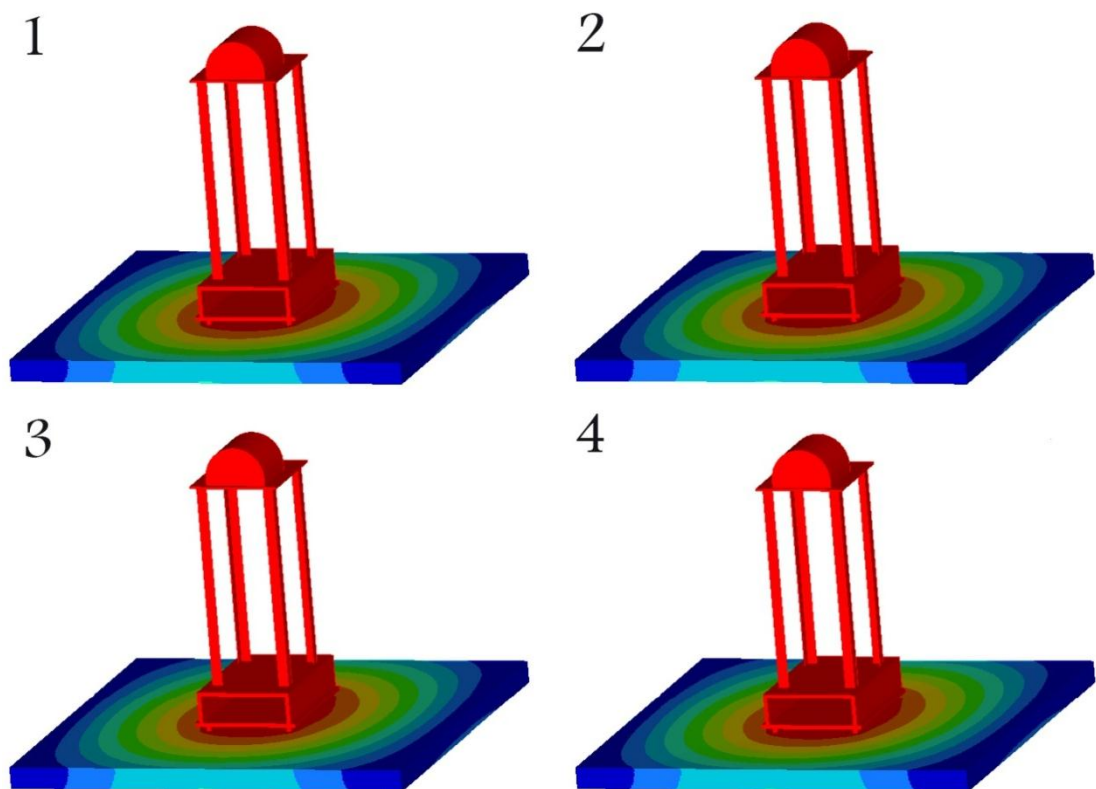


Figure 4.22 : Analytical mode shape- mode3- 28.1 Hz

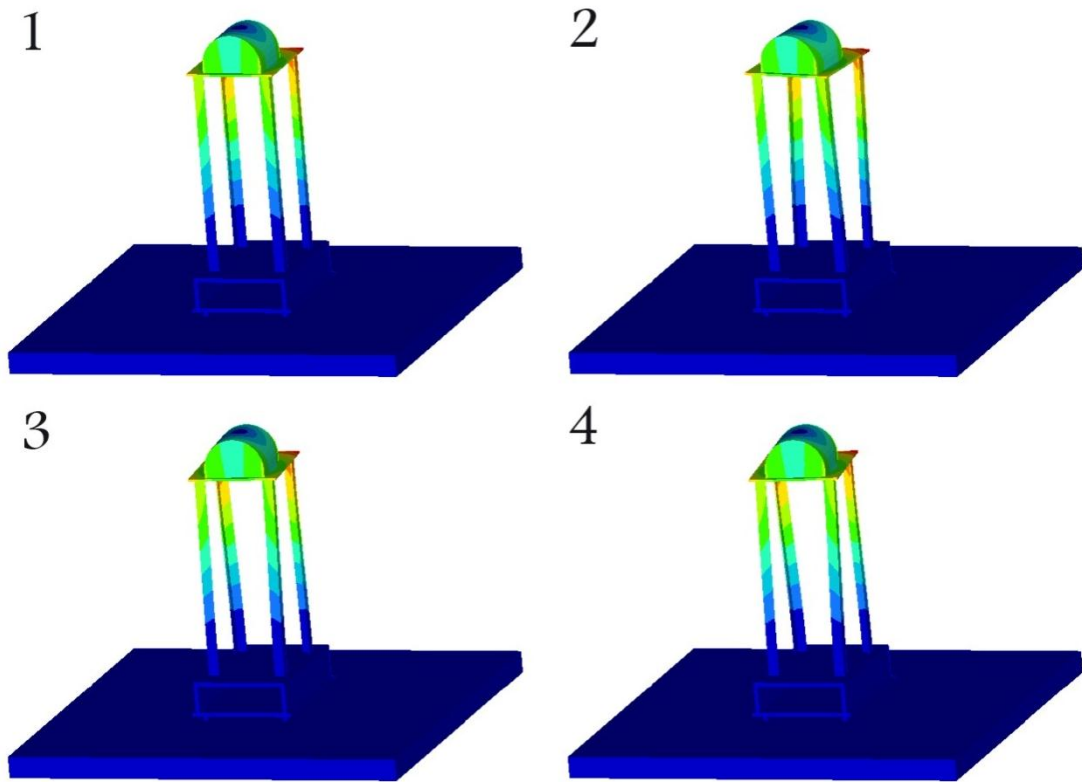


Figure 4.23 : Analytical mode shape- mode4- 58 Hz

#### 4.4 Optimization

As was the case earlier, the optimization of the structure was done to maximize the first and second natural frequencies to allow manufacturability of the new structure. In this way, the operator will be able to optimize the structure by adding simple new parts to the structure and reinforcing it rather than rebuilding the structure.

For this purpose, several responses (objective functions and constraints of optimization) were defined to the Hypermesh. Based on the visual estimation subsequently obtained from the software, a new model of the structure was developed. Modal analysis was then performed on this new model and the results of different assumed models were compared to choose the best one.

Furthermore, the designable area for this work assumed two parts consisting of the pedestal and the platform. The reason is that the movement of the structure in resonances comes not only from the pedestal but the platform also shows deformation.

The results of modal analysis in the form when only the pedestal was optimized show that the natural frequencies did not observe significant changes due to the deformation of the platform. These results are tabulated in Table 4.3.

**Table 4.3 : Finite Element modal analysis results after optimization of the pedestal only**

FEA results before optimization (Hz)	FEA results after optimization of the pedestal only (Hz)	deviation
12.2	12.5	2%
16.2	18.7	15%
33.7	33.4	0%
55	67.4	22%

Due to the limitation of adding new parts to reinforce the structure, the designable area in the pedestal was defined as a 3 mm-thick plate between the columns. Furthermore, the platform was defined as the designable area to identify the areas which need to be reinforced. The designable areas are depicted in Figure 4.24.

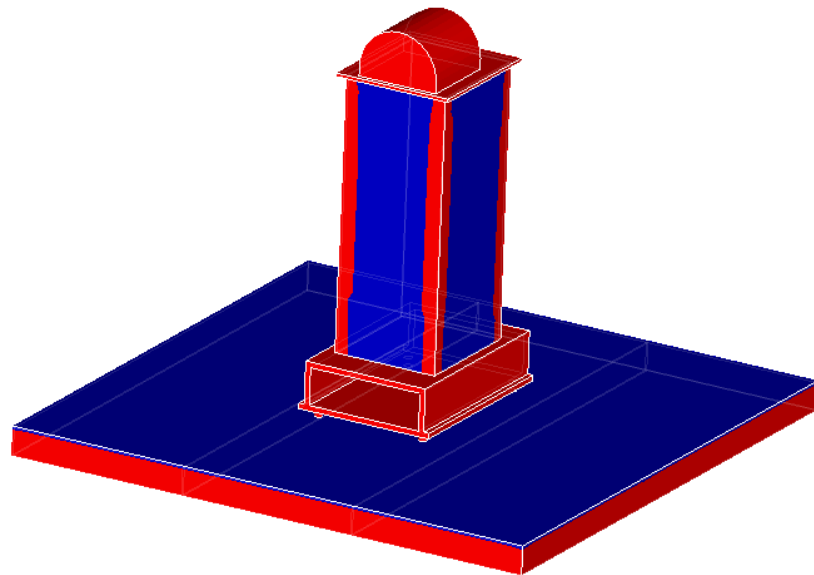


**Figure 4.24 : designable area of pedestal and platform**

The constraint of the optimization was chosen as volume-fraction, which has an amount equal to 50% of the designable area. This amount was chosen due to the

concept of reinforcement for this work, and the fact that a limitation for the weight of the structure did not exist.

The mesh size was the same as for modal analysis to increase the accuracy of the analysis. This is because changing the mesh size is one of the factors that will affect the results and we have got the best results from that mesh size. The model was meshed with a fixed element size of 15 mm and a minimum of 3 mm for Proximity. The element type was the 3D tetra-mesh for solid volumes.

Also, because the aim of the optimization was defined to shift the natural frequencies out of the excitation frequency range, and since there are two natural frequencies below 20 Hz, the first two natural frequencies were maximized. For this purpose, initially, the first natural frequency was maximized. For maximizing the second mode, two approaches were employed; maximizing the second mode based on the original model, and maximizing the second mode based on the results obtained from the optimized model for the first mode.

#### **4.4.1 Maximizing the First Natural Frequency**

In order to maximize the first natural frequency, as described above, the designable area was chosen as plate with 3mm of thickness between the columns of pedestal and the platform. The objective function was defined as maximizing the first natural frequency with 50% volume-fraction of the designable area as the optimization constraint. The results of optimization after 30 iterations are depicted in Figure 4.25 and Figure 4.26.

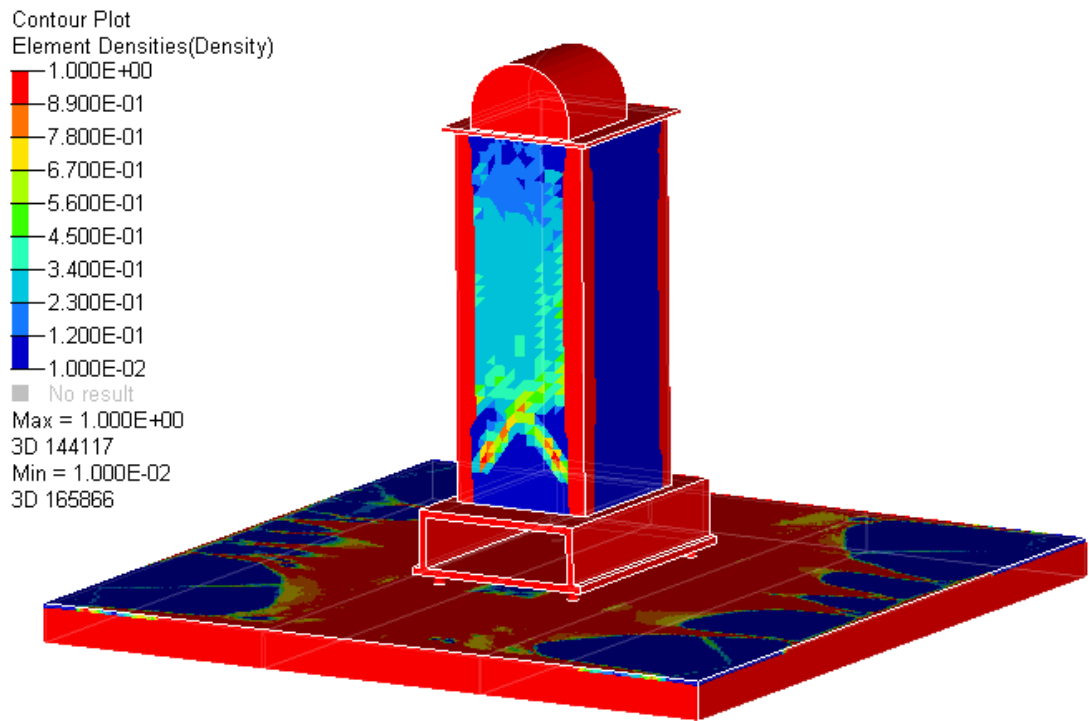


Figure 4.25 : Visual estimation results for optimizing the first mode after 30 iterations

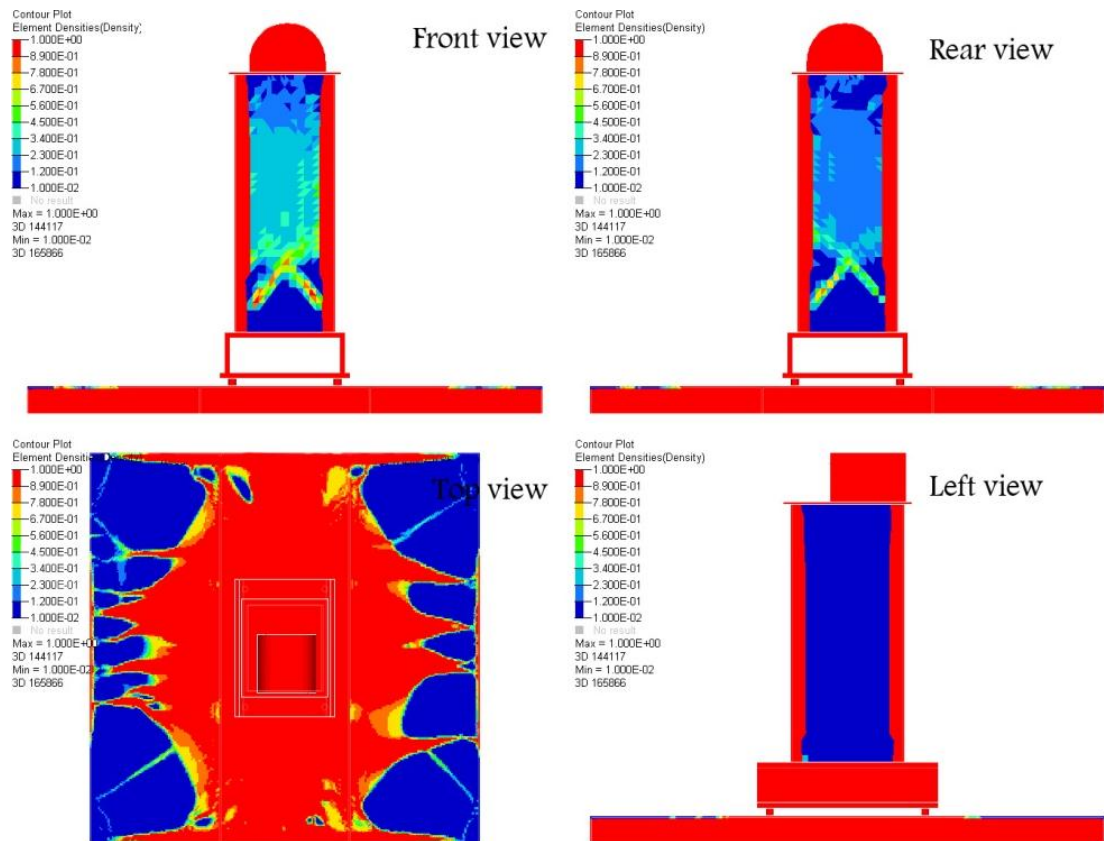
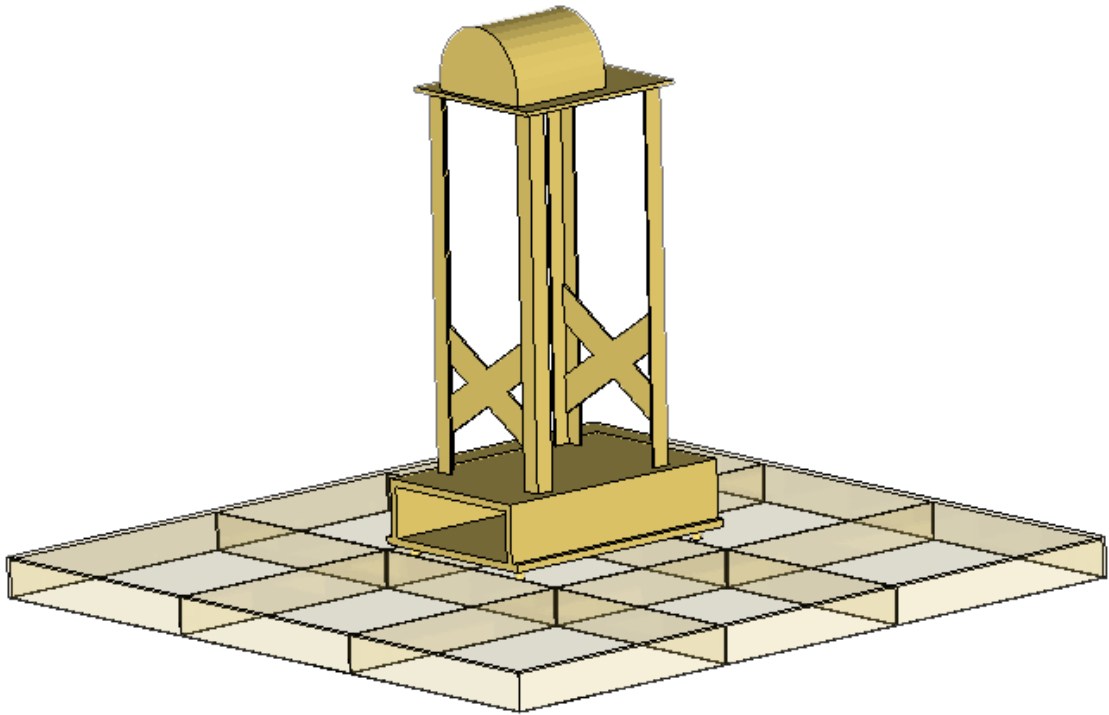


Figure 4.26 : Visual estimation results for optimizing the first mode after 30 iterations

In this contour plot, the red area shows the area with solid elements, and the blue one shows the area with void element. According to this estimation, the structure was

reinforced in both the platform and the pedestal. The pedestal was reinforced by adding two cross-plates, and the platform was reinforced by adding two vertical plates. Optimized structure is depicted in Figure 4.27 and Figure 4.28. The mode shapes and the natural frequencies for the optimized structure are tabulated in Table 4.4.



**Figure 4.27 : Optimized design structure according to visual estimations for the first mode**

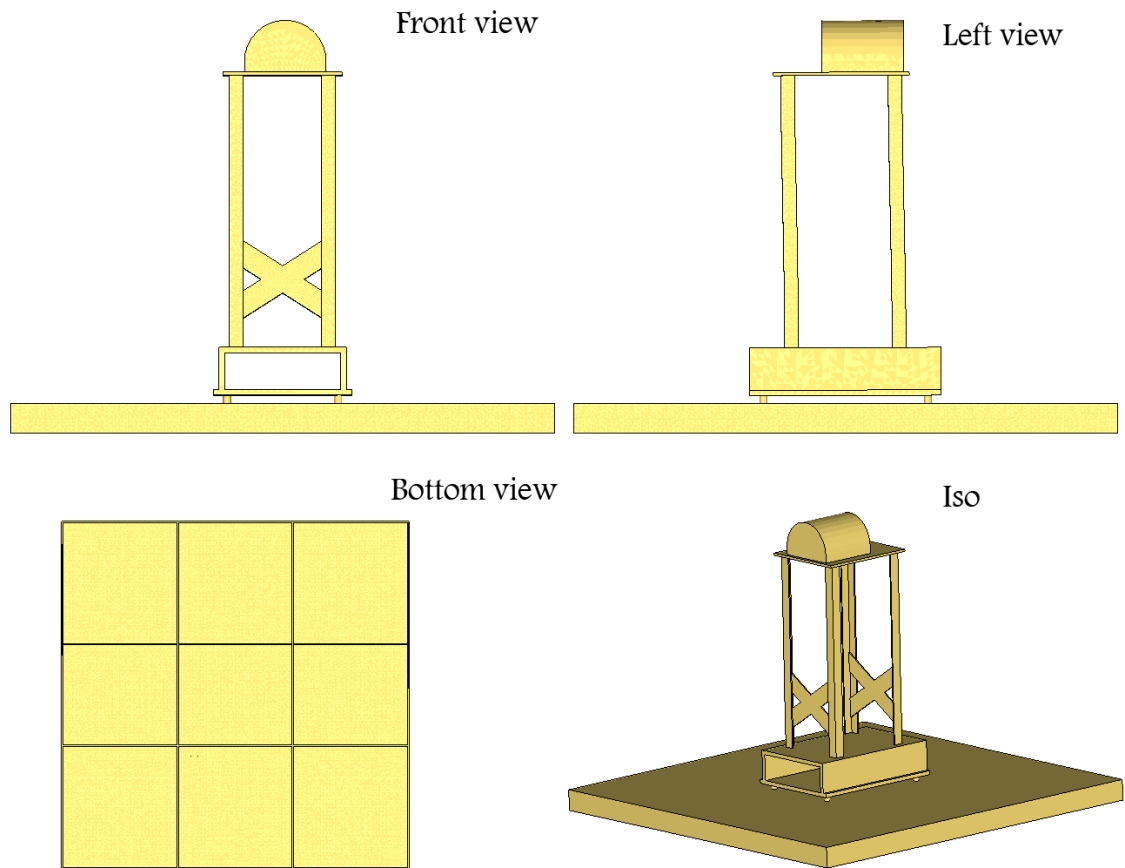


Figure 4.28 : Optimized design structure according to visual estimations for the first mode

Table 4.4 : Modal properties of the optimized structure for the first mode

Natural frequency after optimization (Hz)	Mode shape
26.4	Left to right bending
19.5	Front to rear bending
37.3	Bouncing
76.3	Torsional

#### 4.4.2 Maximizing the Second Natural Frequency- First Approach

As it can be seen in Table 4.4, there is still a frequency below 20 Hz. Therefore, the second natural frequency was maximized as well. In the first approach, the situation was completely similar to the first natural frequency optimization except the objective function, which was chosen to optimize the second natural frequency. The optimization result after 26 iterations is shown in Figure 4.29 and Figure 4.30.



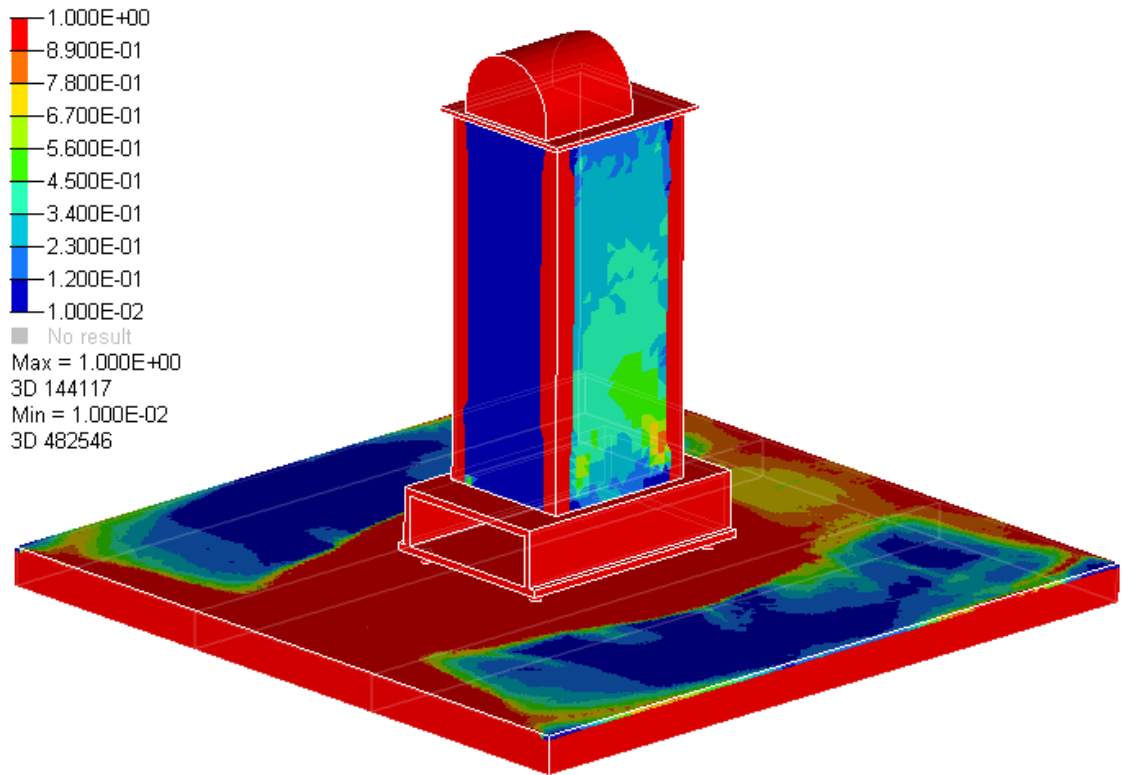


Figure 4.29 : Visual estimation results for optimizing the second mode after 26 iterations, first approach

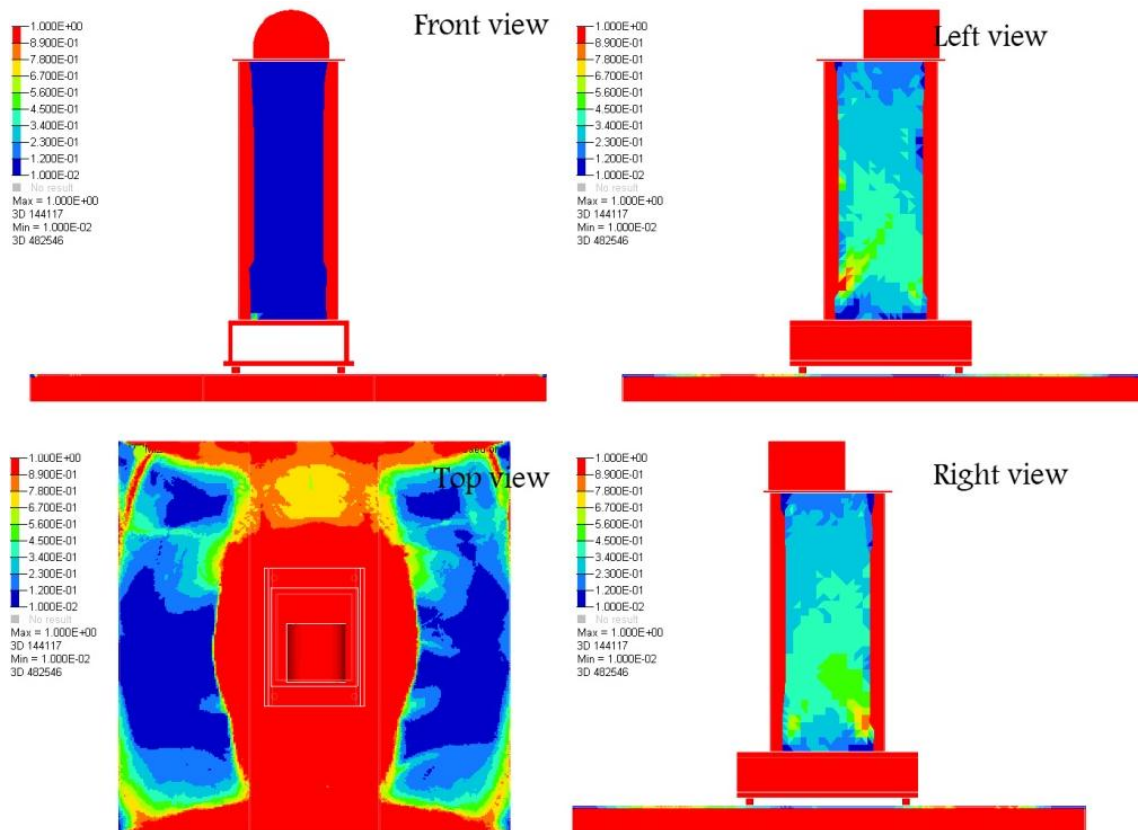
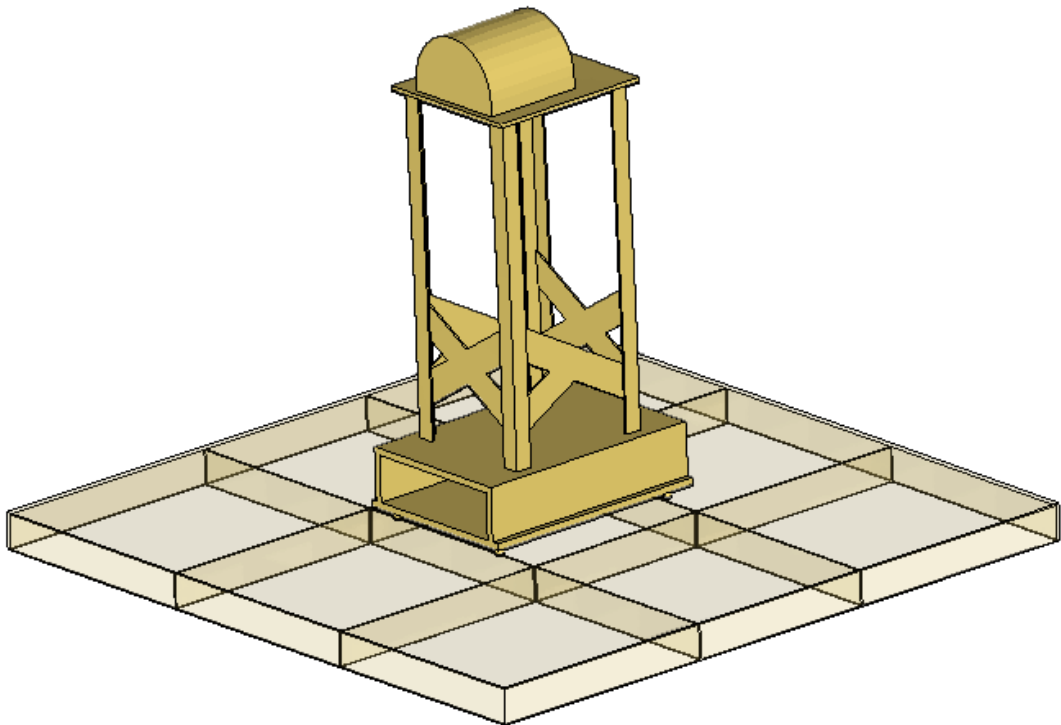


Figure 4.30 : Visual estimation results for optimizing the second mode after 26 iterations, first approach

According to the contour plot estimation, the structure was reinforced to maximize the second natural frequency. The result of this step was combined with the result obtained from the first step. The optimization for the platform was almost the same for both optimizations, but the reinforcement of the pedestal was completely separate from the first mode. Therefore, these two are combined together and the result is depicted in Figure 4.31 and 4.32. The natural frequencies and the mode shapes for the first and second mode optimized structure are tabulated in Table 4.5. It should be mentioned that since the fourth natural frequency after optimization exceeds the frequency limitation range of 70 Hz, it was neglected in the results.



**Figure 4.31 : Optimized design structure according to visual estimations for the first and second mode, first approach**

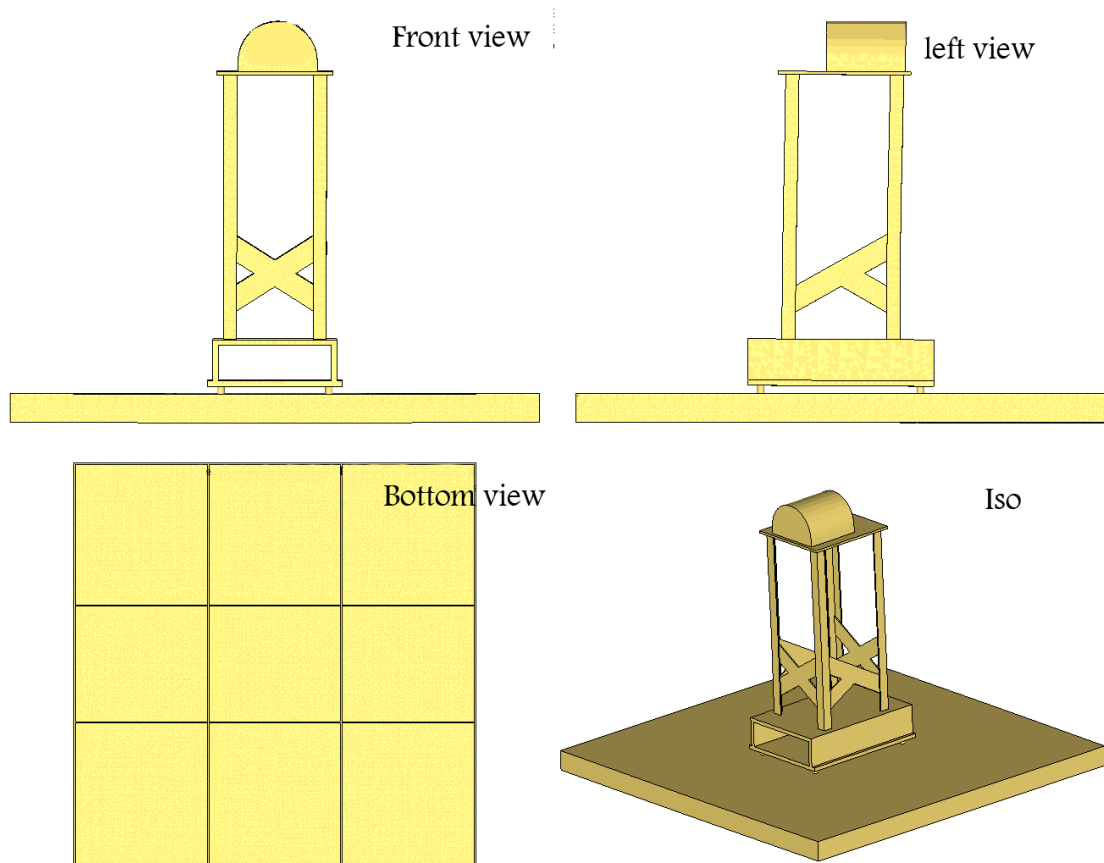


Figure 4.32 : Optimized design structure according to visual estimations for the first and second mode, first approach

Table 4.5 : Modal properties of the optimized structure for the first and second mode, first approach

Natural frequency after optimization (Hz)	Mode shape
27.3	Left to right bending
25.9	Front to rear bending
37.1	Bouncing

#### 4.4.3 Maximizing the Second Natural Frequency- Second Approach

This time the structure was optimized based on the results obtained from the optimized model for the first mode. In other words, the optimized form of the platform was used but the pedestal is assumed to be the same as the first step. It also should be stressed that after the first step of optimization, the arrangement of the first and second natural frequencies were changed. Therefore, for this approach, the optimization was done to maximize the first natural frequency that has front to rear mode shape and is

equal to the second mode of the original structure. The optimization result after 30 iterations is shown in Figure 4.33 and Figure 4.34.

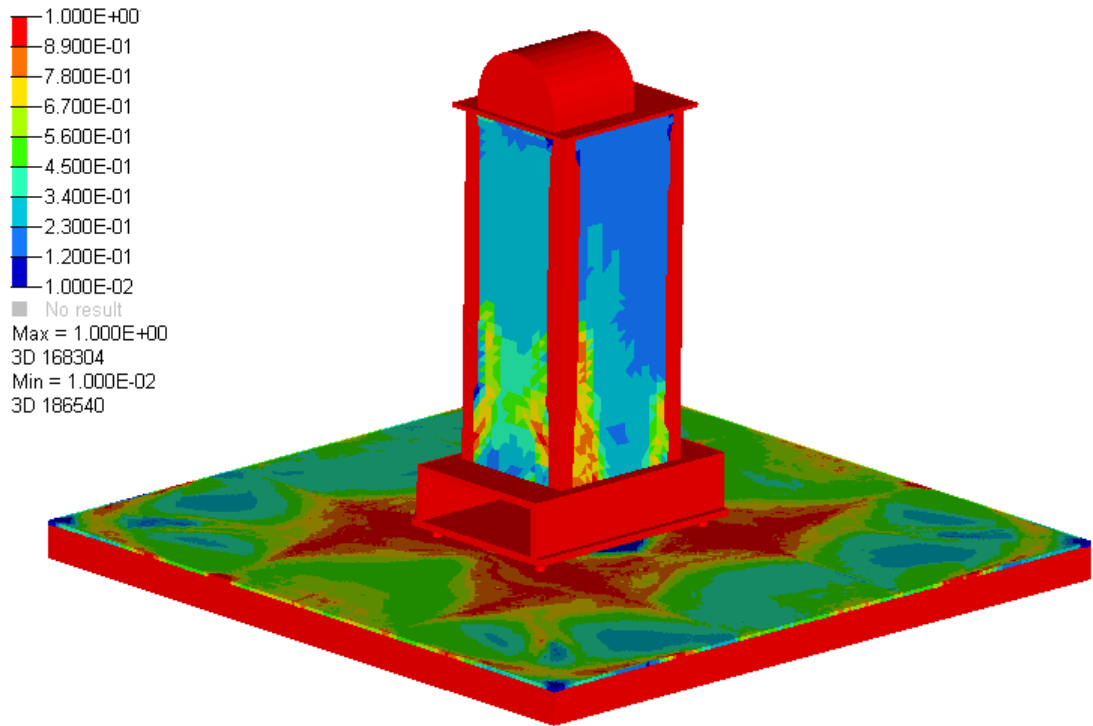


Figure 4.33 : Visual estimation results for optimizing the second mode after 26 iterations, second approach

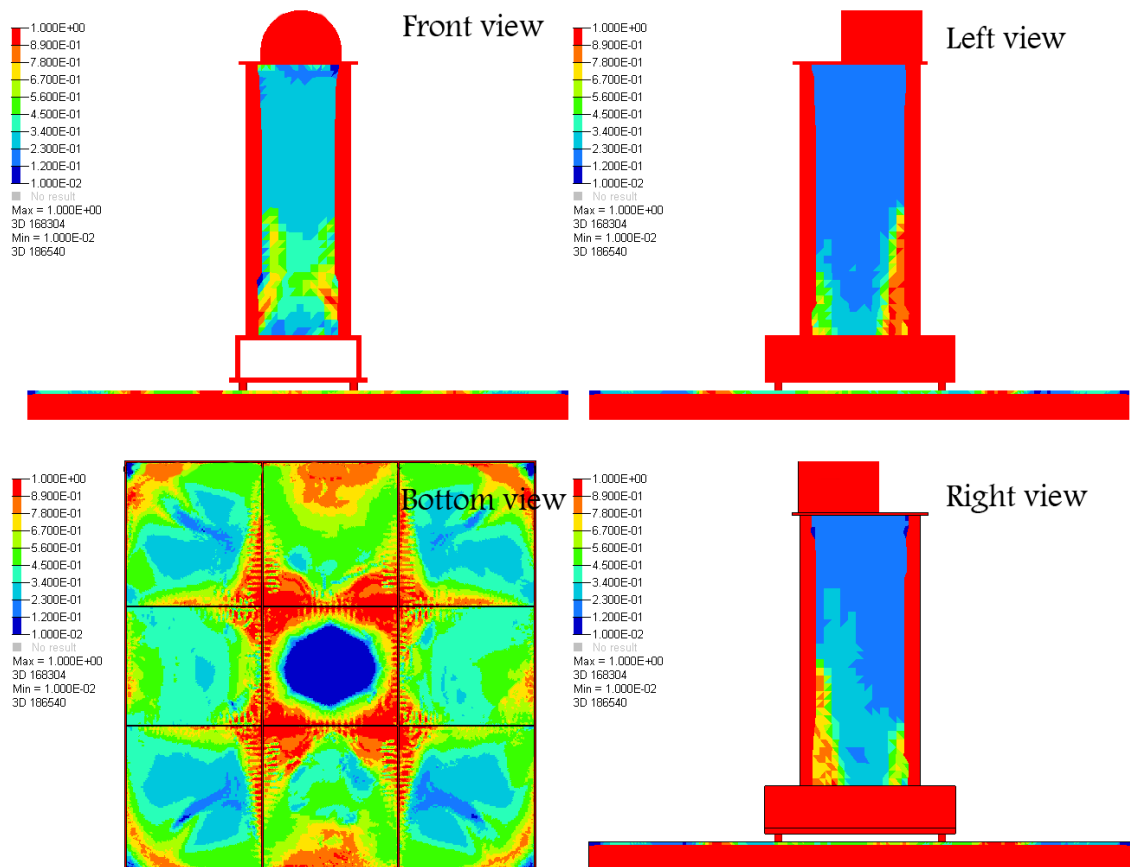


Figure 4.34 : Visual estimation results for optimizing the second mode after 26 iterations, second approach

According to the contour plot estimation, the structure was reinforced for maximizing the second natural frequency of the original structure. The combined model of this approach and the model obtained from the first step are depicted in Figure 4.35 and Figure 4.36. The natural frequencies and the mode shapes for the first and second mode optimized structures are tabulated in Table 4.6.

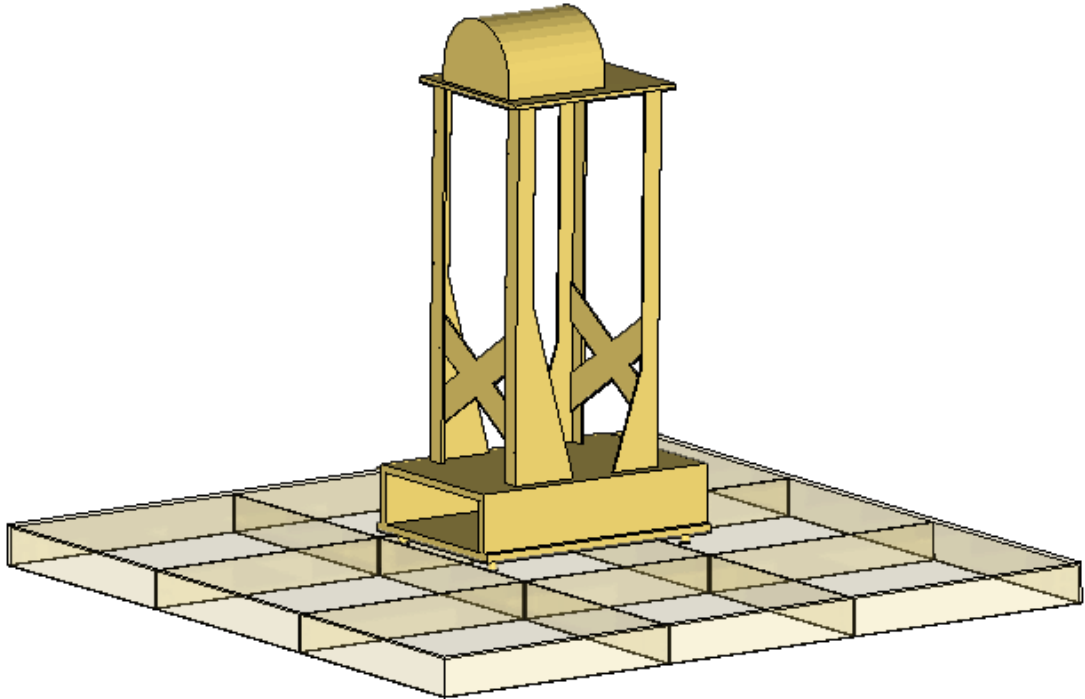


Figure 4.35 : Optimized design structure according to visual estimations for the first and second mode, second approach

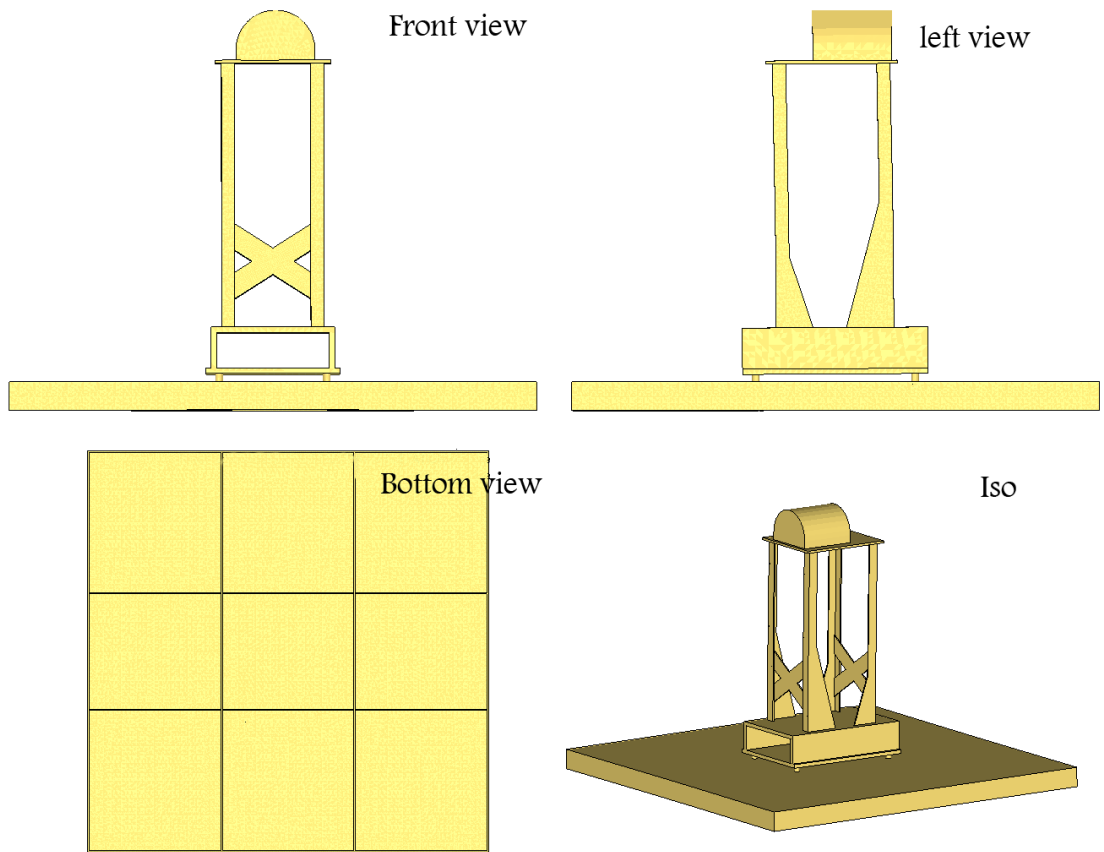


Figure 4.36 : Optimized design structure according to visual estimations for the first and second mode, second approach

Table 4.6 : Modal properties of the optimized structure for the first and second mode, second approach

Natural frequency after optimization (Hz)	Mode shape
27.5	Left to right bending
25.7	Front to rear bending
37.2	Bouncing

## **Chapter Five**

### **5 Discussion**

This chapter discusses the results obtained from the different parts of this research presented in pervious chapter. It contains four subchapters; Experimental modal analysis, ODS measurement, Finite element modal analysis, and structural optimization.

#### **5.1 Experimental Modal Analysis**

Every vibration analysis needs experimental data to describe dynamic properties of the system. As it has been mentioned earlier, these experimental data can be obtained by collecting modal data (modal testing) or by collecting operating data (ODS). But it is always difficult to distinguish the preferred one. To optimize the system, we needed the modal data since it is only the modal data that gives true principle characteristics of the system. On the other hand, the optimization was supposed to be performed in order to decrease vibration failures of the system due to the motor operating effects. Hence, we needed the force response of the system that only the ODS measurement can provide such information, because the modal data are independent of the forces on the system. Furthermore, only ODS can depict how the structure behaves in service. It is very important for optimization of the system because it can present an initial estimation which shows the parts of the structure that is needed to be reinforced. As it came in the results, both the Modal testing and the ODS measurement have been carried out for this research as discussed below.

### 5.1.1 Modal Testing

The aim of this research is to optimize the structure for the occasions that the motor operates below 50 Hz. Therefore, it is important to identify the modes below 50 Hz. For this purpose, the Modal testing has been performed on the structure and as the results show, this structure has 4 modes below this frequency. Such data are the most basic data that are used to validate the FEA model and after the optimization, the results compared with the pervious data have been already done on this structure by (Chiat, 2008). The results are compared in Table 5.1.

Table 5.1 : Comparison of obtained modal parameters with results from (Chiat, 2008)

EMA results from (Chiat, 2008) (Hz)	EMA results from my experience (Hz)	Mode Shape	Error
12	12.1	Left-right bending	0.8%
16	16.7	Front-rear bending	4.4%
31.4	31.4	Bouncing	0%
47.1	53	Torsional	12.5%

The maximum operating frequency of the motor is 50Hz but the using frequency range of the motor will be at most 20 Hz. obviously, the structure has two modes in the low frequency, below 20 Hz, that can cause resonant vibration and make the structure unstable. The first mode occurs at 12.1 Hz and is a left-right bending mode. The second mode occurs at 16.7 Hz and is a rear-front bending mode. Furthermore, from the results obtained from MEScope, it can be observed that these two modes lead to deformation not only in the pedestal, but also a deformation in the platform. It is important because to optimize the structure we needed to know what parts of the structure should be selected as the designable area. Otherwise, the optimization will not be reliable.

On the other hand, optimization of the structure was going to perform by FEA based software. Therefore, an exact Finite-Element model was vital for this research.



The finite element model is not reliable on its own and needs to be validated by experimental data. Hence, the experimental modal parameters were used to validate the Finite Element model.

## **5.2 ODS Measurement**

As it has already been mentioned, recognizing the natural frequencies is crucial to optimize the structure. However, along with reorganization of the natural frequencies and the mode shapes, the real deflection of the structure is also quite important that has been done by performing the ODS measurement. Similarly, the results of the ODS can validate the Modal Testing data. Therefore, the ODS measurement has been done for two natural frequencies at 12.1 Hz and 16 Hz.

As it has been mentioned in the methodology, the deflection shape resulted from ODS measurement at the natural frequencies should be similar to the mode shapes of the structure. The animation results of the ODS measurements show that the deflection shape of the structure at 12.1 Hz is a combination of both left-right bending and rear-front bending whose major part is left-right bending. This is very close to the mode shape of the structure at 12.1 Hz. Furthermore, FRFs show a high peak at 12.1 Hz that validate the existence of a natural frequency at this frequency. The results at the 16 Hz are as well as 12.1 Hz. The major part of the deflection shape at 16 Hz is rear-front bending that is similar to the second mode shape of the structure. Furthermore, the FRFs show a high peak at 16 Hz that validate existence of a mode at this frequency.

The EMA data show that there are two modes that need to be maximized out of the using frequency range of the motor. Furthermore, these results illustrate that the two parts of the structure have the most deformation due to resonant vibration, pedestal and the platform. Therefore, these two parts are selected as the designable areas for the optimization. These data also used to validate the Finite Element model by comparing the results obtained from Finite element modal analysis and EMA data.

### 5.3 Finite Element Modal Analysis

The aim of this part of research was to make a finite-element model of the structure for optimization section. To this end, the finite-element model needed to be validated by experimental data. Since the optimization was going to be performed according to vibration parameters of the system, the EMA data was used to validate the model.

Since the HyperMesh is not a user friendly software for modelling, the geometry model was built by SolidWorks software and exported to HyperMesh as an \*.igs file to perform modal analysis and topology optimization on the structure.

Since one of the most important factors in doing FEA is memory usage and the duration of the analysis, some simplicities were used during the modelling and analysis but in a way that it does not decrease the accuracy significantly. These simplicities specially were important for optimization process because it is an iterative process with huge memory usage. Totally, two simplicities were used to simplify the motor shape, namely, model the structure as one component, and using a same element type. The shape of the motor does not have a considerable role in natural frequency or mode shape; however, its weight was significantly important. So, according to the weight of the motor, the shape was made in a way that its density is equal to the density of the rest of the structure parts. It should be stressed that the position of the motor on the plate is the same as the real structure. In this way, no more than one property was assigned to all elements. The other simplicity was that the whole structure was modelled as if only one component and connectors were modelled as welded connectors. The third simplicity was that the whole structure was meshed by solid elements. Shell element type could have been used, but since the solid element was reliable for modal analysis, it was used to simplify the analysis preparation.

Another thing that should be mentioned here is that mesh properties such as the mesh size and the mesh shape have a significant influence on the results of the analysis. Therefore, a fixed mesh property was used during the modal analysis and optimization because the optimization was done based on the finite-element model validated by that mesh property.

The comparison of natural frequencies from FEA and EMA has been done employing two methods; calculating the error which should be less than 10%, and a graphical comparison. As it has been discussed in the methodology, the diagram of identified values from EMA versus the calculated ones from FEA should lay on a straight line with a slope of 1. This graphical correlation is depicted in Figure 5.1 and the error method is tabulated in Table 5.2.

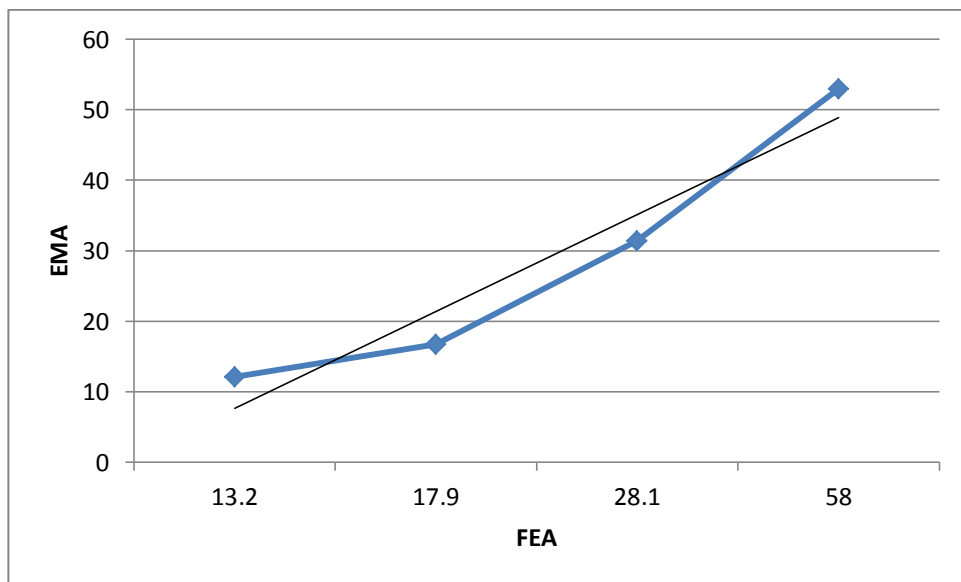


Figure 5.1 : graphical validation of FEA results

**Table 5.2 : comparison of FEA and EMA results by error method**

Mode Number	EMA result (Hz)	FEA result (Hz)	Error (%)
1	12.1	13.2	8%
2	16.7	17.9	6.7%
3	31.4	28.1	10%
4	53	58	8.6%

As it can be seen from the results of two methods, the graphical validation is satisfied because the slope of the average line is almost 1. Furthermore, by calculating the number of errors, it can be observed that the error for every value is less than 10%. Therefore, it can be said that the finite-element model is validated to be used in the optimization process.

#### **5.4 Structural Optimization**

As the results shoes, the structure was optimized to shift the first and second natural frequencies out of the performing frequency range of the motor through employing of a finite element based software, HyperMesh. Since the software is able to consider only one mode at a time, structural optimization for the first and second natural frequencies was conducted separately and in sequence, and then, the results were combined together to get the final model.

This optimization was done according to the simplest manufacture able structure. This point was considered by only adding simple new parts and reinforcing of the structure. Furthermore, due to the influence of the mesh property on the results, mesh properties used for optimization were the same as the ones used for modal analysis.

The form of optimization is related to the designable area, boundary conditions, objective function, and optimization constraints. By considering the aims of the project

and by changing the effective parameters, several models were obtained during the optimization process and the most efficient and effective ones were chosen that are discussed below.

#### 5.4.1 Maximizing the First Natural Frequency

As it is shown in the results, the structure was optimized to maximize the first natural frequency by adding two crossed plates between the columns and some vertical plates on the platform as depicted in Figure 4.27 and Figure 4.28. The estimated changes of the natural frequencies before and after the reinforcements are tabulated in table 5.3.

**Table 5.3 : Estimated changes of natural frequencies before and after the reinforcement for maximizing the first mode**

Natural frequency before optimization (Hz)	Natural frequency after optimization (Hz)	Mode shape	deviation
13.2	26.4	Left to right bending	100%
17.9	19.5	Front to rear bending	9%
28.1	37.3	Bouncing	3%
58	76.3	Torsional	3%

As the results indicate, the estimated frequency of the first mode was increased by 100% in comparison with the frequency prior to the optimization. As it was expected, the first natural frequency was shifted out of the motor operating frequency range that satisfies the expectations. Furthermore, the other result that can be inferred from the table is that the structural optimizations for the first and second modes are independent since the deviation of the frequencies before and after the optimization for the second mode is only 9%. It was predictable from the mode shapes because the first two mode shapes are bending modes in different directions, so the reinforcement of the structure in one direction is independent of the other.

Due to this independency, after maximizing the first natural frequency, the second natural frequency is in the low frequency range and is needed to be maximized. The second mode was optimized by using two approaches. The first one was done based on the original structure, and the second one was done based on the resulted structure from the first mode optimization.

#### 5.4.2 Maximizing the Second Natural Frequency- First Approach

As it has been already mentioned, the first approach towards optimization was conducted based on the original structure. As it was illustrated in the section 5.4.1, optimization for the first and second modes is independent due to the mode shapes of the structure. It means that we can perform superposition principle and therefore, the results for the first and second mode were combined together. The shape of this approach is depicted in Figure 4.31 and Figure 4.32. The estimated changes of natural frequencies before and after the reinforcement are tabulated in Table 5.4. Since, the frequency of the fourth mode was more than 70 Hz after optimization; it was not considered here in the following table.

**Table 5.4 : Estimated changes of natural frequencies before and after the reinforcement for maximizing the second mode, first approach**

Natural frequency before optimization (Hz)	Natural frequency after optimization (Hz)	Mode shape	deviation
13.2	27.3	Left to right bending	107%
17.9	25.9	Front to rear bending	45%
28.1	37.1	Bouncing	32%

As it is evident in the table, the frequency of the second mode has increased from 17.9 Hz to 25.9 Hz and it is 45% deviation between the frequencies before and after the optimization. The results of this approach were satisfactory because after combination of two modes, the frequencies of the first and the second modes are more than 20 Hz, the operating frequency of the motor.

### 5.4.3 Maximizing the Second Natural Frequency- Second Approach

In the second approach to optimization of the second mode, the concentration was on the results of the optimized structure from the first mode. The shape of this approach is depicted in Figure 4.35 and Figure 4.36. The estimated changes of natural frequencies before and after the reinforcements are tabulated in Table 5.5.

Table 5.5 : Estimated changes of natural frequencies before and after the reinforcement for maximizing the second mode, second approach

Natural frequency before optimization (Hz)	Natural frequency after optimization (Hz)	Mode shape	deviation
13.2	27.5	Left to right bending	107%
17.9	25.7	Front to rear bending	45%
28.1	37.2	Bouncing	32%

The results of this approach are almost the same as the result of the first approach and shift the second natural frequency of the structure out of the motor operating frequency range, to 25.7 Hz.

### 5.4.4 Benefits of Each Approach for Optimization of Second Mode

Since the optimization of the structure was done based on the manufacturability and reinforcement of the structure, one of the assumptions of the optimization is that the operator should be able to perform the structural optimization results in the easiest way. According to this assumption, each result has its benefits and limitations.

The benefit of optimization for the first mode is that its installation is easy, and it can be bolted to the pedestal. The first approach of the optimizing the second mode has this benefit as well, and it can be easily bolted to the columns of the pedestal. On the other hand, in the second approach, the plate should be welded to the pedestal. In comparison to bolting, welding is more difficult but the shapes of the plates are simpler.

## **Chapter Six**

### **6 Conclusion and Recommendations**

General conclusions of this research are summarized in this chapter. Furthermore, suggested areas for additional works are introduced.

#### **6.1 Conclusions**

The aim of this research was structural dynamic modification of a vibrating structure by using of the topology optimization method in order to find the most effective design of a pedestal structure on which an electrical motor is installed. So, by applying modal testing and ODS measurement, the dynamic characteristics of a vibrating structure was ascertained. Furthermore, based on topology optimization method, the optimum design of the structure was determined.

In this work, according to the defined objectives, a structural vibration analysis was successfully done to get the vibration properties of the structure. At first, a modal testing and an ODS measurement have been applied on the structure to recognize the natural frequencies, mode shapes, and exact deflection shape of the structure. The modal testing showed that the structure has two modes at 12.1 Hz and 16.7 Hz which are below the assumed motor operating frequency range. The first two mode shapes of this structure were also determined which are “left to right bending” and “rear to front bending,” respectively. The ODS measurement showed the exact deflection shapes related to these natural frequencies. Afterwards, the finite element model of the structure was verified by comparing with the experimental data. Two parameters were evaluated for verification of the FEM results: The first one was about the error between the values obtained from finite element modal analysis and EMA, which were less than



10%, and the second one was a direct correlation between the values, which the points were laid on a straight line with a slope of 1.0. Next, a topological optimization was applied to get the new structure condition and shape. According to the visual estimation resulted from topology optimization, the modified structure of the pedestal was proposed. Then, by applying the FEA modal testing to the new design, it was observed that both of the natural frequencies shifted from 12.1 Hz and 16.7 Hz to 27.5 Hz and 25.7 Hz, respectively. Accordingly, there would not be any natural frequency under motor operating frequency range. In addition, the fabrication of this new proposed design will have an uncomplicated fabrication procedure.

As a conclusion, topology optimization method could be used to find the most effective design for structural dynamic modification of vibrating structures. Moreover, less time is needed to achieve to the results compared with trial and error methods.

## **6.2 Recommendations for Future Works**

In this work, the objective function of the optimization was maximizing natural frequency, and the constraint was the volume fraction. Other works that can be done in this area can focus on the change in these conditions, i.e. objective function, constraint, designable area, etc. and a comparison of the results could be presented. Furthermore, the results of more complicated optimized structure, without considering the manufacturability of the structure can be compared to the results of this work, and the efficiency of each model can be further discussed.

## Bibliography

- Agilent. (2008). The fundamentals of modal testing, application note In A. Technologies (Ed.). U.S.A.
- Arora, J. S. (1993). Sequential linearization and quadratic programming techniques. in: Kamat M. (Ed.). *Structural Optimization: Status and Promise*, AIAA, 71-102.
- Babuska, I. (1976). Solution of interface problems by homogenization I. *Journal of Mathematical Analysis*, 7, 603-634.
- Bendsøe, M. P., & Kikuchi, N. (1988). Generating optimal topologies in structural design using a homogenization method. *Comp. Meth. Appl. Mech. Eng.*, 71.
- Bendsøe, M. P., & Kikuchi, N. (1988). Generating optimal topologies in structural design using a homogenization method. *Computer Methods in Applied Mechanics and Engineering*, 71, 197-224.
- Bendsøe, M. P., & Kikuchi, N. (1989). Optimal shape design as a material distribution problem. *Structural Optimization*, 1, 193-202.
- Bendsøe, M. P., & Mota Soares, C. A. (1993). *Topology design of discrete structures*. In *Topology Design of Structures*. Netherlands: Kluwer Academic Publishers.
- Bendsøe, M. P., & Sigmund, O. (1999). Material interpolation schemes in topology optimization. *Archive of Applied Mechanics*, 69.
- Bendsøe, M. P., & Sigmund, O. (2003). *Topology optimization : theory, methods, and applications*. Berlin ; New York: Springer.
- Bulman, S., Siens, J., & Hinton, E. (2001). Comparisons between algorithms for structural topology optimization using a series of benchmark studies. *Computers & Structures*, 79, 1209-1218.
- Cardoso, E. L., & Fonseca, J. O. F. (2003). Complexity control in the topology optimization of continuum structures. *Journal of the Braz. Soc. of Mech. Sci. & Eng.*, 3.
- Chiat, L. W. (2008). *Design and Optimization of a Dynamically-Tuned Vibration Absorber Using Experimental and Computational Methods*. Bachelor's degree, University of Malaya.
- Chu, D. N. (1997). *Evolutionary Structural Optimization Method for Systems with Stiffness and Displacement Constraints*. PhD, Victoria University of Technology, Melbourne, Australia.
- Cioranescu, D., & Paulin, J. S. J. (1979). Homogenization in open sets with holes. *Journal of Math. Analysis and Appl*, 71, 590-607.
- Diaz , A. R., & Kikuchi, N. (1992). Solutions to shape and topology eigenvalue optimization problems using a homogenization method. *Int. J. Num. Meth. Engng*, 35.
- Dobbs, M. W., & Felton, L. P. (1969). Optimization of truss geometry. *J. Struct. Div., ASCE 100 (ST1)*, 2105-1118.
- Dorn, W. C., Gomory, R. E., & Greenberg, H. J. (1964). Automatic design of optimal structures. *J. de Mecanique*, 3, 25-52.
- Fiacco, A. V., & McCormick, G. P. (1968). *Nonlinear programming: sequential unconstrained minimization techniques*. New York: Wiley.
- Fleury, C. (1979). Structural weight Optimization by dual methods for convex programming. *International Journal for Numerical Methods in Engineering*, 14, 1761-1783.
- Haftka, R. T., & Grandhi, R. V. (1986). Structural optimization-a survey. *Computer Methods in Applied Mechanics and Engineering*, 57, 91-106.
- Haftka, R. T., & Gürdal, Z. (1992). *Elements of structural optimization* (3rd rev. and expanded ed.). Dordrecht ; Boston: Kluwer Academic Publishers.

- Heyman, J. (1951). Plastic design of beams and frames for minimum material consumption. *Quarterly of Applied Mathematics*, 8.
- Holland, J. H. (1975). *Adaptation in natural and artificial systems*. Ann Arbor, USA: University of Michigan Press.
- Huang, X., & Xie, Y. M. (2010). *Evolutionary topology optimization of continuum structures : methods and applications*. Chichester, West Sussex, U.K. ; Hoboken, NJ: Wiley.
- Jensen, J. S., & Pedersen, N. L. (2006). On maximal eigenfrequency separation in two-material structures: the 1D and 2D scalar cases. [doi: 10.1016/j.jsv.2005.03.028]. *Journal of Sound and Vibration*, 289(4-5), 967-986.
- Jog, C. S. (2002). TOPOLOGY DESIGN OF STRUCTURES SUBJECTED TO PERIODIC LOADING. [doi: 10.1006/jsvi.2001.4075]. *Journal of Sound and Vibration*, 253(3), 687-709.
- Jung, E.-I., Park, Y.-S., & Park, K. C. (2005). Structural dynamics modification via reorientation of modification elements. [doi: 10.1016/j.finel.2005.05.004]. *Finite Elements in Analysis and Design*, 42(1), 50-70.
- Kang, Z., Wang, X., & Wang, R. (2009). Topology optimization of space vehicle structures considering attitude control effort. [doi: 10.1016/j.finel.2008.12.002]. *Finite Elements in Analysis and Design*, 45(6-7), 431-438.
- Kirsch, U. (1989). Optimal topologies of Structures. *Appl. Mech. Rev*, 42, 223-239.
- Krog, L. A., & Olhoff, N. (1999). Optimum topology and reinforcement design of disk and plate structures with multiple stiffness and eigenfrequency objectives. [doi: 10.1016/S0045-7949(98)00326-5]. *Computers & Structures*, 72(4-5), 535-563.
- Ma, Z. D., Cheng, H.-C., & Kikuchi, N. (1994). Structural design for obtaining desired eigenfrequencies by using the topology and shape optimization method. [doi: 10.1016/0956-0521(94)90039-6]. *Computing Systems in Engineering*, 5(1), 77-89.
- Ma, Z. D., Kikuchi, N., & Cheng, H. C. (1995). Topology design for vibrating structures. *Computer Methods in Applied Mechanics and Engineering*, 121, 259-280.
- Maxwell, C. (1895). *Scientific Papers II*: Cambridge University Press.
- Michell, A. G. M. (1904). *The limit of economy of material in frame-structures*.
- Molter, A., Fonseca, J. S. O., Bottega, V., & Alves da Silveira, O. A. (2010). *Simultaneous topology optimization and optimal control for vibration suppression in structural design*. Paper presented at the 2nd International Conference on Engineering Optimization, Lisbon, Portugal.
- Molter, A., Fonseca, J. S. O., Bottega, V., Otávio, A., & Silveira, d. (2010). *Simultaneous topology optimization and optimal control for vibration suppression in structural design*. Paper presented at the 2nd International Conference on Engineering Optimization, Lisbon, Portugal.
- Nagendra, S., Haftka, R. T., & Giirdal, Z. (1993). *Design of blade stiffened composite panels by a genetic algorithm approach*. Paper presented at the Proceedings of the 34th AIAA/ASME/AHS SDM Conference, La Jolla, USA.
- Olhoff, N., Bendsoe, M. P., & Rasmussen, J. (1991). On CAD-integrated structural topology and design optimization. *Comp. Meth. Appl. Mech. Engrg.*, 89.
- Ou, J. S., & Kikuchi, N. (1996). Integrated optimal structural and vibration control design. *Structural Optimization*, 12.
- Prager, W., & J.E., T. (1968). Problems of optimal structural design. *Journal of Applied Mechanics*, 35, 102-106.
- Prager, W., & Shield, R. T. (1968). Optimal design of multi-purpose structures. *Int. J. Solids and Structures*, 4, 469-475.

- Ramli, R. (1998). *Structure-borne Noise Problems in a Passenger Car*. Master, University of Malaya.
- Richardson, M. H. (1997). Is It a Mode Shape, or an Operating Deflection Shape? (Vol. 30th Anniversary). Jamestown, California: Vibrant Technology, Inc.
- Rong, J. H., Xie, Y. M., Yang, X. Y., & Liang, Q. Q. (2001). Topology optimization of structures under dynamic response constraints. *Sound & Vibration*, 23(4), 177-189.
- Rosen, J. B. (1961). The gradient projection method for nonlinear programming. *Journal of the Society for Industrial and Applied Mathematics*, 8.
- Rozvany, G. I. N. (1995). *What is meaningful in topology design? An engineer's viewpoint*, *Advances in Structural Optimization*. Netherlands: Kluwer Academic Publishers.
- Schedlinski, c., Wagner, F., Bohnert, K., Frappier, J., Irrgang, A., Lehmann, R., & Muller, A. (2004). *experimental modal analysis and computational model updating of a car body in white*. Paper presented at the ISMA 2004, Leuven, Belgium.
- Schmit, L. A. (1960). *Structural design by systematic synthesis*. Paper presented at the Proceedings of the 2nd conference on Electronic Computation, New York.
- Schwarz, B. J., & Richardson, M. H. (1999). Experimental Modal Analysis. *Vibrant Technology, Inc*.
- Schwarz, B. J., & Richardson, M. H. (1999). Introduction to operating deflection shapes. *Vibrant Technology, Inc*.
- Taylor. (1977). Optimal truss design based on an algorithm using optimality criteria. *Int. J. Solids Struct*, 13, 913-923.
- Tenek, L. H., & Hagiwara, I. (1993). Static and vibrational shape and topology optimization using homogenization and mathematical programming. *Computer Methods in Applied Mechanics and Engineering*, 109, 143-154.
- Venkayya, V. B., Khot, N. S., & Reddy, V. S. (1968). *Optimization of structures based on the study of strain energy distribution*. Paper presented at the DTIC.
- Xie, Y. M., & Steven, G. P. (1993). A simple evolutionary procedure for structural Optimization. *Computers and Structures*, 49, 885-896.
- Xie, Y. M., & Steven, G. P. (1994). Optimal design of multiple load case structures using an evolutionary procedure. *Engineering Computations*, 11, 295-302.
- Yoon, G. H. (2010). Maximizing the fundamental eigenfrequency of geometrically nonlinear structures by topology optimization based on element connectivity parameterization. [doi: 10.1016/j.compstruc.2009.07.006]. *Computers & Structures*, 88(1-2), 120-133.
- Zhao, C., Steven, G. P., & Xie, Y. M. (1998). A generalized evolutionary method for natural frequency optimization of membrane vibration problems in finite element analysis. [doi: 10.1016/S0045-7949(97)00054-0]. *Computers & Structures*, 66(2-3), 353-364.
- Zhou, M., & Rozvany, G. I. N. (1991). The COG algorithm, Part II: Topological, geometrical and general shape optimization. *Comp. Meth. Appl. Mech. Eng.*, 89, 309-336.
- Zoutendijk, G. (1960). *Methods for Feasible Direction*. Amsterdam: Elsevier.